Regulation of the stability of the protein kinase DYRK1A: establishing connections with the Wnt signaling pathway

Krisztina Arató

TESI DOCTORAL UPF / 2010

Barcelona, November 2010

Regulation of the stability of the protein kinase DYRK1A: establishing connections with the Wnt signaling pathway

Krisztina Arató

Memòria presentada per optar al grau de Doctora per la Universitat Pompeu Fabra.

Aquesta tesi ha estat realitzada sota la direcció de la Dra. Susana de la Luna al Centre de Regulació Genòmica (CRG, Barcelona), dins del Programa de Genes i Malaltia.

Krisztina Arató **Susana de la Luna**

UNIVERSITAT POMPEU FABRA

CRG Centre for Genomic Regulation

A Pere,
por haberme traído a Barcelona…

Cover design by Luisa Lente (www.yoyo.es).

Index

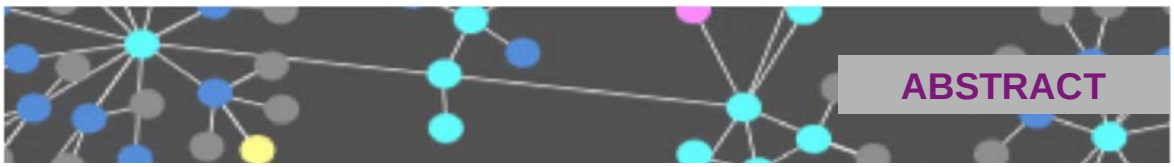

ABSTRACT

DYRK1A is the most studied member of the DYRK family of protein kinases, because is one of the human chromosoma 21 proteins for which changes in gene dosage result in neuropathological alterations. DYRKs are activated by autophosphorylation on a tyrosine residue in the activation loop, a one-off event that takes place during translation. Accordingly, DYRK1A would be constitutively active once is synthesized. However, DYRK1A is extremely sensitive to gene dosage, and thus it is predictable that not only its activity but also its actual protein amounts have to be tightly regulated by mechanisms not yet characterized.

In the present study, the protein kinase NLK has been identified as a novel regulator of DYRK1A protein stability. DYRK1A interacts with NLK in physiological conditions. The interaction results in the phosphorylation of DYRK1A at multiple sites, which have been identified by mass spectrometry analysis. These phosphorylation events promote DYRK1A proteasome-dependent degradation. Moreover, DYRK1A degradation is induced by stimulating cells with Wnt1 or Wnt3a, or overexpressing elements of the Wnt signaling cascade such as the Frizzled-1 receptor or NLK activators such as HIPK2. In addition, DYRK1A interacts with and phosphorylates β-catenin and TCF-4 and enhances β-catenin-dependent transcriptional activity, at least by phosphorylation of β-catenin. Thus, these results suggest that DYRK1A acts as a positive factor in the Wnt-β-catenin signaling pathway and NLK acts as a negative regulator by targeting both DYRK1A and TCF/LEF transcription factors for proteasome-mediated degradation.

DYRK1A es el miembro más estudiado de la familia de proteína quinasas DYRK, porque es una de las proteínas de la cromosoma humano 21 para la que cambios en la dosis génica dan lugar a alteraciones neuropatológicas. Las quinasas DYRK se activan por autofosforilación en un residuo tirosina localizado en el lazo de activación, un evento único que ocurre durante la traducción. Como consecuencia, DYRK1A sería constitutivamente activa una vez se ha sintetizado. Sin embargo, DYRK1A es extremadamente sensible a la dosis génica, y por tanto es predecible que no sólo su actividad, pero también los niveles de proteína han de estar estrictamente controlados por mecanismos reguladores que todavía no han sido caracterizados.

En este trabajo, la proteína quinasa NLK ha sido identificada como un nuevo regulador de la estabilidad de DYRK1A. DYRK1A interacciona con NLK en condiciones fisiológicas, y la interacción tiene como resultado la fosforilación de DYRK1A en residuos serina/treonina, varios de los cuales han sido identificados por espectrometría de masas. La interacción con NLK y la subsecuente fosforilación promueven la degradación de DYRK1A vía el proteasoma. Además, la degradación de DYRK1A es inducida por estimulación de la células con Wnt1 o Wnt3a, o por sobreexpresión de miembros de la cascada de señalización de Wnt, como el receptor Frizzled-1 o de un activador de NLK como HIPK2. Finalmente, se ha demostrado que DYRK1A se une y fosforila β-catenina y TCF-4. La fosforilación de, al menos, β-catenina es responsable del incremento de la actividad transcripcional dependiente de esta proteína en presencia de DYRK1A. Todos estos resultados sugieren que DYRK1A actúa como un factor positivo en la vía de señalización Wnt-β-catenina y NLK actúa como un regulador negativo al inducir la degradación vía proteasoma no sólo de los factores de transcripción TCF/LEF sino también del modulador positivo DYRK1A.

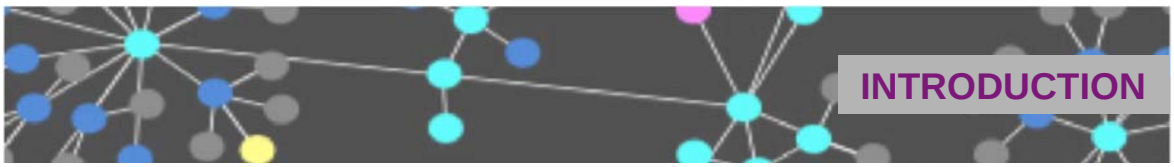

INTRODUCTION

The protein kinase DYRK1A

The DYRK family of protein kinases

DYRK1A belongs to a family of conserved protein kinases named *dual-specificity tyrosine-phosphorylated and regulated kinases* (DYRK), within the CMGC group of the eukaryote kinome, which also includes cyclin-dependent kinase (CDK), mitogen-activated protein kinase (MAPK), glycogen synthase kinase (GSK), CDK-like kinase (CLK), serine-arginine-rich protein kinase, cdc2-like kinase, and RCK kinase families (Manning et al., 2002) (Fig. I1A).

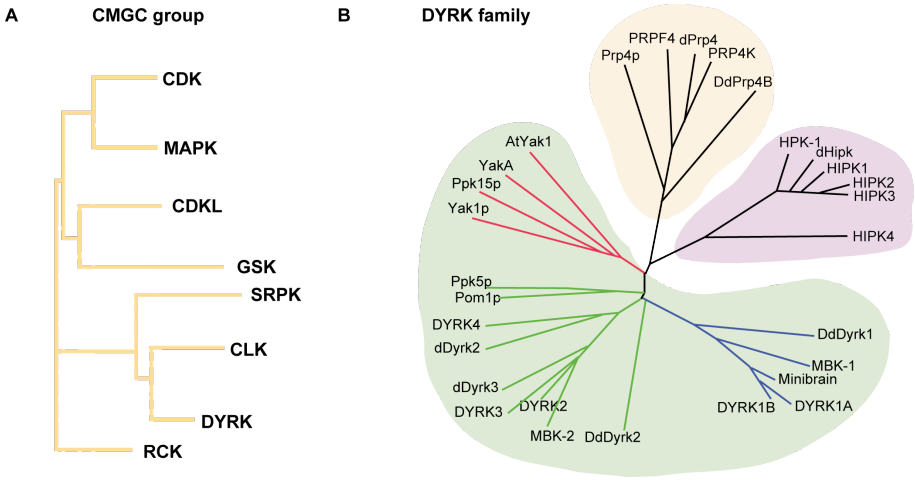

Figure I1: The DYRK family of proteins. **A)** Unrooted phylogenetic tree showing the evolutionary divergence of the different families within the CMGC group (see text for the name of the families). **B)** Unrooted phylogenetic tree showing the three subfamilies, PRP4 (in orange), HIPK (in violet) and DYRK (in green) of the DYRK family (from Aranda et al., 2010).

Homology within the kinase domain allows for the division of the DYRK family into three subfamilies: DYRK kinases, homeodomain-interacting protein kinases (HIPKs) and pre-mRNA processing protein 4 kinases (PRP4s) (Fig. I1B). DYRK subfamily members share a conserved kinase domain and an adjacent DYRK-homology domain, or DH-box (DDDNXDY), but they differ in their N- and C-terminal regions (Becker and Joost, 1999). From a phylogenetic viewpoint, the subfamily can be classified into three classes: a first group includes kinases only present in yeast and plants such as *Saccharomyces cerevisiae* Yak1p or *Dictyostelium discoideum* YakA; a second class includes *Schizosaccharomyces pombe* Pom1p, *Caenorhabditis elegans* MBK-2, *Drosophila melanogaster* dDYRK2 and dDYRK3, and vertebrate

DYRK2, DYRK3, and DYRK4; and a third class includes *C. elegans* MBK-1, *D. melanogaster* minibrain, and vertebrate DYRK1A and DYRK1B (Fig. I1B).

This thesis work is focused on the study of human DYRK1A. For this reason a review on this kinase follows, highlighting both the commonalities and differences with other mammalian DYRKs (DYRK1B, DYRK2, DYRK3 and DYRK4). Particular emphasis has been made on aspects such as regulation of DYRK1A expression and activity and DYRK1A involvement in intracellular signaling pathways. A recent review on all members of the DYRK subfamily can be found in Aranda et al., (2010).

Structure and mechanism of activation of DYRK1A kinase

Several structural features can be distinguished in DYRK1A protein: a conserved catalytic kinase domain, two functional nuclear localization signals (NLS), one at the N terminus and another one within the catalytic domain (Alvarez et al., 2003), a PEST motif, a poly-histidine stretch and a region rich in serine and threonine residues (Fig. I2). PEST domains are protein regions enriched in proline, glutamic acid, serine and threonine residues that have been linked to the control of protein stabilization (Rogers et al., 1986), however the involvement of this motif in the control of the half-life of DYRK1A has not been reported to date. The histidine-repeat targets DYRK1A to the nuclear speckles compartment (Alvarez et al., 2003), and it has also been shown to act as a docking site for recruiting one of the DYRK1A substrates (Aranda et al., 2008). No activities have been associated to the serine and threonine-rich region present in the C-terminal domain.

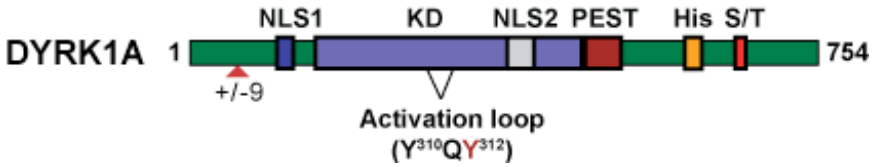

Figure I2: Schematic representation of the protein structure of DYRK1A. The domains shown are explained in the text. The position of the alternative spliced region is indicated with a triangle, and that of the activation loop is shown.

DYRKs are known as dual-specificity kinases, because autophosphorylate on tyrosine and serine/threonine residues, while all the exogenous substrates described till now are phosphorylated in serine and threonine residues. In the case of DYRK1A, a consensus phosphorylation sequence has been defined as RPX(S/T)P, suggesting

that DYRK1A is a proline-directed kinase (Himpel et al., 2000). However, the analysis of all the DYRK1A substrates described to date indicates that not all of the phosphosites fit within the consensus sequence and that other amino acid residues can be accommodated at the P+1 position (Aranda et al., 2010).

All the DYRK family members, including DYRK1A, present a conserved Tyr-X-Tyr motif in the activation loop of the catalytic domain (Becker and Joost, 1999). Phosphorylation of the second Tyr-residue of this motif is essential for DYRK1A kinase activity (Himpel et al., 2001), a requisite that has been proven for other mammalian DYRKs (Lee et al., 2000; Li et al., 2002; Papadopoulos et al., 2010). The mechanism of activation of DYRKs resembles that of the MAPKs, although, unlike MAPKs, Tyr-phosphorylation in the DYRK activation loop is an autophosphorylation event and does not involve an upstream activating kinase (Himpel et al., 2001). Using *Drosophila* DYRKs as the experimental system, a model for the activation of DYRK family members has been suggested (Lochhead et al., 2005). According to this model, autophosphorylation in the activation loop is an intramolecular event mediated by a transitional intermediate form during translation. The Tyr-kinase activity is lost once the protein is fully translated, and the mature kinase can only phosphorylate Ser/Thr residues. Further studies from the same group have shown that the two classes of DYRK subfamily members have distinct structural requirements for the autophosphorylation process (Kinstrie et al., 2010). Class II DYRKs (including DYRK2, DYRK3 and DYRK4) require a conserved domain in the N-terminal region named as the NAPA-domain that provides a chaperon-like function, while class I DYRKs (including DYRK1A and DYRK1B) lack this region and autophosphorylation occurs independently of any N-terminal sequence.

An important characteristic of DYRKs is their ability to act as priming kinases for GSK3. This means that previous phosphorylation by DYRKs of a given residue allows for more efficient phosphorylation of a different residue by GSK3: if the residue is at P-4, it is known as classical GSK3 priming; if the residue is distant from the phosphorylated site, it is known as non-classical or discontinuous GSK priming (Fiol et al., 1988). DYRK1A acts as a classical GSK3 priming kinase in the case of eI2Fβ, tau, MAP1B and CRY2 (Kurabayashi et al., 2010; Scales et al., 2009; Woods et al., 2001), but acts as a non-classical GSK3 priming kinase in the case of nuclear factor of activated T-cells (NFAT) transcription factors (Arron et al., 2006; Gwack et al., 2006).

Two pharmacological inhibitors of DYRK1A have been used to study the function of this kinase. One of them, (-)-epigallocatechin-3-gallate (EGCG) - one of the major polyphenolic components of green tea-, is a potent DYRK1A inhibitor and functions as a noncompetitive inhibitor of ATP. However, EGCG also inhibits other DYRKs and many other kinases (Bain et al., 2007; Yang et al., 2009), and thus it is not useful to elucidate the *in vivo* functionality of DYRK1A. Recently, the alkaloid harmine, a classical inhibitor of monoamine oxidase, was identified as a potent ATP-competitive DYRK1A inhibitor (Bain et al., 2007). With the help of this alkaloid, several new DYRK1A functions have been discovered, as illustrated in the recent identification of DYRK1A as a negative regulator of the intrinsic apoptotic pathway and cardiomyocyte hypertrophy (Kuhn et al., 2009; Laguna et al., 2008; Seifert et al., 2008). However, as harmine also inhibits DYRK1B (5-fold less efficiently) and DYRK2 and DYRK3 (50-fold less efficiently) (Gockler et al., 2009), its use must be complemented with additional techniques.

Regulation of DYRK1A expression

DYRK1A is expressed ubiquitously as it has been detected in almost all tissues analyzed (Becker et al., 1998; Guimera et al., 1996; Wegiel et al., 2004). As other members of the mammalian DYRK family, DYRK1A is expressed as several transcripts, differing in their 5'-ends due to alternative promoter usage and first exon choice (Fig. I3). Experimental evidence suggests that *DYRK1A* contains three putative promoter regions, promoter A (pA) before exon 1A, promoter B (pB) before exon 1B and promoter M (pM) before exon 1M, putative promoter regions. Their use produces distinct transcripts with different 5' ends and they appear to have distinct responses to transcription factors, such as E2F1 in the case of promoter region pB or CRE binding protein (CREB) in the case of promoter region pA, have been described for DYRK1A (Impey et al., 2004; Maenz et al., 2008) (Fig. I3). The transcription factor activator protein 4 (AP4) and its corepressor partner geminin have been shown to repress DYRK1A transcription through recruiting histone deacetylase 3 to pB and pM *DYRK1A* promoter regions (Kim et al., 2006b). Transcription from pM and pB would result in transcripts with an identical coding potential, whereas transcripts generated from pA could potentially encode a protein lacking the first 29 amino acids.

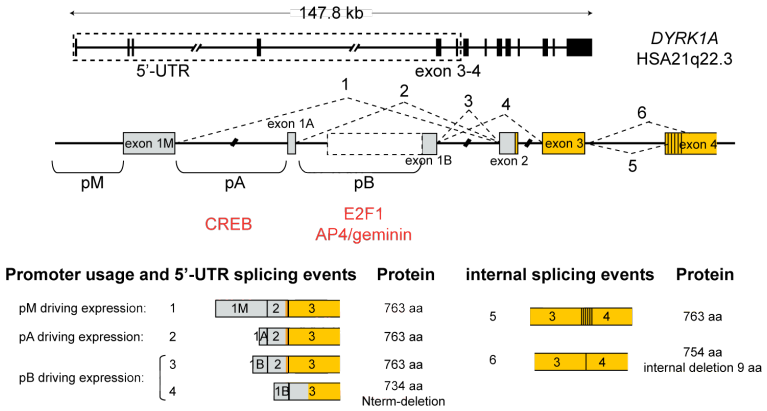

Figure I3: Genomic structure and splicing events of human DYRK1A. Schematic representation of human *DYRK1A* gene: exons are shown as boxes and introns as lines. Gene size and chromosomal location are indicated. The untranslated and the translated exons are shown in grey and orange, respectively. A partial scheme of the transcripts produced by the differential usage of distinct promoters and/or splicing events is included, and the predicted protein produced by each transcript is indicated (adapted from Aranda et al., 2010).

DYRK1A mRNA has been shown to be upregulated in the brain of mice overproducing β-amyloid protein (Aβ), a major component of senile plaques in Alzheimer's disease, and in neuroblastoma cells when incubated with Aβ (Kimura et al., 2007). Transcriptional activation has also been shown in osteoblastoma cells treated with RANKL, very likely through activation of NFATs (Lee et al., 2009). It is worth to note that NFAT and Aβ precursor protein are DYRK1A substrates (Arron et al., 2006; Ryoo et al., 2008), and the transcriptional effects could be part of regulatory loops. Additionally, DYRK1A protein shows circadian oscillation in the mouse liver (Kurabayashi et al., 2010), although it is not known whether the regulation occurs at the transcriptional or post-transcriptional levels. Alternative splicing events within the *DYRK1A* coding region results in the production of distinct protein isoforms. The use of alternative acceptor splicing sites in exon 4 gives rise to two protein isoforms that differ in the inclusion/exclusion of nine amino acids in the N-terminus of the protein (Fig. I3). Up to date, no functional differences among these protein isoforms have been reported. Finally, the control of DYRK1A expression via miRNAs has been proposed and the miRNA let7b suggested as responsible (Buratti et al., 2010).

Regulation of DYRK1A subcellular localization

DYRK1A localizes both in the cytoplasm and in the nucleus of different neuronal types in the human, mouse and chick central nervous system (CNS) (Hammerle et

al., 2003; Marti et al., 2003; Wegiel et al., 2004), while its expression is mostly restricted to the cytosol in glial cells (Marti et al., 2003). Biochemical fractionation experiments indicate that DYRK1A is distributed in different pools in mouse brain cytosolic fraction: a soluble DYRK1A pool, a pool associated with the synaptic plasma membrane and a pool associated with vesicle-containing fractions (Aranda et al., 2008; Murakami et al., 2009).

When exogenously expressed, DYRK1A is only localized in the nucleus of a wide variety of established cell lines (Alvarez et al., 2003; Becker et al., 1998; Fernandez-Martinez et al., 2009; Guo et al., 2010; Mao et al., 2002; Seifert et al., 2008; Sitz et al., 2004), in primary hippocampal neurons (Sitz et al., 2004) and in neural cells of the embryonic neocortex (Yabut et al., 2010). The two predicted NLSs appear to contribute to DYRK1A complete nuclear accumulation (Alvarez et al., 2003); these NLSs are also conserved in the DYRK1A closest homologous DYRK1B and they are also responsible for the accumulation of DYRK1B in the nucleus (Alvarez, Raya, de la Luna, unpublished results). Within the nucleus, DYRK1A accumulates in nuclear speckles through its His-repeat domain, which serves as a nuclear speckle-targeting signal (Alvarez et al., 2003). The presence of DYRK1A in the splicing factor compartment has been also observed in physiological conditions (Fernandez-Martinez et al., 2009; Salichs, Laguna, de la Luna, unpublished results).

A switch from the nucleus to the cytoplasm has been described during Purkinje cells differentiation in chicken (Hammerle et al., 2002), and results from our group indicate that DYRK1A has nucleocytoplasmic shuttling activity (Alvarez, 2004). All these data suggest that DYRK1A subcellular localization may be a control point to regulate substrate accessibility, although whether it is regulated at the nuclear import, nuclear export or nuclear/cytosolic retention levels it is still not known. Other DYRK family members also show changes in subcellular localization and in some cases a regulatory mechanism has been identified. DYRK1B shows a predominant nuclear staining in several cell lines, whereas major cytosolic staining is observed in rhabdomyosarcomas and pancreatic ductal carcinomas (Deng et al., 2006; Mercer et al., 2006). DYRK2 is present in the cytosol, however it translocates to the nucleus upon DNA damage (Taira et al., 2007), by using a NLS at the N-terminus of the protein (Taira et al., 2010). DYRK3 has been observed so far to be predominantly nuclear (Lord et al., 2000), while DYRK4 is expressed as two main isoforms with tissue-specific patterns. One of these variants contains a NLS in its extended N-terminus that targets the protein to the nucleus (Papadopoulos et al., 2010).

Regulation of DYRK1A activity

One consequence of the mechanism of activation of all DYRKs is that the activation loop would be constitutively phosphorylated, and consequently the kinase would be constitutively active. However, the study of animal models in which the dosage of DYRK1A has been manipulated shows that DYRK1A is extremely sensitive to gene dosage (Ahn et al., 2006; Altafaj et al., 2001; Fotaki et al., 2002; Laguna et al., 2008; Ortiz-Abalia et al., 2008), and thus it is sensible to think that its activity has to be tightly regulated. This could happen not only by controlling protein amounts by regulatory mechanisms at the transcriptional and post-transcriptional levels as discussed in the previous section, but also by actions at the post-translational level such as the control of the protein amounts, the regulation of the catalytic activity, the interaction with substrates or the accessibility to substrates or regulators (summarized in Fig. I4):

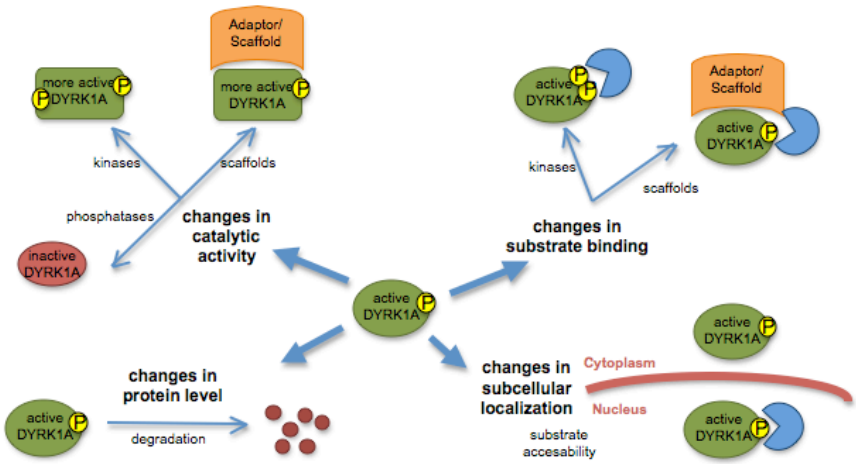

Figure I4: Schematic representation of possible mechanisms by which DYRK1A kinase activity can be regulated. Changes in DYRK1A phosphorylation state, in the interaction with other proteins, in the subcellular localization, in the protein turn-over, alone or in combination, might lead to changes in the overall DYRK1A biological activity.

i- Dephosphorylation of the activation loop should turn off DYRK1A kinase activity, but no specific phosphatases have been described yet. Additionally, phosphorylation events outside the activation loop might contribute to DYRK1A full activity or to substrate recognition. In this regard, it has been shown that MKK3 enhances the activity of DYRK1B by an unknown mechanism (Lim et al., 2002), that ATM activates DYRK2 by phosphorylation within the α-G helix in the catalytic domain (Taira et al., 2010) and that MAP3K10 negatively regulates DYRK2 activity through phosphorylation of the threonine of its YTY motif (Varjosalo et al., 2008).

ii-Two examples of mechanisms by which the modulation of DYRK1A kinase activity relies on the interaction with regulatory proteins have been already proposed. One of them has been described by our group and involves DYRK1A autophosphorylation on Ser520 residue outside the catalytic domain. This event triggers the association with 14-3-3β and induces a conformational change, resulting in increased DYRK1A catalytic activity (Alvarez et al., 2007). Another example is the binding of Sprouty-related protein with an EVH1 domain (SPRED1/2) to the kinase domain of DYRK1A; this interaction appears to compete for the same binding site with other substrates and inhibit therefore DYRK1A-dependent phosphorylation (Li et al., 2010a).

iii- Regulation of the subcellular localization may represent another way of controlling DYRK1A activity. As DYRK1A has both nuclear and cytoplasmic proteins as substrates and DYRK1A is shuttling protein, changes in DYRK1A subcellular localization may represent a way of controlling substrate accessibility. However, the knowledge on the regulatory mechanisms acting at this level is still very poor.

iv- Several observations suggest that DYRK1A protein levels could be regulated, although no regulatory mechanisms have been reported so far. DYRK1A is predicted to have a short half-life, as it harbors a PEST motif. Moreover, results from our group suggest that active DYRK1A has a longer half-life than the kinase inactive form, suggesting that DYRK1A might regulate its own stability (Alvarez, 2004). We have also observed that DYRK1A protein levels change during cell cycle with lower levels in G1 that gradually increase during S phase until reaching the highest levels in G2/M (C di Vona, S de la Luna, unpublished results). Whereas the increase in S phase appears to be at the transcriptional level, the decrease in the M to G1 transition could involve protein stability. Another DYRK family member, DYRK2, which does not contain a PEST motif, has been found to escape from degradation through ATM-induced phosphorylation upon DNA damage (Taira et al., 2010).

DYRK1A as a regulator of signaling pathways

Substrates of DYRK1A have been identified among different classes of proteins, both nuclear and cytosolic (for a complete list, see Aranda et al., 2010). These include proteins involved in transcription, splicing, translation, apoptosis, endocytosis and metabolism (summarized in Fig. I5). In fact, the role of DYRK1A in all these processes has been inferred from the activity of all these substrates. DYRK1A

phosphorylation can affect different aspects of the biology of its substrates including changes in protein stability (HPV16E7; Liang et al., 2008), in subcellular localization (NFAT; Arron et al., 2006; Gwack et al., 2006), in the ability to interact with different partners (dynamin; Huang et al., 2004) or in enzymatic activity (glycogen synthase; Skurat and Dietrich, 2004).

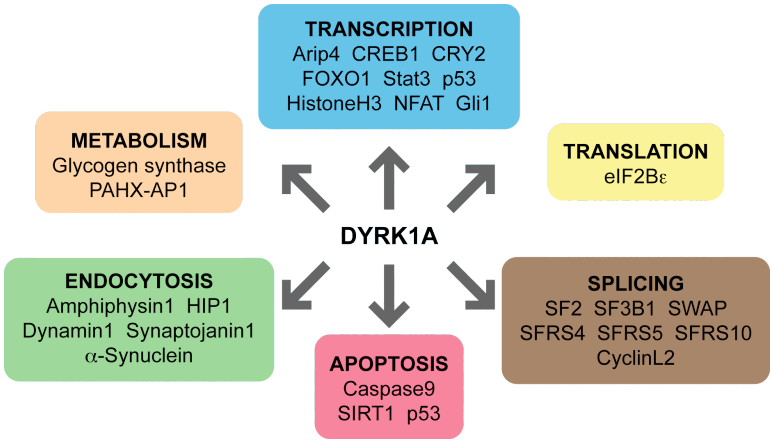

Figure I5: Substrates of DYRK1A. Substrates were classified into groups according to their involvement in different cellular processes. As shown, DYRK1A has multiple putative roles in transcription, translation, splicing, apoptosis, endocytosis, and metabolism.

A role for DYRK1A in the development and homeostasis of the CNS has been proposed based on the phenotype of *Dyrk1A* mouse models. *Dyrk1A* knock-out mice died at embryonic mid-stages and show severe developmental delay (Fotaki et al., 2002). Heterozygotes are viable, but exhibit reduced size that is most noticeable in liver and brain (Fotaki et al., 2002). Reduction in both the number of neurons in the superior colliculus (Fotaki et al., 2002), and in the complexity of the dendritic tree in the cortex (Benavides-Piccione et al., 2005) has been described. Moreover, transgenic mice carrying *Dyrk1A* extra copies exhibit hippocampal-dependent spatial learning and memory defects and motor abnormalities (Ahn et al., 2006; Altafaj et al., 2001; Branchi et al., 2004; Martinez de Lagran et al., 2004; Smith et al., 1997). In *Drosophila*, loss-of-function of the *DYRK1A* orthologue *minibrain*, results in defective neurogenesis (Tejedor et al., 1995). Mutant flies present reduction in the volumes of the adult optic lobes and central brain hemispheres due to abnormal spacing of neuroblasts in the outer proliferation center of the larval brain. In humans, *DYRK1A* truncating mutations or loss-of-copy in hemizygosis result in microcephaly (Fujita et al., 2010; Moller et al., 2008). All these findings indicate that the role of DYRK1A in CNS development has been highly conserved during evolution. However, the particular functions of DYRK1A in CNS development are still not well known.

The fact that both gain-of-copy and loss-of-copy of *Dyrk1A* leads to growth retardation and developmental delay indicates that misexpression of a single gene, *DYRK1A*, can impair multiple physiological functions likely through a signal amplification effect. This hypothesis predicts that DYRK1A is involved in the regulation of several cellular processes and signaling transduction pathways, and indeed, several of its substrates are known to be involved in signaling pathways, which regulate proliferation, differentiation and cellular survival. A summary of the involvement of DYRK1A in these signaling pathways follows.

The Notch signaling pathway

The Notch signaling pathway is a highly conserved developmental pathway, which plays a critical role in cell-fate decisions, tissue patterning and morphogenesis, cell differentiation, proliferation and death in which cell-to-cell communication needs to be established (recently reviewed in, for instance, Kageyama et al., 2009; Phng and Gerhardt, 2009; Roca and Adams, 2007; Yuan et al., 2010). The major players of the pathway are the Notch receptors and their ligands. Notch receptors, Notch1–4 in mammals, are single-pass transmembrane proteins that have dual functions as both cell surface receptors and nuclear transcriptional regulators. Notch ligands, Jagged 1-2, Delta-like (Dll) 1, 3 and 4, are also transmembrane proteins (D'Souza et al., 2008). A schematic representation of how the pathway works is shown in Fig. I6 (recent reviews on the pathway and the many levels of regulation can be found in Fortini and Bilder, 2009; Kopan and Ilagan, 2009; Kovall, 2008; Poellinger and Lendahl, 2008; Tien et al., 2009).

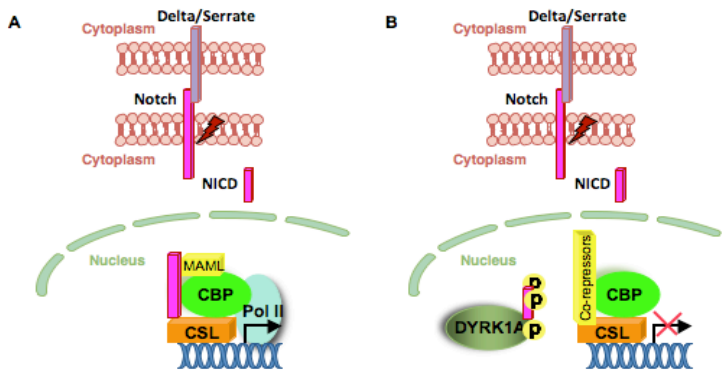

Figure I6: Involvement of DYRK1A in the Notch signaling pathway. (A) Notch signaling activation is initiated by ligand–receptor binding between two adjacent cells. This interaction induces a conformational change in Notch receptors that leads to their proteolytic cleavage. Then, the Notch intracellular domain (NICD) is released to the cytoplasm, and enters into the nucleus binds to the transcriptional repressor CSL and switches CSL into an activated state. Additionally, NICD/CSL complex recruits co-activators, such as mastermind-like (MAML) and p300 that facilitate the transcriptional activation of Notch target genes. **(B)** Notch-pathway repressive state due to the phosphorylation of NICD by DYRK1A.

The activity of the pathway is regulated by many different posttranslational modifications (see Fortini, 2009). In particular, the function of NICD is regulated by several phosphorylation events (Espinosa et al., 2003; Foltz and Nye, 2001; Foltz et al., 2002; Ingles-Esteve et al., 2001). DYRK1A has been shown to interact with NICD and to promote its phosphorylation at multiple sites, which leads to the repression of its transcriptional activity in neural cells (Fernandez-Martinez et al., 2009). In agreement with the DYRK1A repressive activity on Notch signaling, the negative role of Notch on neuronal maturation and neurite development is reverted by the presence of DYRK1A (Fernandez-Martinez et al., 2009).

Receptor tyrosine kinase signaling

Receptor tyrosine kinases (RTKs) transmit signals that regulate cell proliferation and differentiation, promote cell migration and survival and modulate cellular metabolism. They play a critical role in a wide range of biological processes, including embryonic development, angiogenesis, synaptic plasticity and oncogenesis. RTKs are membrane-spanning, cell surface proteins that contain an extracellular ligand binding domain and an intracellular tyrosine kinase domain, which is responsible for transducing the signal. Most RTKs exist as inactive monomers and form dimers following binding to their ligands, the vast majority of which are soluble peptides (i.e. nerve growth factor or NGF, fibroblast growth factor or FGF, epidermal growth factor or EGF, etc.). Many RTKs have been described in mammals, and although their activation leads to specific intracellular responses, a common mechanism of activation can be delineated for most of them and involves the RAS-RAF-ERK cascade (Fig. I7) (for recent reviews Hubbard and Miller, 2007; Lemmon and Schlessinger, 2010; McKay and Morrison, 2007). The signal output from this cascade is finely modulated by positive and negative regulators that contribute to determine both the magnitude and the duration of ERK signaling (reviewed in, for instance, Ebisuya et al., 2005).

An important class of regulators of RTK-dependent pathways is the Sprouty (Spry1 to -4 in mammals) family of proteins, which interferes with RTK-signaling cascade in a growth-factor and tissue-specific manner (for a recent review see Guy et al., 2009). Another way to fine-tune the output of the signal is through regulated endocytosis of the RTKs, which then can be recycled to the cell surface or targeted for degradation (reviewed in Sorkin and von Zastrow, 2009).

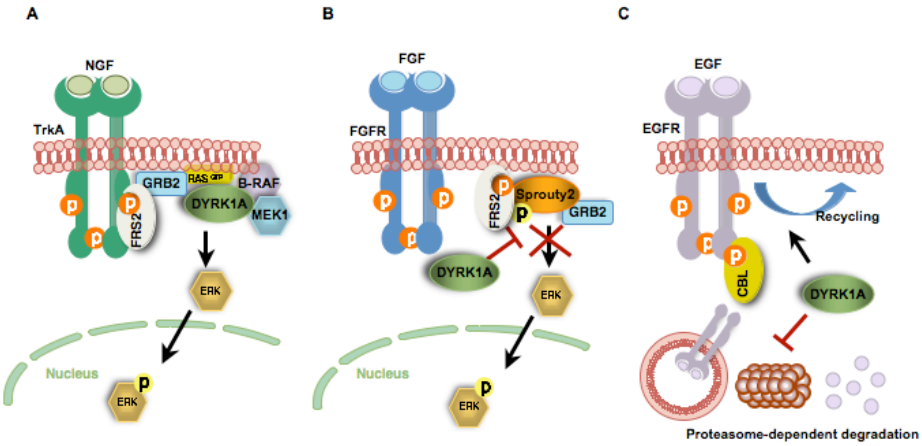

Figure I7: Involvement of DYRK1A in RTK signaling pathways. Upon ligand binding, the dimerization of the receptors induce their activation and the autophosphorylation of tyrosine residues in the RTK intracellular domains that serve as specific binding sites for a wide variety of proteins (FRS, GRB, CBL). The GTPase RAS is the critical link that allows RTKs to signal to ERK via a MAPK cascade involving the MAPKKKs RAF-1 or BRAF. The scheme summarizes the findings on DYRK1A activity within the NGF (**A**), FGF (**B**) and EGF (**C**) -dependent signaling pathways. For details see the text.

The involvement of DYRK1A in RTK signaling has been shown by several groups, although a common picture cannot be extracted yet.

i.- DYRK1A has been reported to potentiate the differentiation of PC12 cells induced by NGF through its interaction with components of the signaling cascade RAS-BRAF-MEK1 (Kelly and Rahmani, 2005) (Fig. I7A). Given that this effect is independent of DYRK1A kinase activity, a role as a scaffold has been suggested.

ii.- DYRK1A has been demonstrated to enhance FGF-dependent signaling in a kinase-dependent manner (Aranda, 2007; Aranda et al., 2008). On one side, knock-down of DYRK1A reduces FGF-dependent MAPK signal by acting downstream of RTK activation (Aranda, 2007). Similarly to the PC12 and NGF paradigm, DYRK1A is present in complexes with BRAF in HEK-293 cells, and it could be therefore one of the DYRK1A targets in this context; however, the complexes are detected independently of the activation status of the pathway suggesting that a triggering mechanism should exist (Aranda et al., 2008). On the other side, DYRK1A phosphorylates Spry2 at residue Thr75 and negatively regulates its inhibitory action on FGF-dependent MAPK activation (Aranda et al., 2008) (Fig. I7B). DYRK1A and Spry2 colocalize in growth cones of dissociated cortical neurons and copurify with the synaptic plasma membrane fraction from mouse brain extracts, pointing to their functional interaction occurring very close where the signals are received by RTKs in neurons.

iii.- DYRK1A acts as a brake for EGF-induced EGF receptor (EGFR) degradation, once EGFR is internalized by endocytosis (Ferron et al., 2010) (Fig. I7C). DYRK1A exerts this role, at least in part, through binding to and phosphorylation of Spry2. The effect of DYRK1A on EGFR cell surface levels is important for the self-renewal capability and long-term persistence of dividing neural stem cells of the adult subependymal zone (Ferron et al., 2010).

Hedgehog Signaling

Vertebrate hedgehog (Hh) signaling is a key regulator of proper morphogenesis of several organs, such as the skin, eye, lung, and pancreas, and for patterning of the neuronal tube and limb bud (for a recent review Jiang and Hui, 2008; Wong and Reiter, 2008). It also acts as a mitogen for a number of neuronal precursor cells located in the spinal cord and retina, in the neural tube, and in the cerebellum (reviewed in Briscoe, 2009; Ruiz i Altaba et al., 2002). A schematic representation of how the pathway works is shown in Fig. I8 and recent reviews can be found in Aikin et al., (2008), Ayers and Therond (2010), Ruiz i Altaba et al., (2007).

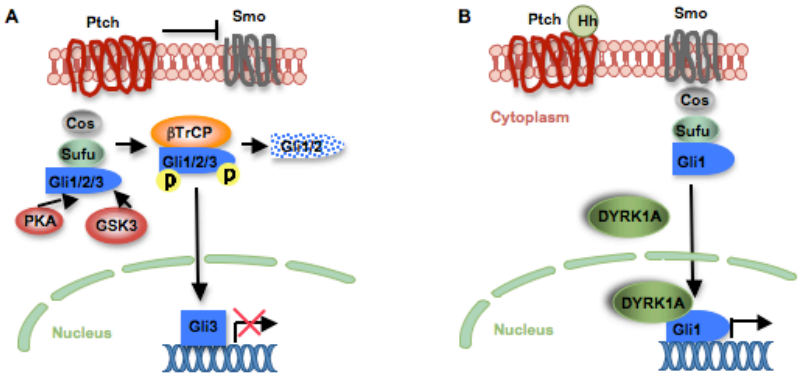

Figure I8: Involvement of DYRK1A in the Hedgehog signaling pathway. (A) In the absence of Hh, Ptch inhibits the downstream pathway by repressing the function of Smoothened (Smo), a seven-transmembrane protein that acts as the central positive mediator of Hh signaling. Gli1/2 and Gli3 are phosphorylated by kinases, including protein kinase A (PKA) and GSK3, to generate phosphopeptide-binding motifs for β-TrCP, an important substrate recognition component of the E3 SCF ubiquitin ligase complex. Ubiquitination of Gli targets these proteins to the proteasome, which processes Gli3 into a C-terminal-truncated repressor form and degrades Gli1/2. **(B)** Upon binding of Hh to Ptch, inhibition of Smo is relieved and its associated G-protein activity likely blocks inhibitory kinase action on Gli which is now free to translocate to the nucleus and activate transcription of Hh target genes including *Ptch1* and *Gli1*, whose protein products negatively and positively, respectively, feed-back on the pathway. Another negative regulator of Hh signaling is Supressor of Fused (SuFu), which retains Gli transcription factors in the cytosol. For details on the DYRK1A activity on the pathway, see the text.

Hhs are secreted lipoproteins that initiate signaling by binding to their receptor, the transmembrane protein Patched (Ptch), which initiates a signaling cascade

including the Gli family (Gli1–3) of transcription factors as final effectors. Gli1 functions only as a transcriptional activator, Gli2 functions similarly and mainly as an activator, whereas Gli3 functions primarily as a repressor (reviewed in Ruiz i Altaba et al., 2007; Varjosalo and Taipale, 2008). Several DYRK family members have been shown to be involved in Hh signaling. DYRK1A retains Gli1 in the nucleus, and enhances the transcriptional activity of full-length Gli1 but not of a natural N-terminally truncated DYRK1A variant (Mao et al., 2002; Shimokawa et al., 2008) (Fig. I8B); both activities depend on DYRK1A kinase activity and Gli1 was shown to be a DYRK1A substrate (Mao et al., 2002). Very importantly, Hh fails to stimulate DYRK1A kinase activity, and thus, DYRK1A might not be directly regulated by this pathway (Mao et al., 2002). In contrast, DYRK1B and DYRK2 have been found to negatively regulate Gli-dependent transcription. DYRK2 does it through phosphorylation and degradation of Gli2 and Gli3 via the ubiquitin/proteasome pathway (Varjosalo et al., 2008). The mechanism of action of DYRK1B has been studied in pancreatic cancer cells. In these cells, the mutated RAS, KRAS, acts through DYRK1B and SUFU to block Gli2 function to negatively regulate cell-autonomous Hh signaling (Lauth et al., 2010). The exact mechanism by which DYRK1B exerts its role is still unknown.

Calcineurin-NFAT signaling

Calcineurin-NFAT signaling is essential in regulating a diverse range of biological processes, including T lymphocyte development and reactivity, development of the nervous and vascular systems, fibre-type switching in skeletal muscle, development of heart valves, development of bone and control of cardiac hypertrophy (Macian, 2005; Mancini and Toker, 2009; Molkentin, 2004; Oh-hora and Rao, 2008; Schulz and Yutzey, 2004). Calcineurin is a calcium–calmodulin-activated, Ser/Thr protein phosphatase that is activated by sustained elevations in intracellular calcium. Once activated, calcineurin directly dephosphorylates NFAT transcription factors within the cytoplasm, promoting their translocation into the nucleus and activation of gene expression (reviewed in Hogan et al., 2003). A schematic representation of how the pathway works is shown in Fig. I9.

NFAT is phosphorylated, and therefore inactivated through cytosolic retention, by the action of different kinases, such as CK1, MEKK1 (Zhu et al., 1998) and GSK3 (Beals et al., 1997). DYRK1A and DYRK2 have been reported to directly phosphorylate NFAT, which in turns prime further phosphorylation by CK1 and GSK3 promoting NFAT translocation to the cytosol (Arron et al., 2006; Gwack et al., 2006).

DYRK1A-induced inhibition of NFAT transcription attenuates the hypertrophic response of cardiomyocytes, which may develop upon arterial hypertension or heart valve disease (Kuhn et al., 2009). It also results in the blockade of osteoclast differentiation, which seems to act as a negative regulatory feed-back loop, as DYRK1A expression is induced upon osteoclast differentiation (Lee et al., 2009). DYRK3-mediated inhibition of NFAT transcription attenuates red blood cell production selectively during aneamia (Bogacheva et al., 2008).

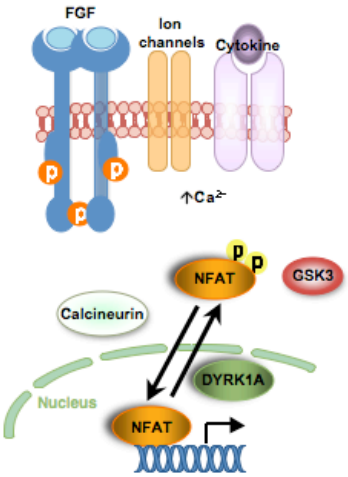

Figure I9: Involvement of DYRK1A in the Calcineurin-NFAT signaling pathway. The increase in intracellular concentration of calcium by activation of RTKs, ion channels or cytokine receptors leads to the activation of calcineurin and the nuclear translocation of NFAT. NFAT is kept in the cytosol in its hyperphosphorylated state by the action of several kinases. For details on the activity of DYRK1A in the pathway see the text.

DYRK1A and disease

Dyrk1A is one of the genes located on the Down syndrome (DS) critical region (DSCR) in human chromosome 21. This chromosomal segment when present in trisomy is associated with some DS characteristics including mental retardation, and motor defects (Dahmane et al., 1995). In the brain of DS fetuses and patients, the extra copy of *DYRK1A* gene leads to elevated mRNA and protein levels (Dowjat et al., 2007; Guimera et al., 1999). The phenotype of mouse models of DYRK1A overexpression (Ahn et al., 2006; Altafaj et al., 2001; Smith et al., 1997) together with its expression profile during neurogenesis (Hammerle et al., 2008; Hammerle et al., 2002) and in the adult central nervous system (Marti et al., 2003; Okui et al., 1999; Wegiel et al., 2004) has led to propose DYRK1A as one of the candidates to be responsible of some of the neuropathological features of DS (Arron et al., 2006; Epstein, 2006; Park et al., 2009).

Most individuals with DS show early onset of Alzheimer disease (AD). Involvement of DYRK1A in AD phenotypes has been suggested based on several

evidences. First, scanning for chromosome 21 genetic markers found association of *DYRK1A* and AD phenotype in the Japanese population (Kimura et al., 2007). Second, DYRK1A is increased in DS and AD brains correlating with increased phosphorylated Tau (Liu et al., 2008; Wegiel et al., 2008). Third, Aβ and phosphorylated Tau and APP are increased in mouse models of gain-of-function of DYRK1A (Liu et al., 2008; Ryoo et al., 2008), in agreement with the fact that both Tau and APP are *in vitro* substrates of DYRK1A (Kimura et al., 2007; Liu et al., 2008; Ryoo et al., 2008; Ryoo et al., 2007; Woods et al., 2001). Four, increased dosage of DYRK1A induces an imbalance of Tau isoforms by phosphorylation of the splicing factor ASF (Shi et al., 2008). Finally, DYRK1A has been shown to phosphorylate key molecules in neurodegenerative processes such as Parkinson's disease and Huntington's disease including septin 4 (Sitz et al., 2008), α-synuclein (Kim et al., 2006a) or the huntingtin interacting protein Hip-1 (Kang et al., 2005).

In humans, *DYRK1A* truncating mutations result in intrauterine growth retardation, microcephaly and developmental delay (Fujita et al., 2010; Moller et al., 2008). Additionally, the potential participation of DYRK1A in other pathologies such as cardiac hypertrophy, bone homeostasis or tumor growth has also been suggested (Baek et al., 2009; Kuhn et al., 2009; Lee et al., 2009; Raaf et al., 2009).

All these data suggest that DYRK1A may participate in different cellular processes and signal transduction pathways that have an impact in CNS development. An interacting screen with DYRK1A identified Nemo-like kinase (NLK) and an overview on the current knowledge on this kinase follows. The results obtained during the investigation of the functional interaction between DYRK1A and NLK led us to hypothesize the involvement of DYRK1A in the Wnt signaling pathway. Therefore, a brief summary on aspects of the Wnt signaling pathway relevant for this work is also included.

Nemo-like kinase (NLK)

The protein kinase NLK was first identified in *Drosophila* as *nemo*, and described as a gene required for proper photoreceptor cells rotation during ommatidia morphogenesis in the eye (Choi and Benzer, 1994). An ortholog of NLK, known as LIT-1, was later on identified in *C. elegans* as a gene product that regulates asymmetric cell division in the early embryo and antagonizes the Wnt-β-catenin signaling activity (Kaletta et al., 1997; Meneghini et al., 1999). All multicellular eukaryotes contain only a single functional *Nlk* gene (Brott et al., 1998). However, in rodent genomes the existence of two evolutionarily not conserved *Nlk* homologs has been reported: a predicted retrotransposed *Nlk2* gene encoding a non-functional NLK with a deletion within the kinase domain (Katoh, 2005) and a transcriptionally silent processed Nlk pseudogene (Kortenjann et al., 2001).

Human NLK is a 527-amino acid protein with a central kinase domain. The N-terminal sequence, which is enriched in alanine, glutamine, proline and histidine residues, is poorly conserved among NLK orthologues and its function remains obscure. The C-terminal extension is conserved from *C. elegans* to human and it has been suggested that may contribute to the interaction of the kinase with specific substrates or targets (Ishitani et al., 1999; Yamada et al., 2003; Yamada et al., 2006).

Regulation of NLK expression

NLK is expressed ubiquitously in fetal and adult tissues as a unique mRNA (Brott et al., 1998; Harada et al., 2002). Studies in *Drosophila* have shown that Wnt-β-catenin signaling enhances the transcription of *nemo,* which is induced only upon high levels of Wnt (Zeng and Verheyen, 2004). Several dTCF binding sites are found in the 5'-region of the *nemo* gene that may represent enhancer elements. These observations have led to propose a negative feedback circuit in which Wnt induces expression of its own antagonist *nemo*. In the sea urchin embryo, *nlk* is a transcriptional target of Delta/Notch signaling (Rottinger et al., 2006). In mammals, it is not known yet how NLK is regulated at the transcriptional or post-transcriptional level. However, NLK has been described as a target of miRNA-181 (Ji et al., 2009) and to be ubiquitinated and respond to the proteasome inhibitor MG-132 (Zhou et al., 2007).

The subcellular localization of NLK

The subcellular localization of NLK seems to respond to extracellular stimuli based on the only study analyzing the subcellular localization of endogenous NLK: under normal growing conditions, NLK accumulates in the cytoplasm of PC12 cells, but it translocates to the nucleus and leading edges upon stimulation of neuronal differentiation with NGF. When exogenously expressed, NLK localizes predominantly in the nucleus (Brott et al., 1998; Kanei-Ishii et al., 2004), and accumulation in perinuclear compartments has been also observed (Ishitani et al., 2009; Kim et al., 2010; this thesis work). Once in the nucleus, NLK localizes in nuclear speckles through its histidine-rich segment, similarly to DYRK1A and other histidine repeats-containing proteins (Salichs et al., 2009). NLK does not appear to possess a basic sequence that might clearly be identified as a NLS, and thus it has been suggested that it might complex with other proteins for its nuclear translocation, as it has been described for some MAPKs (Fukuda et al., 1997). Furthermore, it is not known whether activation of NLK influences its cellular distribution, although work on the *C. elegans* orthologous LIT-1 has shown that the nuclear levels of the kinase increase in response to Wnt activation (Lo et al., 2004).

Mechanism of activation of NLK

NLK belongs to the MAPK family within the CMGC group of protein kinases (Manning et al., 2002) (Fig. I10). One distinctive feature of MAPKs is the presence of a TXY motif in the activation loop, which is the site for the activating phosphorylation by the MAPKK family members. In NLK a glutamic acid residue replaces the tyrosine (TQE), and thus it is considered an atypical MAPK (Coulombe and Meloche, 2007). Nevertheless, it is predicted that NLK is regulated by phosphorylation of its activation loop Thr298. Mutation of Thr298 abolishes the ability of NLK to autophosphorylate, indicating that activation loop phosphorylation is necessary for its activity

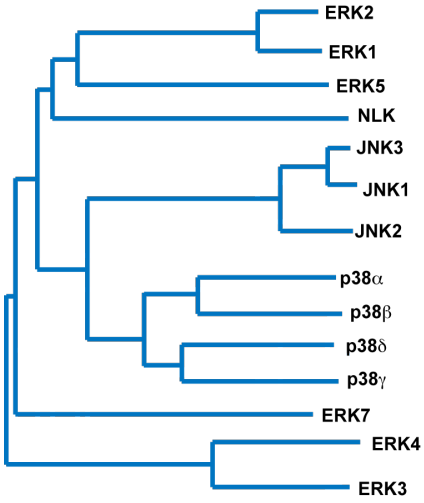

Figure I10: The MAPK family. Unrooted phylogenetic tree showing the evolutionary relationship of MAPKs.

(Brott et al., 1998; Kanei-Ishii et al., 2004). However, and although the residue has been detected as phosphorylated *in vivo* (Phosphosite database), there is no data supporting that the phosphorylation is required for the *in vivo* activation. There are very few phosphosites described for NLK (Table I1), so it is difficult to define a consensus phosphorylation site. Nonetheless, several of the NLK phosphorylation sites identified to date are followed by a proline (Table I1), suggesting that NLK has proline-directed specificity like conventional MAPKs.

Table I1: List of NLK substrates in which the phosphorylation sites have been identified. The substrates are mouse or human proteins, except ***a*** (*D. melanogaster*) and ***b*** (*X. laevis*).

Substrate	Phosphorylation site	Reference
TCF-4	HPL**T**^{178}P, EHF**T**^{189}P	(Ishitani et al., 2003)
LEF-1	HPL**T**^{155}P, EHF**S**^{166}P	(Ishitani et al., 2003)
STAT3	LPM**S**^{727}P	(Ohkawara et al., 2004)
c-Myb	15 S/TP	(Kanei-Ishii et al., 2004)
Mad[a]	SFT**S**^{25}P	(Zeng et al., 2007)
MEF2A[b]	PLA**T**^{310}P, GFT**S**^{353}P	(Satoh et al, 2007)
SETDB1	SEE**T**^{976}P	(Takada et al., 2007)
Paxillin	KQK**S**^{126}A	(Ishitani et al., 2009)
FOXO1	8 S/TP	(Ishitani et al., 2009)
FOXO4	6 S/TP and 22 S/TX	(Szypowska et al., 2010)
SMAD4	ITN**T**^{9}P RVV**S**^{138}P	(Shi et al., 2010)

NLK is activated by various extracellular ligands, such as the Wnt ligand Wnt-1, the cytokines interleukin-6 and granulocyte colony-stimulating factor, transforming growth factor-β (TGF-β), NGF and EGF (Ishitani et al., 2009; Kanei-Ishii et al., 2004; Kojima et al., 2005; Ohkawara et al., 2004; Smit et al., 2004), but in most cases the elements of the MAPK signaling cascade have not been clearly elucidated. Moreover, in certain cell types, elevation of intracellular Ca^{2}+ is sufficient to stimulate NLK enzymatic activity, by a mechanism dependent on Ca^{2}+/calmodulin-dependent protein kinase II activation (Ishitani et al., 2003). For several of the extracellular ligands, the MAPKKK TGF-β-activated kinase 1 (TAK1) is involved in NLK activation (Ishitani et al., 1999; Meneghini et al., 1999; Ohkawara et al., 2004; Shin et al., 1999; Smit et al., 2004). However, TAK1 cannot directly interact with NLK (Kanei-Ishii et al., 2004; Kojima et al., 2005), and it is unclear whether an intermediate kinase is functioning between the MAPKKK TAK1 and the MAPK NLK. In this regard, HIPK2, a DYRK kinase belonging to the HIPK subfamily, was shown to interact with and phosphorylate NLK *in vitro* (Kanei-Ishii et al., 2004). The HIPK2 phosphorylation

site(s) on NLK has not been identified and it is not known whether HIPK2 directly phosphorylates NLK in the activation loop or induces its autophosphorylation. Recently, TAK1 binding protein 2 (TAB2) was found to directly interact with NLK and function as a scaffold protein to facilitate TAK1-dependent NLK activation (Li et al., 2010b; Takada et al., 2007), and therefore it is possible that in certain situations an intermediate kinase would not be required.

The existence of other NLK activating kinases is inferred from several reports as in the case of the NLK-dependent repression of Nurr1 activity, which does not depend on TAK1 (Saijo et al., 2009). In this line, the MAPK p38β has been identified as an activator of NLK in *Xenopus* oocytes. p38β, or p38α but not δ/γ, regulates the function of NLK via phosphorylation of two evolutionarily conserved serine residues outside the catalytic domain (Ohnishi et al., 2010). Given that p38β can be activated by TAK1 (Ninomiya-Tsuji et al., 1999; Wang et al., 2001), it is therefore possible that this mechanism is used as an alternative to TAK1 directed phosphorylation via TAB2 recruitment.

Physiological functions of NLK

NLK/Nemo has been suggested to be a very important regulator of cell growth, patterning, and death based on the phenotype of loss of function mutants. In fact, loss of NLK/Nemo results in significant embryonic lethality in *C. elegans* (Rocheleau et al., 1999), *Drosphila* (Mirkovic et al., 2002), and mice (Kortenjann et al., 2001) and in several defects during development, mostly related with processes in which regulation of asymmetry is required (Table I2).

Mice with a targeted disruption of *Nlk* have been generated (Kortenjann et al., 2001). The phenotype of $Nlk^{-/-}$ mice is modulated by the genetic background; whereas NLK-null mice die during the third semester of pregnancy in a C57BL/6 background, mutant mice bred to a 129/Sv background survive for up to 4–6 weeks. These mutant mice exhibit growth retardation and suffer from neurological abnormalities. The Nlk deficiency includes aberrant differentiation of bone marrow stromal cell with increased number of adipocytes, large blood sinuses and absence of bone-lining cells in the bone marrow.

Table I2: Summary of phenotypes described in *NLK* deletion mutants. The phenotypes of the *NLK* null mutants in different organisms is presented.

Organism	Phenotype	Reference
C. elegans	Defects in asymmetric cell divisions during embryogenesis	(Kaletta et al., 1997)
	Embryonic lethality	(Rocheleau et al., 1999)
	Loss of endoderm	(Rocheleau et al., 1999)
	Defects in anterior-posterior asymmetry in intestinal twist	(Hermann et al., 2000)
	Defects in basement membrane invasion	(Matus et al., 2010)
Drosophila	Eye and wing defects	(Choi et al., 1994)
	Embryonic lethality	(Verheyen et al., 2001)
	Head defects	(Mirkovic et al., 2002)
	Altered patterns of apoptosis	(Mirkovic et al., 2002)
	Synaptic growth defects at the neuromuscular junction	(Merino et al., 2009)
	Patterning defects in cuticle	(Braid et al., 2010)
Zebrafish	Defects in ventrolateral mesoderm formation	(Thorpe et al., 2004)
Xenopus	Defects in patterning of the midbrain	(Thorpe et al., 2004)
	Defects in neurogenesis	(Ishitani et al., 2010)
	Inhibition of mesoderm induction	(Ohkawara et al., 2004)
	Severe defects in anterior development	(Satoh et al., 2007)

NLK as a regulator of signaling pathways

Several substrates of NLK have been identified in the recent years (Table I3). Among them, transcription factors are highly represented. Some of the substrates are known to be involved in signaling pathways and a summary of the involvement of NLK in these signaling pathways follows.

NLK negatively regulates Wnt-β-catenin signaling by inactivating the transcriptional unit composed of β-catenin/TCF/LEF (Ishitani et al., 1999). NLK phosphorylates LEF-1 and TCF-4, which results in the inhibition of TCF/LEF binding to DNA (Ishitani et al., 1999). Moreover, TCF/LEF phosphorylation by NLK triggers their ubiquitination and subsequent degradation dependent on the E3 ubiquitin-ligase NARF (Yamada et al., 2006). NLK also induces the nuclear accumulation of a deubiquitinating enzyme, Ubiquitin specific protease 4 (USP4), which interacts with a subpopulation of post-translationally modified TCF4 and represses β-catenin/TCF-dependent transcription (Zhao et al., 2009). In *C. elegans*, LIT-1 (NLK orthologue) - induced POP-1 (TCF orthologue) phosphorylation leads to POP-1 interaction with PAR-5 (14-3-3 orthologue) and subsequent POP-1 nuclear export (Lo et al., 2004), rather than inhibiting its DNA binding capability or inducing its degradation. Therefore, the signaling complexes in which NLK participates might differ between species.

Table I3: List of NLK interactors. ***a***, interaction/phosphorylation described in mammals; ***b***, interaction/phosphorylation described in *Xenopus*; ***c***, interaction/phosphorylation described in *Drosophila*; ***d***, interaction/phosphorylation described in *C. elegans;* ***e***, involves target phosphorylation by NLK.

Interactor	Activity	Effect on target	Functional output	References
Androgen Receptor[a]	Nuclear receptor	n.d.	Decrease AR-transcription	(Emami et al., 2009)
CBP/p300[a]	Transcription factor	Inhibition of CBP co-activator activity[e]	Inhibition of CBP-transcription (NF-κB, AP-1, Smad, p53)	(Yasuda et al., 2004)
CHD7[a]	Chromodomain ATPase	n.d.	Inhibition of PPARγ-transcription; induction of osteoblastogenesis	(Takada et al., 2007)
Cul1[a]	E3 ubiquitin ligase (SCF compex)	n.d.	Enhance c-Myb degradation	(Kanei-Ishii et al., 2008)
FOXO1[a]	Transcription factor	Increase nuclear export[e]	Increase nuclear export[e]	(Kim et al., 2010)
Fbxw4/5[a]	E3 ubiquitin ligase (SCF compex)	n.d.	n.d.	(Kanei-Ishii et al., 2008)
HMG2L1[b]	Transcription factor	n.d.	n.d.	(Yamada et al, 2003)
LEF-1[a,c,d]	Transcription factor	Increase degradation[e]	Inhibition of canonical Wnt	(Ishitani et al., 2003)
Mad[c]	Transcription factor	Promotes nuclear export[e]	Inhibition of BMP-dependent wing development	(Zeng et al., 2007)
MAP1B[a]	Cytoskeleton regulation	Unknown[e]	NGF-induced neurite outgrowth	(Ishitani et al., 2009)
MEF2A[a,b]	Transcription factor	Increase in transcriptional activity[e]	Development of anteroneural structures[e]	(Satoh et al., 2007)
A-Myb[a]	Transcription factor	Inhibition of association with CBP[e]	Decrease A-Myb trans-activation	(Kurahashi et al., 2005)
c-Myb[a]	Transcription factor	Increase interaction with Fbxw7[e]	Increase in degradation	(Kanei-Ishii et al., 2004; 2008)
NARF[a,b]	E3 ubiquitin ligase	n.d.	Increase TCF/LEF ubiquitination	(Yamada et al., 2006)
Paxillin[a]	Focal adhesion regulation	Unknown[e]	NGF-induced re-distribution of F-actin	(Ishitani et al., 2009)
PPAR-γ[a]	Nuclear receptor	n.d.	Inhibition of PPARγ-transcription; induction of osteoblastogenesis	(Takada et al., 2007)
Notch1ICD[a]	Transcription factor	Reduction of the Notch1ICD-CSL-Mastemind complex[e]	Inhibition of Notch1-transcription; inhibition of neurogenesis[e]	(Ishitani et al., 2010)
Notch3[a]	Transcription factor	n.d.[e]	Activation of Notch3-dependent	(Ishitani et al., 2010)
Nurr1[a]	Nuclear receptor	Increase binding to CoREST repressor[e]	Inhibits Nurr1-repression upon LPS stimulus	(Saijo et al., 2009)
SMAD4[a]	Transcription factor	n.d.[e]	n.d.	(Shi et al., 2010)
SETDB1[a]	Histone methyltransferase	Assembly of the repressive complex SETDB1-CHD7-PPARγ[e]	Inhibition of PPARγ-transcription; induction of osteoblastogenesis	(Takada et al., 2007)
Skp2[a]	E3 ubiquitin ligase (SCF compex)	n.d.	n.d.	(Kanei-Ishii et al., 2008)
Sox11[b]	Transcription factor	n.d.	n.d.	(Hyodo-Miura et al., 2002)
STAT3[a,b]	Transcription factor	Increase transcriptional activation[e]	Scaffold in IL-6 activation of NLK; mesoderm induction[b]	(Ohkawara et al., 2004; Kojima et al., 2005)
TCF-4[a,c,d]	Transcription factor	Inhibition of β-catenin/TCF-4 DNA binding[e]; increase degradation[e]; increase cytoplasmic TCF[d]	Inhibition of canonical Wnt	(Rocheleau et al., 1999; Ishitani et al., 1999; Ishitani et al., 2003; Yamada et al., 2006)
USP4[a]	Deubiquitinase	Increase in nuclear localization[e]	Repression of Wnt signaling	(Zhao et al., 2009)

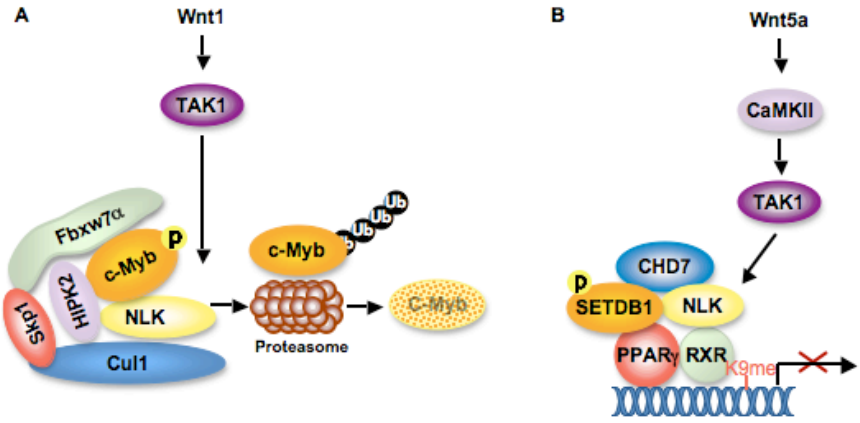

Figure I11: Functional activities of NLK. Schematic representation of the protein complexes in which NLK participates. **(A)** The interactions among c-Myb, HIPK2, NLK, and each component of the SCF complex are shown schematically. The assembly of the complex leads to c-Myb degradation. **(B)** Stimulation of Wnt non-canonical signaling cascade results in activation of NLK, phosphorylation of SETDB1 and assembly of an active histone H3K9 methyl transferase complex. For details on the NLK activity on these pathways, see the text.

NLK phosphorylates the Myb family members c-Myb and A-Myb at multiple sites acting as a negative regulator (Kanei-Ishii et al., 2004; Kurahashi et al., 2005) (Fig. I11A). In response to Wnt-1, c-Myb is degraded and the effect involves TAK1, HIPK2, and NLK. NLK directly binds c-Myb, which results in the phosphorylation of c-Myb at multiple sites, and induces its ubiquitination and proteasome-dependent degradation. Molecularly, this is explained because the NLK-dependent phosphorylation of c-Myb enhances its interaction with Fbxw7α, an E3 ubiquitin-ligase (Kanei-Ishii et al., 2008). NLK and HIPK2 directly interact with components of the SCF complex (Table I3), suggesting that these kinases may participate in the degradation of other proteins mediated by the SCF complexes (Kanei-Ishii et al., 2008). In the case of A-Myb, NLK inhibits A-Myb activity by blocking the interaction between A-Myb and CBP and inducing the methylation of histone H3 at Lys9 (Kurahashi et al., 2005). In this context, NLK also inhibits peroxisome proliferator-activated receptor (PPAR)-γ activity by binding and phosphorylating a histone methyltransferase, SET domain bifurcated 1 (SETDB1), which leads to methylation of histone H3 at Lys9 at PPAR-γ target gene promoters (Takada et al., 2007) (Fig. I11B). These findings suggest that histone modification might be another way that NLK uses to control target gene expression.

NLK has also been found to inhibit Notch1 ICD in its ability to form a transcriptionally active complex (Ishitani et al., 2010), which has been found to be important in the regulation of zebrafish neurogenesis. By contrast, during early

development of the sea urchin embryo, *nlk* and Delta, a Notch receptor ligand, strongly synergize during mesoderm formation through down-regulation of TCF (Rottinger et al., 2006). Therefore, the role of NLK in the regulation of the Notch signaling pathway is not clear yet.

NLK and disease

As NLK negatively regulates the Wnt-β-catenin signaling pathway, it is predicted to act as a tumor suppressor. In fact, several observations support this role. First, NLK expression is decreased in prostate cancer metastases in comparison to normal prostate epithelium (Emami et al., 2009) and in some hepatocellular carcinomas (Ji et al., 2009). In this case, up-regulation of microRNA-181, which targets NLK, appears to be responsible (Ji et al., 2009). Second, NLK suppresses cell growth in human colon carcinoma cells (DLD-1) (Yasuda et al., 2003) and induces apoptosis in prostatic tumor cells (Emami et al., 2009). In fact, the involvement of NLK in the induction of apoptosis has been also suggested by studies in *Drosophila* (Mirkovic et al., 2002). However, other authors have found quite opposite results regarding induction of apoptosis. A large-scale RNAi screen to identify human kinases that regulate cell survival and apoptosis identified NLK as one of the most potent survival kinase (MacKeigan et al., 2005). In agreement with this antiapoptotic role, NLK negatively regulates FOXO1 (Kim et al., 2010), a known activator of the expression of target genes involved in apoptosis (Fu and Tindall, 2008). Therefore, and in line with these findings, results that link NLK to tumor progression have been found by other groups. Up-regulation of NLK has been observed in hepatocellular carcinoma and targeted-disruption of NLK suppressed cell growth and arrested cell cycle (Jung et al., 2010). Additionally, NLK appears to be required for invasion in breast carcinoma cells (Matus et al., 2010). In conclusion, further work needs to be done to have a clearer picture of the role of NLK in tumor progression.

Wnt signaling pathway

Wnt proteins are soluble molecules that mediate intracellular signaling pathways involved in the control of a wide variety of cellular processes such as cell proliferation, cell polarity, survival, migration and adhesion and as such is crucial for normal embryonic development, organized cell movements, establishment of tissue polarity, morphogenesis and patterning, and tissue homeostasis in various systems, including the nervous system, the immune system and the bones. Mutations in the Wnt pathway are often linked to human birth defects, cancer and degenerative diseases. The importance of the pathways is reflected in the many recent reviews that can be found on the subject in the literature as for instance (Angers and Moon, 2009; Clevers, 2006; Huang and He, 2008; Ille and Sommer, 2005; Krishnan et al., 2006; MacDonald et al., 2009; Moon et al., 2004; Nusse, 2008; Reya and Clevers, 2005; Staal et al., 2008; van Amerongen and Nusse, 2009).

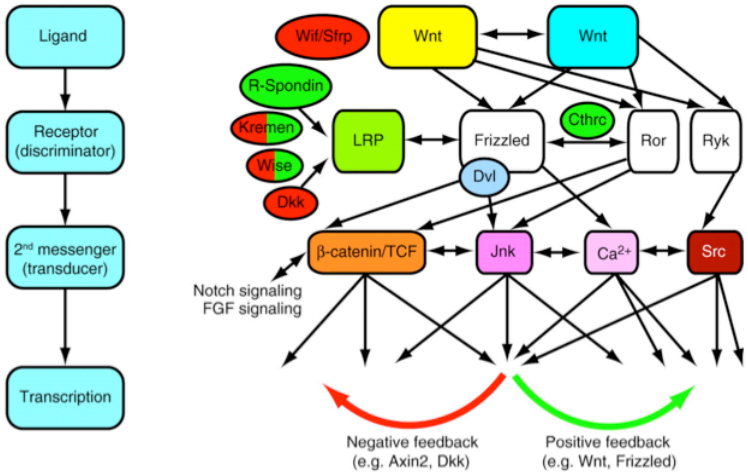

Figure I12: The Wnt signal transduction network. The mammalian genome, encodes 19 different Wnt ligands. Multiple receptor homologs (ten Frizzled receptor homologs in mammals), different receptor families and additional co-receptors further diversify the signal transduction cascade. Signals can branch off at virtually every step, modifiers can represent a parallel input that affects the outcome of signal transduction independently of extracellular ligand stimulation, intense cross-talk (depicted by double-headed arrows) exists between different signaling cascades, and feedback mechanisms provide an additional layer of control. (Adapted from van Amerongen et al., 2009).

As in other signal transduction pathways, the Wnt pathway consists in three main elements: the extracellular ligands - Wnts -, the membrane receptors - the Frizzled (Fz or Fzd) receptors and the low-density lipoprotein (LDL) receptor-related proteins 5 and 6 (LRP5 and LRP6) -, and a group of intracellular proteins in charge of transducing the signal, including specific transcription factors - a heterodimer of β-catenin with the T cell factor/lymphoid enhancer factor (TCF/LEF) family of proteins -

responsible for the induction of the expression of the target genes (Fig. I12) (a good source of information for all the components of the Wnt signaling pathway is the Wnt Homepage at Stanford University maintained by the Nusse's group: www.stanford.edu/~rnusse/wntwindow.html). Given that the Wnt pathway has been so extensively studied, this section does not intend to be a thorough review, but just offer a short overview on specific aspects of the pathway that are relevant for this thesis project and will provide references for Reviews on each of them.

Wnt ligands, biogenesis and extracellular transport

Wnts are secreted signaling molecules that are conserved in all metazoan animals, of which 19 different proteins are found in humans (a description, including the phenotypes of loss-of-function mouse models, is found at the Wnt Homepage: www.stanford.edu/~rnusse/wntgenes/humanwnt.html). Wnts are cysteine rich, glycosylated and lipid-modified proteins of approximately 350-400 amino acids that contain an N-terminal signal peptide for secretion. The post-translational modifications occur in the endoplasmic reticulum (ER) and the proteins are secreted via the Golgi apparatus and dedicated secretory vesicles (Fig. I13). Wnt secretion is a complex and highly regulated process that influences the spreading and signaling activity of Wnt (for recent reviews see Bartscherer and Boutros, 2008; Hausmann et al., 2007; Lorenowicz and Korswagen, 2009). Studies in *Drosophila* and in *C. elegans* have identified several molecules that regulate Wnt biogenesis and secretion such as Porcupine, a multipass transmembrane ER protein with acyl-transferase activity involved in the post-translational modifications of Wnts (Takada et al., 2006), and Wntless (Wls or Gpr177), a multipass transmembrane protein that localizes to the Golgi, endocytic compartments and the plasma membrane and is in charge to escort Wnts from the Golgi to the plasma membrane for secretion. Wls is recycled by endocytosis and trafficked back to Golgi by the retromer complex (Hausmann et al., 2007).

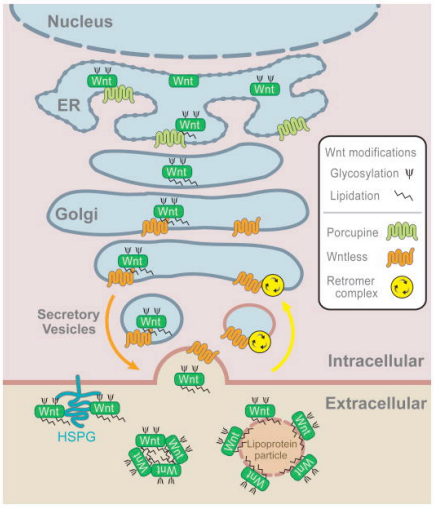

Figure I13: Wnt biogenesis and secretion. See the text for explanations (from MacDonald et al., 2009).

To establish morphogenetic gradients, Wnt molecules have to move from the secretory site to the target cells. Recently, large particles called lipoprotein particles have been implicated in moving Wnts and other lipid-modified proteins such as Hedgehog (Panakova et al., 2005). The retromer complex appears to promote the association of secreted Wnts with lipoprotein particles on the extracellular face of cells (Coudreuse et al., 2006; Prasad and Clark, 2006). Wnts may also form multimers to bury lipid modifications inside (Katanaev et al., 2008). It have been speculated that lipoprotein particles and multimers may be involved in long-range signaling, while acylated Wnt binding to membranes might act in short-range signaling.

Receptors dictate Wnt activity

The high degree of conservation and evolutionary constraint of Wnt proteins suggests that each Wnt is likely to have a specific function. In mammals, complexity and specificity in Wnt signaling are, in part, achieved through 19 Wnt ligands and 10 Fzd receptors, and, in theory, 190 potential Wnt-Fzd combinations exist. The complexity increases, because activation of some, but not all, Wnt pathways requires co-receptors such as LRP5 and LRP6 (Fig. I12).

Fzd proteins are seven-pass transmembrane receptors that contain a large extracellular domain with a conserved motif comprised of 10 cysteine residues called the cysteine-rich domain (CRD). The CRD domains from various Fzd receptors have been shown to bind multiple Wnts with high affinity (reviewed in Schulte and Bryja, 2007; Wang et al., 2006). Following Wnt binding, it is thought that Fzds form a co-receptor complex with LRP proteins, single-pass transmembrane proteins with a relatively small intracellular domain and a large extracellular domain containing several potential protein interaction domains. At the cytoplasmic side, Fzds interact directly with the Dishevelled protein, a known mediator of Wnt signaling (reviewed in Gao and Chen, 2010). The Axin protein, a negative regulator of Wnt signaling, binds to the cytoplasmic tail of LRP6, providing a mechanism by which Axin is released from β-catenin and inducing β-catenin accumulation (see below). The binding of Axin to the LRP6 tail is promoted by phosphorylation of LRP6 on several clusters of serines and threonines, with a central PPPSP motif that is phosphorylated by GSK3 (Zeng et al., 2005).

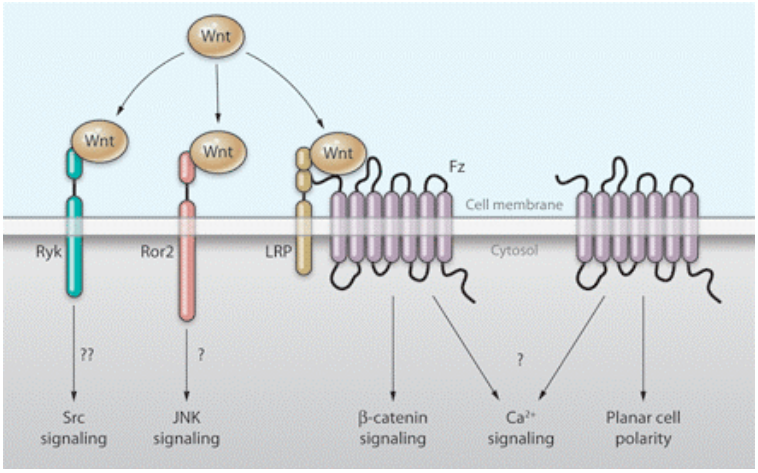

Figure I14: Current model of receptor-dependent Wnt signaling. See the text for explanations (from van Amerongen et al., 2008).

Historically, Wnt-Fzd complexes have been divided into “canonical” (Wnt1, Wnt3A, or Wnt8) and “non-canonical” (Wnt5A or Wnt11) classes, which activate β-catenin-dependent and -independent signaling pathways, respectively. However, several experimental evidences indicate that there is a cross-talk between different members of the two classes (for a recent review van Amerongen et al., 2008), thus, the subdivision of Wnts into these two categories is not completely right. Instead, the group of R. Nusse and others propose that Wnts themselves are not intrinsically canonical or non-canonical but determined by distinct sets of receptors (Liu et al., 2005; van Amerongen et al., 2008). According to this, the following signaling pathways are distinguished: Wnt-β-catenin signaling, Fzd-planar cell polarity (PCP) signaling, Wnt-Ca^{2+} signaling, Wnt-Ryk signaling and Wnt-Ror2 signaling (Fig. I14). Given that this thesis project has only explored the relationship of DYRK1A with Wnt signaling depending on β-catenin, a summary on this specific pathway follows. Recent reviews on the Fzd-PCP signaling pathway can be found in Seifert and Mlodzik (2007) and Wang and Nathans (2007), on the Wnt-Ca^{2+} signaling in Kohn and Moon (2005), on the Wnt-Ryk signaling in Fradkin et al., (2010) and Hendrickx and Leyns (2008), and on the Wnt-Ror2 signaling in Minami et al., (2010).

Wnt-β-catenin signaling

This signaling cascade has been broadly studied due to its importance not only in metazoan development, but also in degenerative diseases and cancer (Clevers,

2006; Polakis, 2000). In the vertebrate nervous system it is involved in cell fate decisions and possibly synaptogenesis. In addition, Wnt signaling has been shown to regulate the cytoskeleton through a pathway that diverges downstream of GSK-3β. Inhibition of the phosphorylation of some GSK-3β substrates such as microtubule-associated protein 1B (MAP1B) changes the organization of microtubules and increases microtubule stability (Ciani et al., 2004).

In the absence of Wnt, cytoplasmic β-catenin is constantly degraded by the action of the Axin complex, which is composed of the scaffolding protein Axin, the tumor suppressor *adenomatous polyposis coli* gene product (APC), CK1 and GSK3. CK1 and GSK3 sequentially phosphorylate the N-terminal region of β-catenin, resulting in its recognition by β-Trcp, an E3 ubiquitin ligase subunit, and subsequent β-catenin ubiquitination and proteasomal degradation (Su et al., 2008). This continual β-catenin elimination prevents β-catenin from reaching the nucleus, and Wnt target genes are thereby repressed by the DNA-bound TCF/LEF family of proteins. Upon activation, the inhibition of Axin-mediated β-catenin phosphorylation leads to the stabilization of β-catenin, which accumulates and travels to the nucleus to form complexes with TCF/LEF and initiates transcription of Wnt target genes (Fig. I15) (for a recent review, see MacDonald et al., 2009).

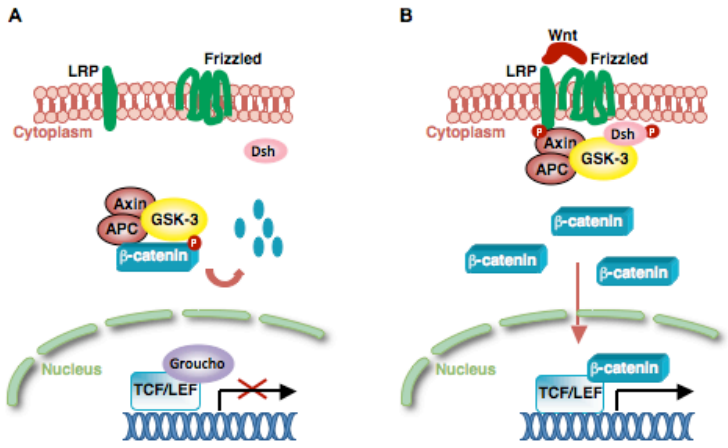

Figure I15: Schematic representation of the Wnt-β-catenin signaling pathway. In **A)** the pathway is represented in the absence of Wnt signaling, whereas in **B)** the active pathway is depicted. See text for details.

Moreover, β-catenin/TCF form multiple protein complexes with either Wnt pathway inhibitors, such as ICAT and Chibby, or transcriptional co-activators, including BCL9/BCL9-2, CBP/p300, pygopus, Brg-1, Pontin-52, MED12 and

parafibromin/Hyrax (Mosimann et al., 2009; Willert and Jones, 2006). Numerous β-catenin/TCF target genes have been identified in diverse biological systems and the majority of the target genes appear to be cell type specific (Logan and Nusse, 2004; Vlad et al., 2008). An emerging feature is that Wnt signaling components, including Fzd, LRP6, Axin2, NLK, and TCF/LEF, are often regulated positively or negatively by TCF/β-catenin (for an updated overview see the Wnt homepage).

The majority of β-catenin in the cell is associated with adherens junctions, where it interacts with the cytoplasmic region of cadherin, and only a small and dynamic pool of β-catenin in the cytosol and nucleus is responsible for the transduction of Wnt signals. β-catenin has a central armadillo repeat domain composed of 12 armadillo repeats, an N-terminal domain that harbors the binding site for α-catenin as well as the GSK3 and CK1 phosphorylation sites that are recognized by the β-TrCP ubiquitin ligase (see Table I4 for references), and a C-terminal domain with regulatory activities (Fig. I15). The N- and C-termini were suggested to directly bind the armadillo repeats and regulate β-catenin interaction with certain ligands (Castano et al., 2002; Cox et al., 1999). However, it has been recently shown that the termini remain unstructured, and speculated that the terminal regions may effectively shield the armadillo repeats from nonspecific interactions (Xing et al., 2008). Crystal structures of several proteins in complexes with the β-catenin armadillo repeat have revealed that numerous β-catenin-binding partners have overlapping binding sites in the armadillo repeat domain (Fig. I16). Therefore, competition between binding partners could be important for regulating the Wnt-β-catenin signaling pathway (Xu and Kimelman, 2007).

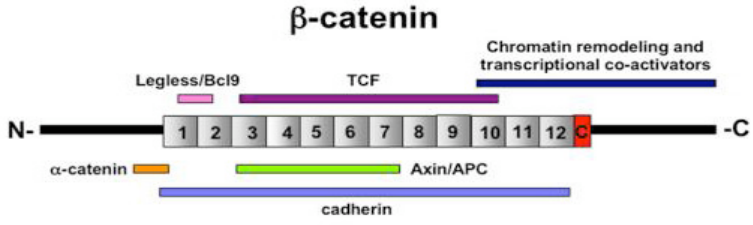

Figure I16: Primary structure of β-catenin. The binding regions for several of the β-catenin partners are shown (adapted from Gottardi and Peifer, 2008).

It is not well understood how β-catenin enters the nucleus, but it is postulated that β-catenin can mediate its own nuclear import through direct interaction with nucleoporins based on the fact that its armadillo repeat region resembles the HEAT

repeats found in the nuclear import factor importin-β (Suh and Gumbiner, 2003). β-catenin also exits the nucleus via export involving APC (Henderson and Fagotto, 2002), Axin (Cong and Varmus, 2004), and RanBP3 (Ran binding protein 3), which binds to β-catenin in a Ran-GTP dependent manner (Hendriksen et al., 2005). Thus β-catenin is thought to continually shuttle in/out of the nucleus, and interactions with either cytosolic or nuclear proteins ultimately influence the distribution of β-catenin.

β-catenin is tightly regulated by several post-translational modifications, including phosphorylation, ubiquitination and acetylation (a complete list on these modifications can be found at Phosphosite web page). Regarding phosphorylation, serine, threonine and tyrosine residues have been identified as phosphorylated, with many different functional outputs that include protein destabilization/stabilization, nucleocytoplasmic transport and interaction with partners, which could modulate β-catenin-mediated transcription in (Table I4).

Table I4: Summary of the phosphorylated sites found in β-catenin.

Residue	Protein kinase	Functional output	Reference
S33	JNK, GSK3	Promotes protein destabilization	(Liu et al., 2002; Hino et al., 2005)
S37	JNK, GSK3	Promotes protein destabilization	(Liu et al., 2002; Hino et al., 2005)
S41	JNK, GSK3	Promotes protein destabilization	(Liu et al., 2002; Hino et al., 2005)
S45	CK1, PKA, IKK	Promotes protein destabilization	(Amit et al., 2002; Liu et al., 2002; Hino et al., 2005)
Y64	PTK6	n.d.	(Palka-Hamblin et al., 2010)
Y86	Bcr-Abl	Promotes protein stabilization	(Coluccia et al., 2007)
Y142	Met receptor, PTK6	Promotes Bcl9-2 binding	(Brembeck et al., 2004; Palka-Hamblin et al., 2010)
S191	Cdk5	Binding to Pin1 and displacement of APC	(Munoz et al., 2007)
S246	Cdk5	Binding to Pin1 and displacement of APC	(Munoz et al., 2007)
T393	CK2	Promotes protein stability, interaction with Axin and transcriptional activity	(Song et al., 2003; Wu et al., 2009)
Y489	Abl	Decrease binding to N-cadherin, increase nuclear localization	(Rhee et al., 2007)
S552	AKT, PKA	Promotes β-catenin/TCF reporter activation	(Fang et al., 2007)
Y654	Met, Bcr-Abl	Impairs binding to Axin complexes, promotes nuclear translocation	(Coluccia et al., 2007)
Y670	Met	Promotes nuclear translocation	(Zeng et al., 2006)
S675	AKT, PKA	Promotes β-catenin/TCF reporter activation possibly through association with histone acetylases	(Fang et al., 2007; Taurin et al., 2006; Hino et al., 2005)
S718	PLK1	n.d.	(Arai et al., 2008)

The main partner for β-catenin in Wnt-dependent gene regulation is the TCF/LEF family of DNA-bound transcription factors (Arce et al., 2006; Hoppler and Kavanagh, 2007). While a single TCF gene is found in *Drosophila* and worm, four

TCF genes, TCF-1 (TCF7), LEF-1, TCF-3 (TCF7L1) and TCF-4 (TCF7L2), exist in mammals. Moreover, alternative splicing and promoter usage produce a large number of TCF variants with distinct properties (Arce et al., 2006; Hoppler and Kavanagh, 2007) (Fig. I17).

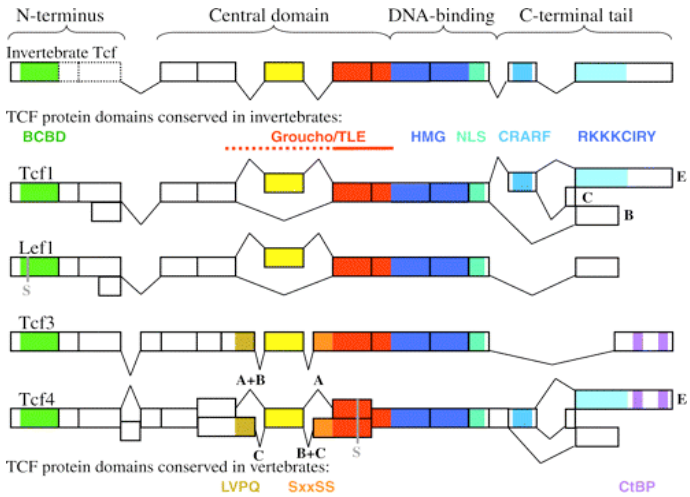

Figure I17: The structural variety of vertebrate TCF/LEFs. Schematic representation of the different TCF family members. The isoforms resulting from alternatively splicing events are also shown. BCBD: β-catenin binding domain; Groucho/TLE: Groucho/TLE-binding domain; HMG: high mobility group domain; NLS: nuclear localization signal; CRARF motif (in mid blue); RKKKCIRY motif (in light blue); LVPQ motif (in brown); SxxSS motif (in orange); CtBP: CtBp-binding domain; S in grey: sumoylation (adapted from Hoppler et al., 2007).

LEF/TCF recognition of DNA can occur independently of β-catenin but weakly and with only moderate specificity (reviewed by Arce et al., 2006). TCF represses gene expression by interacting with the repressor Groucho (TLE1 in human), which promotes histone deacetylation and chromatin compaction; furthermore, another co-repressor, CtBP, may bind directly to an alternative spliced variant of TCF-3 or TCF-4. Post-translational modifications of TCF/LEF exist including phosphorylation, acetylation, sumoylation, and ubiquitination/degradation (Arce et al., 2006; Hoppler and Kavanagh, 2007). For instance, and apart from NLK phosphorylation, TCF-3 phosphorylation by CK1ε and LEF-1 phosphorylation by CK2 enhance their binding to β-catenin and diminishes LEF-1 binding to Groucho/TLE. LEF-1 and TCF-4 sumoylation (by the SUMO ligase PIASy) represses LEF-1 activity by targeting it to nuclear bodies but enhances TCF-4/β-catenin transcription, while CBP-mediated acetylation of TCF results in decreased TCF/β-catenin-binding in *Drosophila* and increased TCF nuclear retention in nematodes, both leading to transcriptional repression.

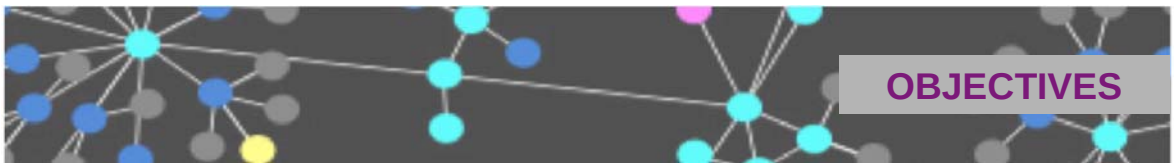

OBJECTIVES

This Thesis work is framed within the general objectives of the research group that try to elucidate the functional roles of the protein kinase DYRK1A as well as the mechanisms that regulate the activity of this protein kinase. An interacting screen for novel DYRK1A partners carried out in the group found the protein kinase NLK as a putative DYRK1A interactor. The interest to further study DYRK1A/NLK interaction was based in several pieces of information:

1.- NLK had been shown to interact with HIPK2, a relative of DYRK1A in the DYRK family of kinases, and HIPK2 acted as an NLK regulator. Thus, the possibility existed of DYRK1A acting as an NLK regulatory kinase.

2.- DYRK1A was known to be highly sensitive to gene dosage, and thus it was predictable that both its protein levels as well as its catalytic activity have to be tightly regulated. Results from the group indicated that DYRK1A is degraded by the proteasome, and it was known that NLK marks several of its substrates for proteasome-mediated degradation. Thus, the possibility existed of DYRK1A being a substrate of NLK and that NLK could regulate several aspects of DYRK1A biology.

3.- The biological activity of NLK was framed within the Wnt signaling pathway. DYRK1A was known to participate in several intracellular signaling pathways. Thus, the interaction with NLK could be a suggestion of DYRK1A being placed in the Wnt signaling pathway.

Therefore, the general objective of this thesis work has been to study the interaction between DYRK1A and NLK from a physical and functional viewpoint. Given that NLK is a regulator of Wnt/β-catenin signaling, the possible functional interaction of DYRK1A with the pathway was also proposed to be analyzed.

The particular objectives are detailed below.

I. To characterize the interaction of DYRK1A with the protein kinase NLK.
II. To elucidate the functional outcome of the interaction of DYRK1A with NLK: Is DYRK1A a substrate of NLK? If so, which aspects of the DYRK1A biology are affected by NLK? Catalytic activity? Protein stability?
III. To analyze the role of DYRK1A in the Wnt/β-catenin signaling pathway.

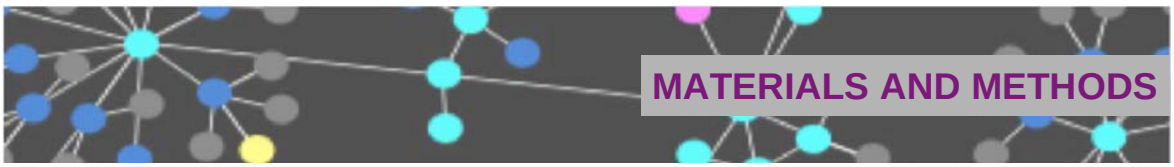

MATERIALS AND METHODS

1. PLASMIDS

In this Section, the construction of the plasmids generated during the thesis work is described in detail. It also includes the description and source of other plasmids used in some experiments. The sequence of oligonucleotides used for the mutagenesis or for PCR amplification of specific DNA fragments is listed in Annex 1. All constructs generated by mutagenesis/PCR were checked by DNA sequencing. The identity of the plasmids obtained from Addgene (www.addgene.org/pgvec1) or RZPD/ImaGenes (http://www.imagenes-bio.de/) was confirmed by DNA sequencing.

1.1 Backbone vectors

- pEGFP-C1 (Clontech)
- pcDNA-3 (Invitrogen)
- pcDNA-HA (de la Luna et al., 1999)
- pGEX-6P1 (Amersham Biosciences)

1.2 DYRK1A expression vectors

All the constructs used to express influenza virus hemagglutinin (HA)-tagged, enhanced green fluorescent protein (GFP)-tagged or glutathione-S-transferase (GST)-tagged DYRK1A wild-type or kinase-inactive versions, and the following deletion mutants (numbers indicate the amino acids included) have been already described (Alvarez et al., 2007; Alvarez et al., 2003): GFP-DYRK1A^{522}; GFP-DYRK1A/378-522; HA-DYRK1A^{664}; HA-DYRK1A^{588}; HA-DYRK1A^{522}; HA-DYRK1A^{474}; HA-DYRK1A^{377}; GFP-DYRK1A^{167}; GFP-DYRK1A^{127}; GFP-DYRK1A^{87}.

The following mutants have been generated by site-directed mutagenesis:

- pHA-DYRK1A$^{\Delta 70\text{-}104}$: Deletion of the indicated 35 aa in pHA-DYRK1A using oligonucleotide D1A/Δ70-104.
- pHA-DYRK1A$^{\Delta 105\text{-}125}$: Deletion of the indicated 21 aa in pHA-DYRK1A using oligonucleotide D1A/Δ105-125rev.
- pGFP-DYRK1A/378-522^{6A}: Substitution of Thr393, Thr422, Ser433, Thr436, Thr457 and Ser468 by Ala in pGFP-DYRK1A/378-522 using oligonucleotides D1A/T393A, D1A/T422A, D1A/S433A,T436A, D1A/T457A and D1A/S468A.
- pHA-DYRK1A^{6A}: Substitution of Thr393, Thr422, Ser433, Thr436, Thr457 and Ser468 by Ala in pHA-DYRK1A using oligonucleotides D1A/T393A, D1A/T422A, D1A/S433A,T436A, D1A/T457A and D1A/S468A.

- pHA-DYRK1A^{K179R,6A}: Substitution of Lys179 by Arg in pHA-DYRK1A^{6A} using oligonucleotide D1A/K179R.

1.3 Other DYRKs expression vectors

The plasmids to express HA- or GFP-tagged DYRK1B (human 629 aa isoform), DYRK2 (human 844 aa isoform), DYRK3 (human 612 aa isoform) and DYRK4 (Papadopoulos et al., 2010); human 520 aa isoform) and other mutant forms of DYRK1A have been generated by different members of the group.

1.4 NLK expression vectors

- pFlag-NLK: To generate an expression vector for human NLK Flag-tagged at its N-terminus, a *Bgl*II-*Kpn*I restriction fragment containing the human NLK open reading frame (ORF) from pGFP-NLK (Salichs et al., 2009) was ligated in-frame into pCMV-Flag, *BamH*I-*Kpn*I.
- pGST-NLK: To generate an expression vector for NLK GST-tagged at its N-terminus, a *Bgl*II-*EcoR*I restriction fragment containing the human NLK ORF from pGFP-NLK was ligated in-frame into pGEX-6P1, *BamH*I-*EcoR*I.
- pFlag-NLK^{K167M}: Substitution of Lys167 (within the conserved ATP-binding pocket) by Met in pFlag-NLK using oligonucleotide NLK-K167M.
- pFlag-NLK^{T298A}: Substitution of Thr298 (within the activation loop) by Ala in pFlag-NLK using oligonucleotide NLK-T298A.
- pFlag-NLK$^{\Delta 430-444}$: Deletion of 15 amino acids in the indicated position in pFlag-NLK using oligonucleotide NLKΔ430-444.
- pFlag-NLK^{C437Y}: Substitution of Cys437 by Tyr in pFlag-NLK using oligonucleotide NLK-C437Y.
- pFlag-NLK^{428}: Substitution of Glu429 by a Stop codon in pFlag-NLK using oligonucleotide NLK429/Stop-r.

1.5 β-catenin expression vectors

- pGST-βCat: mouse β-catenin ORF cloned into pGEX-6P3 was kindly provided by Antonio García de Herreros (Institut Municipal d'Investigació Mèdica, Barcelona, Spain).
- pβCat^{S33Y}: a mammalian cells expression vector for the mouse β-catenin mutant S33Y for was kindly provided by Antonio García de Herreros.

- pβCat^{S33Y,S129A}: Substitution of Ser129 by Ala in pβCat^{S33Y} using oligonucleotide mβcat-S129A.
- pβCat^{S33Y,S552A}: Substitution of Ser552 by Ala in pβCat^{S33Y} using oligonucleotide mβcat-S552A.
- pβCat^{S33Y,S675A}: Substitution of Ser675 by Ala in pβCat^{S33Y} using oligonucleotide mβcat-S675A.
- pβCat^{S33Y,S552,675A}: Substitution of Ser675 by Ala in pβCat^{S33Y,S552A} using oligonucleotide mβcat-S675A.

1.6 Other plasmids

- pCS2-Wnt-1-myc: to express mouse Wnt-1 Myc-tagged at the C-terminus (Addgene plasmid 16851; XE173) (Yang-Snyder et al., 1996).
- pUSE-Wnt3a-HA: to express mouse Wnt3a HA-tagged at the C-terminus, was kindly provided by Anna Bigas (IMIM, Barcelona, Spain).
- pCS2-Frz1: to express rat-frizzled-1 (Addgene plasmid 16821; XE41) (Yang-Snyder et al., 1996).
- pEGFP.C1-hTCF-4E-HA: to express E isoform of human TCF-4 GFP-tagged at the N-terminus and HA-tagged at the C-terminus, was kindly provided Antonio García de Herreros.
- pCMV-HIPK2: to express the protein kinase HIPK2. Mouse *Hipk2* full-length cDNA (Acc. No. BC031904) cloned into pCMV-SPORT6 (IMAGE clone: IRAVp968B0466D) was purchased from ImaGenes.
- pCMV-TCF-4: to express TCF4. Human *TCF4* full-length cDNA (Acc. No.: BC032656) cloned into pCMV-SPORT6 (IMAGE clone: IRATp970B1155D). It was purchased from the RZPD German Resource Center for Genome Research. It corresponds to a spliced variant of TCF4 that does not contain the LVPQ and the SxxSS motifs, and also lacks several conserved regions at the C-terminal tail such as the CRARF and the RKKKCIRY motifs and proposed binding sites for the CtBP co-repressor (Hoppler and Kavanagh, 2007).
- pCMV-VSV-G: to express the glycoprotein of the vesicular stomatitis virus (Addgene plasmid 8454) (Stewart et al., 2003).
- pCMVΔR8.91, lentivirus packaging construct (kindly provided by Cristina Fillat) (Zufferey et al., 1997).
- pLKO.1-puro control vector (Mission clone SHC001) and pLKO.1 shRNA hNLK

(Mission clone SH0111; two clones: 922s1c1, 1320s1c1) were purchased from Sigma.

- TOPFLASH reporter, a β-catenin/TCF reporter plasmid containing the *Firefly* luciferase gene under the control of three TCF-binding sites (Korinek et al., 1997) was kindly provided by Antonio García de Herreros.
- FOPFLASH reporter, a control luciferase reporter with the TCF/LEF sites of TOPFLASH reporter being mutated, was kindly provided by Antonio García de Herreros.
- pCMV-RNL, Renilla luciferase vector (Invitrogene).

2. TECHNIQUES FOR DNA MANIPULATION

2.1 DNA purification and sequencing

For small-scale purification, DNA was extracted from bacterial minicultures using the QIAGEN Plasmid Mini Kit (Qiagen) following manufacturer's instructions. Plasmid DNA purification for cell transfections was done by using the QIAGEN Plasmid Kit (Qiagen), following manufacturer's instructions.

DNA samples (500 ng/reaction) were sequenced at the Genomic Sequencing Service (Universitat Pompeu Fabra-PRBB, Barcelona) using the Big-Dye terminator 3.0 reactive (Applied Biosystems; 2 μl/reaction), 3.2 pmoles of primer (final vol, 10 μl), and the following PCR sequencing conditions: initial denaturation step (1 min, 94ºC) and 28 cycles of denaturation step (30 s, 95ºC), primer annealing (30 s, 55ºC) and extension step (4 min, 60ºC).

PCR reactions were purified using Sephadex G-50 (Pharmacia) columns. Briefly, 800 μl of Sephadex-G50 equilibrated in H_2O were added to a Centristep column and centrifuged for 1 min at 2,600*xg*. After discarding the supernatant, the column was washed with 10 μl of H_2O; the PCR reaction was added and recovered by centrifugation. Finally, DNAs were dried in a Speed-vac for 10 min without heat.

2.2 Cloning of a DNA fragment into an expression vector

In this section, all the procedures carried out to clone a DNA fragment into any of the expression vectors used are described. In general, these steps were followed:

1) PCR amplification of the DNA fragment of interest with specific primers, which also include restriction sites (see *2.2.1*).
2) Ligation into pGEM-T Easy vector (Promega), following manufacturer's instructions.
3) Transformation into competent bacteria (see *2.2.2*).
4) Colony screening by PCR, with appropriate primers, DNA miniprep preparation and sequencing of positive clones.
5) Digestion with restriction enzymes, elution of the DNA fragment and ligation into the expression vector digested with the same enzymes.
6) Transformation into competent bacteria.
7) Colony screening by PCR (see *2.2.3*).
8) DNA extraction and confirmation by restriction enzyme digestion and/or sequencing of the fusions.

When possible, DNA fragments were prepared by restriction enzyme digestion; in those cases, steps 1-5 were omitted.

2.2.1 PCR amplification

PCR reactions were carried out in a total volume of 25 μl with 1 ng of template DNA, 0.4 μM forward and reverse primers, 200 μM dNTPs, 0.5 μl Expand High Fidelity PCR System (Roche) and the following amplification conditions: initial denaturation step (1 min, 94ºC) and 30 cycles of denaturation step (30 s, 94ºC), primer annealing (30 s, Tm-5ºC), extension step (40 s, 72ºC), and final extension (7 min, 72ºC).

2.2.2 Transformation into competent Escherichia coli

All DNA transformations were done using the *E. coli* strain XL1-blue F' (supE44 hsdR17 recA1 endA1 gyrA46 thi relA1 lac- F' [proAB+ laclq lacZ DM15 Tn10 (tetr)]). Frozen competent cells were thawed and kept for 10 min on ice; 5 μl of each ligation were added to 45 μl of cells and kept for 15 min on ice. Cells were incubated for 90 s at 42^{o}C, put on ice for 5 min, resuspended in 200 μl of SOC media (20 g/l triptone, 5 g/l yeast extract, 10 mM NaCl, 10 mM $MgCl_2$, 10 mM $MgSO_4$, 20 mM glucose) and incubated for 45 min in a shaker at 37^{o}C. Finally, cells were plated on LB (Luria Broth medium)-agar plates containing antibiotics (ampicillin, 100 μg/ml; kanamycin, 30 μg/ml).

2.2.3 Colony screening by PCR amplification

Positive colonies were inoculated in 200 μl of LB + antibiotic and incubated for 45 min at 37°C. PCR reactions were performed as described (*2.2.1*) in a final volume of 10 μl, using 1 μl of bacterial culture.

2.2.4 Preparation of DNA fragments and ligation into the expression vector

DNA (2-20 μg) was digested with restriction enzymes (2-20 units) in a final volume of 100 μl (buffer conditions according to manufacturer's instructions) for 2 h at the recommended temperature for each enzyme. Reactions were loaded in Low Melting Agarose (ECOGEN) gels (1-2%, depending of the size of the fragment) – 1xTAE (2 mM Tris, 1 M acetic acid, 50 mM ethylendiamine tetracetic acid [EDTA]) – 0.1 μg/ml ethidium bromide gel and run in 1xTAE at 80 V. DNA was visualized with an ultraviolet transilluminator and the band of the expected molecular weight was cut.

To elute DNA, bands were processed as follows: agarose was melted for 10 min at 65°C, and NaCl plus EDTA were added to final concentrations of 100 mM and 10 mM, respectively. DNA was extracted by adding 1 vol of phenol (Sigma) and precipitated with 2 vol of 100% ethanol at -20°C for 16 h. To dephosphorylate the digested vectors, DNA was treated with shrimp phosphatase (Roche) for 1 h at 37°C and purified by phenol-chloroform (1:1; Sigma) extraction. Ligations were carried out using a molar ratio of 1:3 (vector:insert) in a final volume of 10 μl with 1 μl of T4 DNA ligase (Roche). The reactions were incubated overnight at 16°C and 5 μl of each one were transformed into competent bacteria as described previously (see *2.1.2*).

2.3 Site-directed mutagenesis

Site-directed mutagenesis has been used to generate point mutants of a given amino acid, to introduce stop codons or to generate small deletions. The commercial kit QuickChange Multi Site-Directed Mutagenesis Kit (Stratagene) has been used, following manufacturer's instructions. The mutagenic primers were purchased with a phosphorylated 5' end (Bonsai Technologies). All the mutants have been checked by DNA sequencing of the complete ORF sequence.

3. CELL CULTURE

3.1 Cell lines

The cell lines used in this work are as follows:

- U2-OS: epithelial cell line derived from human osteosarcoma.
- HEK-293: epithelial cell line derived from human embryonic kidney
- HEK-293T: epithelial cell line derived from human embryonic kidney transformed with the SV40 T-Antigen.

All these cell lines were supplied by the American Type Culture Collection (http://www.atcc.org). Cells were cultured in Dulbecco's Modified Eagle's Medium (DMEM, Invitrogen) containing 10% fetal bovine serum (FBS, Invitrogen) and supplemented with antibiotics (100 units/ml penicillin and 100 μg/ml streptomycin, Invitrogen) at 37ºC and in 5% CO_2 atmosphere.

3.2 Cell transfection

Cells were transfected with 1.3 μg (22-mm, MW12), 5 μg (60-mm plates) or 15 μg (100-mm plates) of DNA by the calcium phosphate precipitation method (Graham and van der Eb, 1973), as described in . The optimal pH of the HEPES buffer for each cell line was tested by transfection with a GFP-expressing construct and quantification of fluorescent cells. The DNA-calcium phosphate precipitate was removed after 16 h of incubation by washing the cells with phosphate-buffered saline (PBS) and adding fresh DMEM medium. Cells were washed in PBS at 48 h after transfection and processed accordingly to the purpose of the experiment.

When required, pRNL-Null encoding *Renilla* luciferase was used to normalize transfection efficiencies. For this, an aliquot of the harvested cells were resuspended in Passive lysis buffer (Promega) and Renilla luciferase activity determined with the Stop&Glo Reagent (Promega).

3.3 Cell treatments

To inhibit the proteasome activity, cells were treated with Z-Leu-Leu-Leu-al (MG132, Sigma; 10 mM in dimethyl sulfoxide) at 50 μM final concentration for 7 h. To inhibit the lysosome degradative pathway, cells were treated with chloroquine (Sigma; 100 mM diphosphate salt in H_2O) at 100 μM final concentration for 8 h. To block protein

synthesis, cycloheximide (Sigma; 0.2 g/ml in ethanol) was used at 100 μg/ml final concentration during different time periods (up to 4 h) before lysate preparation.

3.4 Pulse-chase experiments

HEK-293T cells were seeded at a density of $2x10^6$ in 100-mm plates and transfected with the HA-DYRK1A (10 μg) expression vector together with the NLK expression plasmid (wild type or kinase mutant) or control DNA (5 μg). Twenty-four hours after transfection cells were washed, trypsinized and divided into four 3.5-mm wells. Forty-eight hours after transfection, cells were washed and incubated with DMEM (-)methionine, (-)cysteine for 1 h. Cells were labeled with 100 μCi/ml EXPRE^{35}S Protein Labeling Mix ([^{35}S]-methionine and [^{35}S]-cysteine, 11 mCi/ml PerkinElmer) for 40 min (pulse). Then, media was replaced by complete DMEM (chases). At 1-h intervals, soluble lysates were prepared by using lysis buffer A, and immunoprecipitated by anti-HA antibody. The immunocomplexes were analyzed by SDS-PAGE followed by autoradiography.

3.5 Preparation of lentivirus stocks and infection

The CRG has all the permits to work with lentivirus in a biological contention level 2 (A/ES/05/I-13 and A/ES/05/14.). To generate a viral stock, HEK-293 cells were seeded at a density of $2x10^6$ in 100-mm plates and transfected with 15 μg of pCMV-VSV-G, 10 μg of pCMVΔR8.91 packaging construct and 15 μg of pLKO.1-puro control vector or pLKO.1-shRNA hNLK by the calcium phosphate precipitation method. Twenty-four h after transfection, fresh DMEM medium was added, and the lentivirus containing supernatant was harvested at 48 h and 72 h after transfection. The two supernatants were pooled together, spinned at 2,000*xg* for 10 min and filtered through a 0.45 μm filter (Millipore). Viral particles were concentrated by centrifugation through a 4% sucrose cushion (26,700 rpm in a Beckman Coulter centrifuge rotor SW32Ti for 90 min at 4ºC). The supernatant was discarded by inversion and the viral pellet was resuspended in PBS.

For infection, cells were seeded at a density of $7x10^5$ in 60-mm plates in DMEM medium containing 5 μg/ml hexadimethrine bromide (Polybrene, Sigma). The virus was added to the medium and removed 24 h after infection. Cells were processed 72 h after infection. Each stock of vector was titered by infecting HEK-293 cells (10^5 cells in 60-mm plates) with a serial dilution of the viral stock. After 48 h in culture, infected

cells were selected with 1 μg/ml puromycin (Sigma; 2 mg/ml in H_2O) during 8 days, and cell colonies were identified by staining with methylene blue (Sigma). The virus titer was calculated as follows: [number of cell colonies (TU) / viral vol used in the infection (μl)]. The mean value was calculated considering the different viral dilutions.

4. TECHNIQUES FOR PROTEIN ANALYSIS

4.1 Preparation of cell lysates

For total cell lysates preparation, $1x10^6$ cells were resuspended in 150 µl 2x sample loading buffer (100 mM Tris-Cl pH 6.8, 200 mM dithiothreitol [DTT], 4% [w/v] sodium dodecil sulfate [SDS], 20% [v/v] glycerol, 0.2% [w/v] bromophenol blue) and heated for 10 min at 98ºC.

Soluble extracts were prepared by resuspending cells for 15 min at 4°C in lysis buffer A (50 mM HEPES, pH7.4, 150 mM NaCl, 2 mM EDTA, 1% [v/v] Nonidet P-40 [NP-40], protease inhibitor cocktail [Roche Diagnostics], and phosphatase inhibitors [2 mM sodium orthovanadate, 30 mM sodium pyrophosphate, and 25 mM sodium fluoride]), followed by centrifugation for 30 min at 13,000*xg* at 4°C.

4.2 Western blot analysis

Protein samples were resolved on SDS-polyacrylamide gels (SDS-PAGE) of different acrylamide percentage (depending on the molecular weight of the protein to study) at 30 mA in 1x running buffer (25 mM Tris-base, 200 mM glycine, 0.1% [w/v] SDS). Proteins were transferred onto Hybond-ECL nitrocellulose membranes (Amersham Biosciences) at 400 mA for 1 h in 1x transfer buffer (25 mM Tris-HCl pH 8.3, 200 mM glycine, 20% [v/v] methanol). Protein transfer was checked by staining with Ponceau S (Sigma).

Transferred membranes were blocked with 10% (w/v) skimmed milk (Central Lechera Asturiana) diluted in TBS (10 mM Tris-HCl pH 7.5, 100 mM NaCl) -0.1% (v/v) Tween-20 (TBS-T) for 30 min at room temperature (RT), and later incubated with the primary antibody diluted in 5% (w/v) skimmed milk in TBS-T for 1 h at RT or 16 h at 4°C (Table 1). Four washes of 10 min each in TBS-T eluted non-bound primary antibody, and then the secondary antibody (horseradish peroxidase (HRP)-conjugated, Table MM1) was added diluted in 5% skimmed milk in TBS-T and

incubation proceed at RT for 45 min. After four 10 min-washes in TBS-T, membranes were revealed with SuperSignal West Pico Chemiluminescent Substrate (Pierce), and finally exposed in a LAS-3000 image analyzer (Fuji PhotoFilm, Tokyo, Japan) with the LAS3000-pro software. In the case of phosphospecific antibodies and in the case of anti-NLK rabbit polyclonal antibody, antibody incubations were performed with 3% [w/v] bovine serum albumin (BSA) in TBS-T.

Table MM1: Properties and working dilution of the primary and secondary antibodies used.

Primary antibody	Host	Working dilution	Commercial brand
Anti-HA (HA.11)	mouse	1:2000	Babco
Anti-GFP (JL-8)	mouse	1:1000	BD Biosciences
Anti-Flag (M2)	mouse	1:20000	Sigma
Anti-GST (HRP-conjugated, B14)	mouse	1:5000	Santa Cruz
Anti-NLK (H-100)	rabbit	1:500	Santa Cruz
Anti-DYRK1A	mouse	1:1000	Abnova
Anti-β-catenin	mouse	1:2000	BD Biosciences
Anti-β-catenin (phosphoSer552)	rabbit	1:1000	Cell Signaling
Anti-β-catenin (phosphoSer675)	rabbit	1:1000	Cell Signaling
Anti-TCF-4	mouse	1:1000	Sigma
Anti-α-tubulin (DM1A)	mouse	1:10000	Upstate

Secondary antibody (HRP-conjugated)	Host	Working dilution	Commercial brand
Anti-mouse	rabbit	1:2000	DAKO
Anti-rabbit	goat	1:2000	DAKO

4.3 Immunoprecipitation assays

Soluble cell extracts were incubated overnight at 4°C with protein G-Sepharose beads (GE Healthcare) pre-bound with 5 μg of monoclonal antibody (MAb) anti-Flag M2 (Sigma) or MAb anti-HA (Babco) or 2 μg rabbit polyclonal antibody anti-GFP (Invitrogen) antibodies. For immunoprecipitation of endogenous proteins, 700 μg of HeLa nuclear extracts (CIL Biotech) were incubated overnight at 4°C with protein G-magnetic beads (Invitrogen) pre-bound with 1 μg of MAb anti-DYRK1A (Abnova). Beads were washed four times with lysis buffer A, adding 0.1% NP-40 in the two initial washes. Samples were resuspended in 6x sample loading buffer, resolved by SDS-PAGE and analyzed by immunoblotting or used for *in vitro* kinase assays.

4.4 Immunofluorescence

Transfected cells growing on coverslips (12 mm ∅, Afora) were washed in PBS, fixed in 4% (w/v) paraformaldehyde in PBS for 15 min and permeabilized in 0.1% (v/v) Triton X-100 in PBS for 10 min. Cells were blocked in 10% FBS in PBS, incubated with primary antibodies for 1 h and washed extensively with PBS before and after incubation with secondary antibodies for 45 min. All incubations were done at RT. The following primary antibodies have been used: MAb anti-HA (Babco) and MAb anti-Flag M2 (Sigma). Alexa Fluor 488-conjugated donkey anti-mouse and anti-rabbit antibodies or Alexa Fluor 555-conjugated donkey anti-mouse and anti-rabbit antibodies (Invitrogen) were used as secondary antibodies. Coverslips were mounted onto slides using Vectashield Mounting Medium (Vector Laboratories) with 0.2 μg/ml 4,6-diamidino-2-phenylindole (DAPI). Images were viewed under a Zeiss Observer.Z1 and acquired with an AxioCamRM camera. In Figure 13B preparations were observed in a confocal inverted microscope Leica SP2.

4.5 Purification of GST-fusion proteins

To induce the expression of GST-fusion proteins, a fresh colony of *E. coli* BL-21(DE3)pLysS (Stratagene) containing the plasmid of interest was inoculated in 5 ml of LB medium plus 100 μg/ml ampicillin and grown overnight in a shaker at 37ºC. The miniculture was diluted in 100 ml of LB medium plus 100 μg/ml ampicillin, and grown at 37ºC with shaking until the OD_{600} was 0.6-0.8. To induce the expression of the fusion proteins, 0.1 mM isopropyl-β-D-thiogalactoside was added to the cultures that were kept growing for 4 h at 37ºC. In the case of GST-DYRK1A recombinant proteins, induction was performed for 8 h at 20ºC.

To purify the GST-fusion proteins, the bacterial cultures (100 ml) were centrifuged for 10 min at 6,000*xg* and 4ºC and pellets were resuspended in 10 ml of lysis buffer B (10 mM Tris-HCl, pH 8, 100 mM NaCl, 0.5% [v/v] NP-40, 1 mM EDTA and a protease inhibitor cocktail). The cellular suspension was sonicated with 3 pulses for 15 s and 10% amplitude in a digital Branson Sonifier-250, and centrifuged at 13,000*xg* for 15 min at 4ºC. The supernatant was incubated with 100 μl of lysis buffer B-equilibrated glutathione-Sepharose beads (Amersham Biosciences) for 1 h rolling at RT. Finally, beads were washed 3 times with 5 ml of cold lysis buffer B and resuspended in 1 ml lysis buffer B.

When elution from beads was required, as in the case of fusion proteins being used as enzymes or substrates in *in vitro* kinase reactions, beads were incubated in glutathione elution buffer (10 mM Tris-HCl pH 8, 100 mM NaCl; 0.5 % [v/v] NP-40, 1 mM EDTA) three times for 10 min. Between each time beads were centrifuged at 500*xg* for 1 min and supernatant containing the eluted fusion protein was collected and pulled together. Finally, eluted proteins were dialyzed against kinase buffer (50 mM Hepes pH 7.4, 5 mM $MgCl_2$, 5 mM $MnCl_2$) for 16 h at 4ºC.

When removal of the GST-tag from the fusion protein was required, as in the case of GST-β-catenin in pull-down experiments, the fusion protein bound to glutathione-Sepharose beads was diluted in 1 ml lysis buffer B and treated with 2 μl PreScission Protease (Amersham Biosciences) for 16 h at 4ºC. After centrifugation at 500*xg* for 1 min, the supernatant containing the unfused protein was collected.

Protein concentration and purity were estimated by SDS-PAGE and Coomassie blue staining using BSA as standard.

4.6 Pull-down assays

As source of proteins, we have used cell extracts for transiently transfected cells with the plasmids of interest or *in vitro* translated proteins. Proteins were *in vitro* transcribed and translated using the TnT T7 Coupled Reticulocyte Lysate System (Promega) following manufacturer's instructions. Reactions were performed in a final volume of 12.5 μl using 0.25 μg of template DNA, 1 u of T7 RNA polymerase and 30 μCi of [^{35}S]-methionine (1.000 Ci/mmol; Amersham Biosciences) and incubated for 90 min at 30ºC.

For pull-down assays, equivalent amounts of target proteins were incubated with 2.5 μg of purified unfused GST as a control for the specificity of binding or with different GST-fusions as required bound to glutathione beads. Incubations were in 350 μl of binding buffer (20 mM HEPES-KOH, 200 mM KCl, 0.1% [v/v] Triton-X-100, 0.05% [v/v] NP-40, 5 mM EDTA, 0.3% [w/v] BSA and 5 mM DTT) for 3 h rolling at 4ºC. Beads were extensively washed with 1 ml of cold washing buffer (20 mM HEPES-KOH, 500 mM KCl, 0.1% [v/v] Triton-X-100, 0.05% [v/v] NP-40, 5 mM EDTA and 5 mM DTT), resuspended in sample buffer and loaded in a SDS-PAGE gel. The gel was stained with Coomassie blue to ensure that equivalent amounts of bacterially expressed proteins were used, and then either processed for Western blot or for autoradiography. In this case, gels were dried and exposed to a phosphoimager screen (FLA-500, Fujifilm) or to a film.

4.7 In vitro kinase assays

Anti-GFP immunocomplexes (using GFP-tagged proteins as a source of enzyme) or bacterially expressed, purified proteins (using GST-DYRK1A as a source of enzyme) were incubated for 20 min at 30°C in 20 μl of phosphorylation buffer (50 mM HEPES, pH 7.4, 10 mM $MgCl_2$, 10 mM $MnCl_2$, 1 mM DTT and 50 μM ATP) in the presence of 2.5 μCi [γ^{32}P-ATP] (3000 Ci/mmol). ^{32}P incorporation was determined by resolving samples in SDS-PAGE, and then exposing the dried gel to a Phosphoimager screen or to a film. The amount of GFP-tagged proteins present in the immunocomplexes was normalized, as quantified by immunoblot with anti-GFP antibody.

Kinase activity of DYRK1A protein was determined with the peptide substrate DYRKtide (Himpel et al., 2000). To determine the catalytic activity of GFP-DYRK1A, GFP-immunocomplexes were incubated for 20 min at 30°C in 20 μl of phosphorylation buffer containing 200 μM DYRKtide and 1 μCi [γ^{32}P-ATP] (3000 Ci/mmol). Reaction aliquots were dotted onto P81 Whatman phosphocellulose paper, and, after washing extensively with 5% orthophosphoric acid, counts were determined in a liquid scintillation counter (LS6500 Multi-Purpose Scintillation Counter, Beckman Coulter). Each data point was determined in triplicate. For mass spectrometry analysis, cold *in vitro* kinase assays were performed in the presence of 1 mM ATP.

4.8 Mass spectrometry analysis

Mass spectrometry analysis has been performed by Cristina Chivas and Henrik Molina at the Joint CRG/UPF Proteomics Unit. Purified DYRK1A proteins (bacterially expressed as GST-fusion or immunoprecipitated from extracts transiently transfected with plasmids expressing GFP-DYRK1A) were resolved by SDS-PAGE and stained with Coomassie blue. Bands were excised and proteins subjected to in-gel digestion using trypsin (Promega). Each digested sample was split into 3 portions: 15% was analyzed without enrichment while two portions, equal in amount, were subjected to respectively, titanium dioxide (Inertsil, GLSciences) and IMAC (Select Affinity Gel, Sigma-Aldrich) based phosphopeptide enrichment strategies (Thingholm and Jensen, 2009; Thingholm and Larsen, 2009). For LC-MS/MS analysis, peptides were pre-concentrated and desalted using Zorbax 300SB-C18 cartridges (Agilent Technologies). Hereafter, peptides were eluted for MS/MS analysis, via a homemade RP C18 column: 75-μm × 10-mm, 3-μm particle size (Reprosil), using a gradient

delivered at 300 nL/min and increasing from 3% to 45% solvent B in 28 min: solvent A: 0.1% formic acid; solvent B: 0.1% formic acid in acetonitrile (1200-series, Agilent Technologies). Peptides were analyzed on a LTQ Orbitrap XL mass spectrometer (Thermo Fisher Scientific) equipped with a Proxeon nano-ESI source. An electrospray voltage of 2,200 V and a capillary voltage of 14 V at 180°C were used. MS spectra were generated in the FT analyzer using a mass range from 350 to 1,500 *m*/*z* with a resolution of 60,000 at *m/z* 400. For each MS scan, the five most intense ions where selected for fragmentation in the LTQ linear ion trap. MS/MS fragmentation was performed using phosphopeptide-focused multistage activation. Normalized collision energy was set to 35%. MS/MS data were queried against IPI_HUMAN database (version 3.52) using Mascot v2.2 (Matrix Science).

4.9 Reporter assays

HEK293 cells were seeded into 12-well (22-mm) plates ($8x10^4$ cells/well). After 24 h, cells were transfected by the calcium phosphate precipitate method with pTOPFLASH (100 ng/sample) or pFOPFLASH, along with the effector plasmids as indicated in the Figure legends. The total DNA concentration (4 μg/sample) was kept constant by supplementing with empty vector DNAs. Cells were harvested in 150 μl Passive lysis buffer (Promega). Luciferase activity was determined with the Dual-Luciferase Reporter Assay System (Promega). pCMV-RNL (25 ng/sample) encoding *Renilla* luciferase was used to normalize transfection efficiencies. Each data point was determined in triplicate.

4.10 Protein quantification

Protein quantification was performed with the commercial kit BCA Protein Assay Kit (Pierce), following manufacturer's instructions.

5. BIOINFORMATIC TOOLS AND STATISTICAL ANALYSIS

5.1 Search in the databases

Sequence search, both DNA and protein, has been performed basically using the public database from the NCBI (National Centre for Biotechnology Information), through the Entrez system (www.ncbi.nlm.nih.gov/entrez). This includes information

from different sources (GenBank, RefSeq,…). This database has also been used for the search and query of bibliographic references with PubMed.

5.2 DNA sequence analysis

The alignment and comparison of both DNA and protein sequences has been carried out with the BLAST (Basic Alignment Search Tool) and Blast2equences programs from NCBI (www.ncbi.nlm.nih.gov/BLAST).

The analysis of the chromatograms of DNA sequences has been done with the program 4Peaks (www.mekentosj.com).

For the translation from DNA to amino acid sequences and the generation of plasmid maps the program MacVector 3.5 (Accelrys) has been used. The identification of restriction sites and the generation of restriction maps have been performed with the programs DNA Strider and MacVector.

5.3 Protein analysis

The alignment of amino acid sequences was performed with the multiple sequence alignment program CLUSTAL (www.ebi.ac.uk/Tools/clustalw2/index.html). The names and accession numbers of the protein sequences used is shown in Table 2.

Search for phosphorylated sites was carried out at the Phosphosite website (www.phosphosite.org), and for PEST region at the ePESTFIND website (emboss.bioinformatics.nl/cgi-bin/emboss/epestfind)

5.4 Statistical analysis

The significance of differences between samples was evaluated by a two-tailed Student's t-test. A minimum of three independent experiments per condition was included in the analysis. Data are presented as the mean ± standard error of the mean (SEM). Differences were considered significant at p-values <0.05; $^{*}p<0.05$; $^{**}p<0.01$ and $^{***}p<0.001$.

Annex 1: The sequence of oligonucleotides used for the mutagenesis or for PCR amplification of specific DNA fragments.

Name	Sequence (5'->3')
DYRK1A oligonucleotides	
D1AΔ70-104	GCAACCTCTAACTAACCAGAAAAAGAAGCGAAGACACC
D1AΔ105-125rev	CATCATCATAACCATCATTGTAAACTGCATAGTAAACCTCATTAATATGC
D1A/T436A	CTTCAAGTAGTCAGCGACCGCATGACCTGACTCCCCAGCAC
D1A/S468A	CCTTATTATGCTCTGCAGCACGCTTTCTTCAAGAAAACAGC
D1A/T393A	GAGAAGTTGCCAGATGGCGCTTGGAACTTAAAGAAGACC
D1A/T422A	CATAACATTCTTGGAGTGGAAGCAGGAGGACCTGGTGGGCGACG
D1A/S433A,T436A	CAAGTAGTCAGCGACCGCATGACCTGCCTCCCCAGCACGTCGC
D1A/T457A	GGATGCTTGATTATGACCCCAAAGCTCGAATTCAACCTTATTATGC
D1A/K179R	GCAAGAATGGGTTGCCATTAGAATAATAAAGAACAAGAAGGC
NLK oligonucleotides	
NLK-r	CACCATCACTCCCACACCAG
BglII-NLK-f	AGATCTATGGCGGCTTACAATG
NLK-K167M	GGAAAGAGAGTAGCGCTCATGAAGATGCCCAACGTCTTCC
NLK-T298A	GAATCCCGTCATATGGCTCAGGAAGTTGTTAC
NLKΔ430-444	CACTGGTATAAACTCTTCCAGTGGAGGTTTCATCTAGGTAGGGGTGGGC TAAGGC
NLK-C437Y	GGGCGACTACGATATCACACATATATGTGTAAATGTTGCTTTTCC
β-catenin oligonucleotides	
mβcat-S129A	CCAGCGTTTGGCTGAACCAGCACAGATGCTGAAACATGC
mβcat-S552A	CAGGACACCCAACGGCGCACCGCCATGGGTGGAACGCAGCAGC
mβcat-S675A	CAGGATTACAAGAAGCGGCTTGCAGTCGAGCTGACCAGTTCCC

Annex 2: Accession numbers for the protein sequences used in this Thesis work

Name	Species	Accession Number
DYRK1A		
DYRK1A (Hs)	*Homo sapiens*	NP_001387
DYRK1A (Mam)	*Macaca mulatta*	XP_001083622
DYRK1A (Am)	*Ailuropoda melanoleuca*	XP_002929062
DYRK1A (Mm)	*Mus musculus*	NP_031916
DYRK1A (Bt)	*Bos taurus*	XP_612233
DYRK1A (Cf)	*Canis familiaris*	XP_859326
DYRK1A (Gg)	*Gallus gallus*	NP_989881
DYRK1A (Xl)	*Xenopus laevis*	NP_001156669
Minibrain (Dm)	*Drosophila melanogaster*	NP_728104
MBK-1 (Ce)	*Caenorhabditis elegans*	NP_510460
dDYRK1A (Dd)	*Dictyostelium discoideum*	XP_642598
NLK		
NLK	*Homo sapiens*	NP_057315
NLK	*Pan troglodytes*	XP_001147662
NLK	*Bos taurus*	XP_886284
NLK	*Canis familiaris*	XP_548280
NLK	*Mus musculus*	NP_032728
NLK	*Gallus gallus*	XP_415915
NLK	*Danio rerio*	NP_998121
NLK	*Takifugu rubripes*	NP_001027920
Nemo	*Drosophila melanogaster*	NP_729317
LIT-1	*Caenorhabditis elegans*	NP_001022808
MAPK		
MAPK1/Erk2	*Homo sapiens*	NP_002736
MAPK4/Erk4	*Homo sapiens*	NP_002738
MAPK6/Erk3	*Homo sapiens*	NP_002739
MAPK8/JNKα2	*Homo sapiens*	NP_620637
MAPK14/p38α	*Homo sapiens*	NP_001306
MAPK15/Erk7	*Homo sapiens*	NP_620590

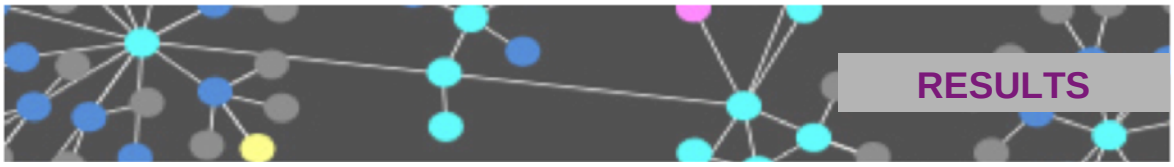

RESULTS

DYRK1A interacts with NLK

To verify the interaction between DYRK1A and NLK, expression vectors in which each of the open reading frames were N-terminally fused to different epitopes recognized by commercial antibodies were prepared: an HA-tagged DYRK1A expression vector was available in the group and a Flag-tagged NLK expression vector was generated. These constructs were transfected into HEK-293T cells and the NLK-DYRK1A interaction was verified by immunoprecipitation experiments either with anti-Flag or with anti-HA antibodies (Fig. R1A). HA-DYRK1A was immunoprecipitated with Flag-NLK in anti-Flag immunocomplexes, but was not precipitated by anti-Flag when expressed alone (Fig. R1A, upper panel), thus indicating specific interaction between the two proteins. The complementary result was obtained when anti-HA immunocomplexes were analyzed (Fig. R1A, middle panel). These results demonstrate that DYRK1A and NLK can interact *in vivo* in mammalian cells when they are exogenously expressed.

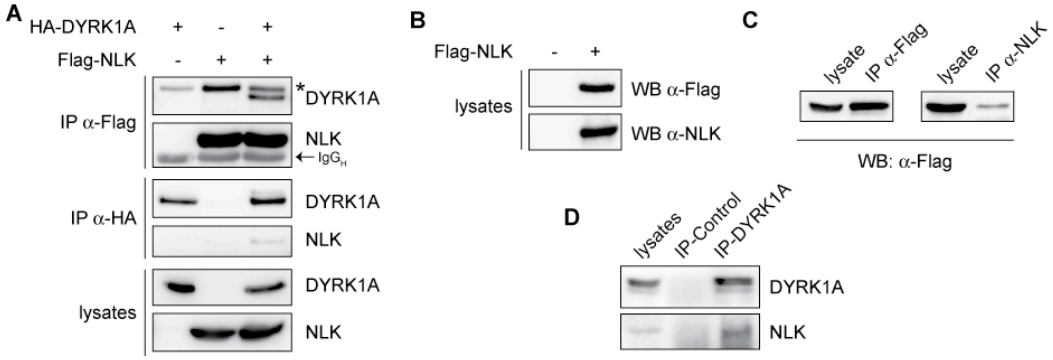

Figure R1: DYRK1A interacts with NLK. (A) DYRK1A and NLK interact when exogenously expressed in cells. Soluble extracts from HEK-293T cells expressing HA-DYRK1A and Flag-NLK were immunoprecipitated with anti-Flag or with anti-HA. Immunoprecipitated proteins (IP) and cell lysates (5% of input) were analyzed by Western blot with anti-HA or anti-Flag. In this and the other Figures, the asterisk indicates a cross-reacting band and IgG_H indicates the position of IgG heavy chain. **(B, C)** Specificity of the anti-NLK antibody. Soluble extracts from cells transfected with Flag-NLK or control plasmid were analyzed by Western blot with anti-Flag and anti-NLK (H-100, Santa Cruz). **(B)** or immunoprecipitated with anti-Flag or with anti-NLK and analyzed by Western blot with anti-Flag **(C)**. The anti-NLK antibody works efficiently in Western blot, but it is not optimal for immunoprecipitation. **(D)** HeLa nuclear lysates were immunoprecipitated with anti-DYRK1A or mouse IgG as a control antibody. Immunoprecipitated proteins (IP) and nuclear lysates (5% of input) were analyzed by Western blot with anti-DYRK1A and with anti-NLK. The position of protein markers (in kDa) is shown.

To confirm the interaction under physiological conditions, nuclear extracts from HeLa cells, in which both proteins were present (Fig. R1D) were used for immunoprecipitation experiments with antibodies recognizing the endogenous proteins. The specificity of a commercial anti-DYRK1A monoclonal antibody has been previously demonstrated (Laguna et al., 2008). In the case of NLK, several

commercial anti-NLK antibodies were analyzed by immunoblot against overexpressed NLK to test their specificity and only one, H-100 from Santa Cruz Biotechnology, recognized NLK (Fig. R1B); however, this antibody did not immunoprecipitate NLK efficiently (Fig. R1C), precluding its use in immunoprecipitation experiments. As shown in Figure R1D, NLK was immunoprecipitated with DYRK1A in anti-DYRK1A immunocomplexes, but it was not precipitated by a control mouse IgG. Therefore, NLK and DYRK1A can form complexes in physiological conditions.

The interaction between DYRK1A and NLK is independent of their kinase activities

For several kinases, enzymatic activity is associated with a conformational change in the protein, which may regulate their interaction with other proteins (for a recent review Rabiller et al., 2010). To test whether the interaction depends on the kinase activity of DYRK1A, a kinase-deficient mutant form in which the conserved lysine of the ATP binding site was mutated to arginine (K179R) (Fig. R2A and B). The interaction with NLK was detected both with DYRK1A wild type and with the kinase-inactive form (Fig. R2C), indicating that the kinase activity of DYRK1A is not necessary for the interaction.

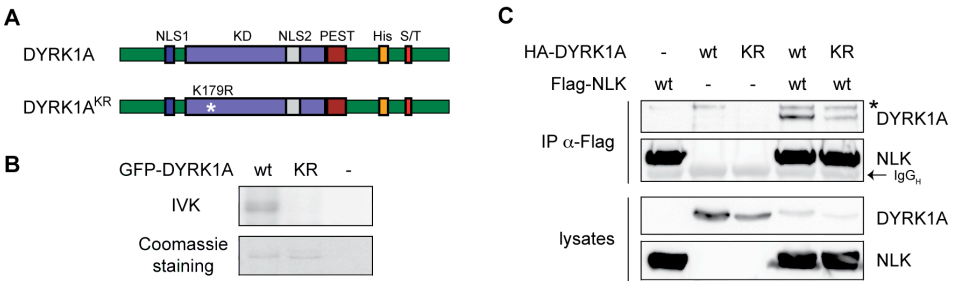

Figure R2: DYRK1A-NLK interaction is independent of DYRK1A kinase activity. (A) Schematic representation of DYRK1A wild type (wt) or the inactive-kinase mutant (KR): labelling is according to Figure I2. **(B)** HEK-293T cells were transfected with pGFP-DYRK1A wt or pGFP-DYRK1A^{KR} expression vectors as indicated. Anti-GFP-immunoprecipitates were subjected to an *IVK* assay in the presence of [γ^{32}P-ATP]. Proteins were separated by SDS-PAGE and analyzed by autoradiography. The gel was stained with Coomassie to check for equal loading. **(C)** Soluble cell extracts from HEK-293T cells expressing HA-DYRK1A wt or the inactive-kinase mutant HA-DYRK1A^{KR} and Flag-NLK were immunoprecipitated with anti-Flag. Immunoprecipitated proteins (IP) and cell lysates (5% of input) were analyzed by Western blot with anti-HA or anti-Flag.

In the case of NLK, two distinct mutant forms of NLK deficient in the kinase activity were prepared. In one of them, the lysine residue 167 within the ATP binding

site was mutated to methionine (NLK^{KM}); in the second one, the threonine residue 298 in the activation loop, which has to be phosphorylated for complete kinase activation (Brott et al., 1998), was replaced by alanine (NLK^{TA}) (Fig. R3A). Given that NLK has been shown to autophophorylate (Brott et al., 1998), the two mutant forms were analyzed in autophosphorylation assays and found that were indeed inactive (Fig. R3B). As Figure R3C shows, the NLK-DYRK1A interaction was detected with both NLK kinase inactive proteins in co-immunoprecipitation experiments, suggesting that NLK kinase activity is not necessary for the interaction.

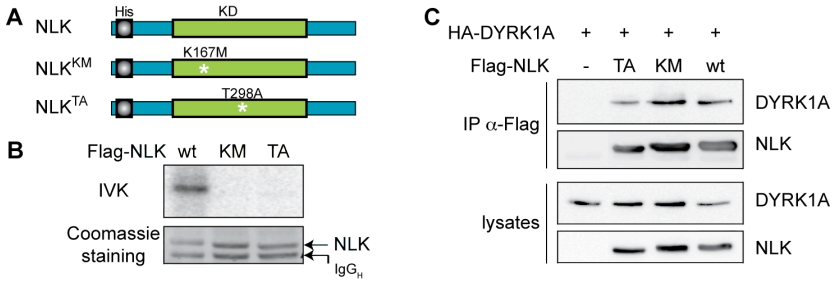

Figure R3: DYRK1A-NLK interaction is independent of NLK kinase activity. (A) Schematic representation of NLK wild type (wt) or its kinase-inactive mutants (NLK^{KM} and NLK^{TA}): His, region rich in histidine residues; KD, kinase domain. **(B)** HEK-293T cells were transfected with pFlag-NLK wt, pFlag-NLK^{KM} (KM) or pFlag-NLK^{TA} (TA) expression vectors as indicated. Anti-GFP-immunoprecipitated complexes were subjected to an *IVK* assay in the presence of [γ^{32}P-ATP]. Phosphorylated proteins were separated by SDS-PAGE and analyzed by autoradiography (IVK). The gel was stained with Coomassie to check for equal protein amounts. **(C)** Soluble cell extracts from HEK-293T cells expressing Flag-NLK wt or its kinase-inactive mutants together with HA-DYRK1A were immunoprecipitated with anti-Flag. Immunoprecipitated proteins (IP) and cell lysates (5% of input) were analyzed by Western blot with anti-HA or anti-Flag.

NLK interacts with all DYRK family members

As indicated in the *Introduction* section, DYRK family consists of five different members in humans: DYRK1A, DYRK1B, DYRK2, DYRK3 and DYRK4 that can be classified as Class I and Class II members based on phylogenetics and on the presence of the NAPA domain in their N-terminal regions (Aranda et al., 2010; Kinstrie et al., 2010) (Fig. R4A). To check whether interaction occurs between NLK and other DYRK family members, immunoprecipitation experiments using HA-tagged versions of DYRK1B, DYRK2, DYRK3 and DYRK4 and Flag-NLK were performed. As Figures R4B and R4C show, all DYRK family members were present in immunocomplexes with NLK, although with different efficiencies. Whereas DYRK1A, DYRK1B and DYRK4 interacted similarly with NLK, DYRK2 and DYRK3 were bound to NLK less efficiently. These results indicate that NLK can interact with all human DYRK kinases.

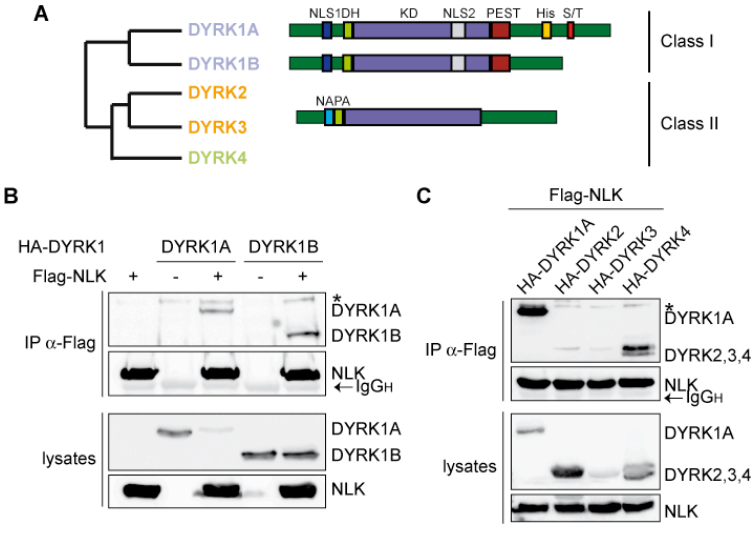

Figure R4: NLK interaction is shared by all DYRK family members. (A) Schematic representation of DYRK proteins: on the left, the tree shows the phylogenetic relationship; on the right, the primary structure is depicted and the DYRK homology box (DH) and the NAPA domain (NAPA) are shown. **(B, C)** Soluble extracts from HEK-293T cells expressing Flag-NLK and HA-tagged DYRK family members, as indicated, were immunoprecipitated with anti-Flag followed by Western blot with anti-HA or anti-Flag. Cell lysates representing 5% of inputs are shown.

The N-terminal region of DYRK1A has an NLK-binding site

To define the region in DYRK1A necessary for the interaction with NLK, co-immunoprecipitation experiments were first carried out with a series of C-terminal deletion mutants of DYRK1A up to amino acid 522. All these DYRK1A mutant proteins interacted with Flag-NLK in co-immunoprecipitation experiments (Fig. R5).

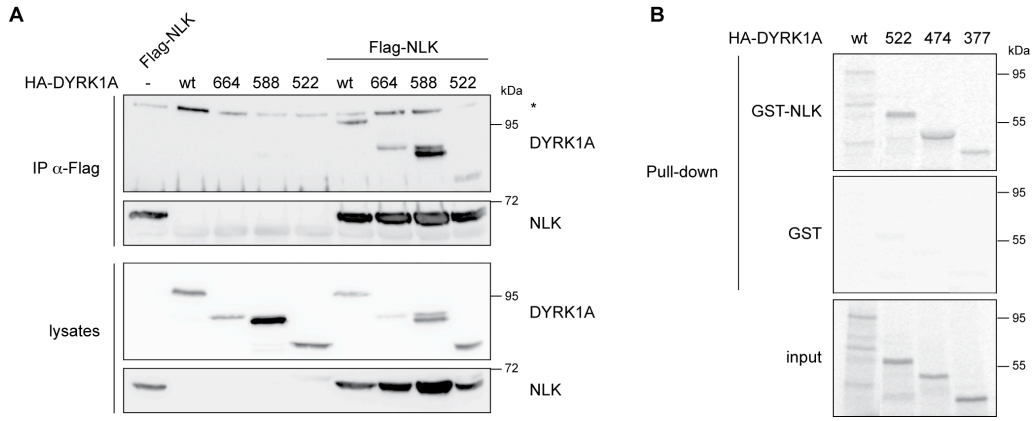

Figure R5: The C-terminal region of DYRK1A is dispensable for binding to NLK. (A) Soluble extracts from HEK-293T cells expressing Flag-NLK and HA-tagged DYRK1A wt or deletion mutants as indicated (the numbers indicate the last amino acid present) were immunoprecipitated with anti-Flag followed by Western blot with anti-HA or anti-Flag. Cell lysates representing 5% of input are shown. **(B)** HA-DYRK1A and the deletion mutants indicated were *in vitro* translated in the presence of radiolabeled methionine and incubated with unfused GST or GST-NLK immobilized on gluthatione-Sepharose beads. Bound protein was detected by autoradiography. An autoradiograph representing 10% of the input is shown.

Further upstream deletions, including the PEST region or part of the kinase domain, yielded proteins that were not stable when expressed in cells by transient transfection (data not shown). For this reason, the DYRK1A deletion mutants were

synthesized *in vitro* by coupled transcription/translation in rabbit reticulocyte extracts in the presence of radioactive-labeled methionine. The extracts were then incubated with a GST-NLK fusion protein expressed in *E. coli* and purified by glutathione-Sepharose affinity chromatography, and bound proteins were analyzed by autoradiography. All the C-terminal DYRK1A deletion mutans tested, up to amino acid 377, were pulled down by the GST-NLK fusion protein, but not by unfused GST (Fig. R5B). These results allow to conclude that the C-terminal region of DYRK1A is dispensable for the interaction with NLK.

We then asked whether a binding site for NLK was present within the N-terminal region of DYRK1A. Therefore, co-immunoprecipitation experiments using soluble extracts expressing different DYRK1A mutants containing a series of N-terminal fragments fused to GFP were performed. Whereas GFP-DYRK1A fusion proteins containing the first 167 or 127 amino acids were co-immunoprecipitated with NLK (Fig. R6A), a GFP fusion containing the first 84 amino acids could not bind to NLK (Fig. R6B). A summary of the NLK-DYRK1A experiments is shown in Fig. R6C. These results suggest therefore that the region in DYRK1A required for NLK interaction is located between amino acids 88 and 127.

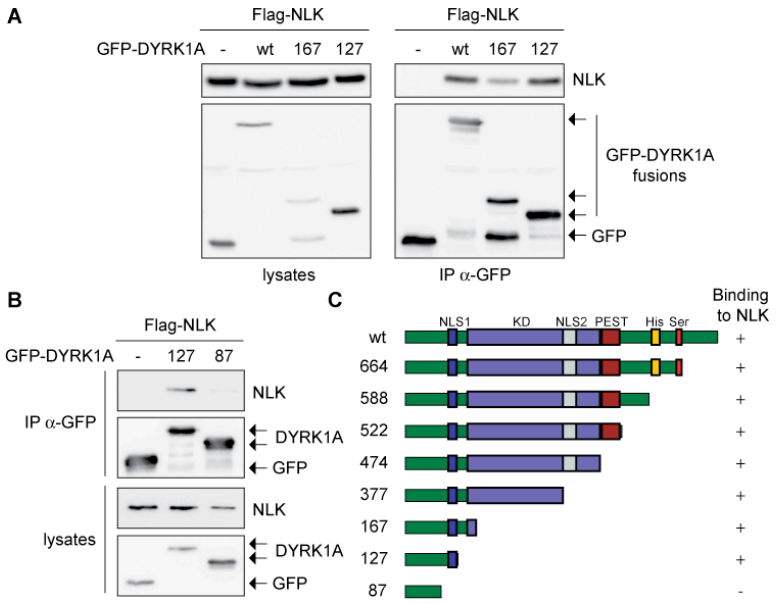

Figure R6: A binding site for NLK is present within amino acids 87-127 in DYRK1A. (A, B) Soluble extracts from HEK-293T cells expressing Flag-NLK and GFP-tagged DYRK1A wt or the indicated deletion mutants (the numbers indicate the last amino acid) were immunoprecipitated with anti-GFP followed by Western blot with anti-GFP or anti-Flag. Cell lysates representing 5% of input are shown. **(C)** Summary of the DYRK1A-NLK interaction results shown in Figures 5 and 6.

The NLK interacting region in DYRK1A harbors the predicted bipartite NLS responsible for targeting DYRK1A to the nucleus (Alvarez et al., 2003). To test whether this domain is important for the interaction with NLK, two distinct mutant forms of DYRK1A were prepared: DYRK1A$^{\Delta 105\text{-}125}$, in which the NLS1 of DYRK1A

was deleted and DYRK1A$^{\Delta 70\text{-}104}$, in which the rest of the putative DYRK1A binding site was deleted but the NLS1 kept intact (Fig. R7A). The subcellular localization of these mutants was assessed by immunofluorescence analysis. As predicted, deletion of the region between amino acids 105 and 125 affected the subcellular localization of DYRK1A, which shows more cytosolic staining when compared to DYRK1A wt but it still localizes to the nucleus through its NLS2 (Fig. R7B). DYRK1A$^{\Delta 70\text{-}104}$ was present in the nucleus. Despite their nuclear localization, HA-DYRK1A$^{\Delta 105\text{-}125}$ was immunoprecipitated with NLK, whereas the interaction of NLK with HA-DYRK1A$^{\Delta 70\text{-}104}$ was impaired (Fig. R7C and quantification shown in Fig. R7D). These results suggest that the region in DYRK1A required for NLK interaction is located between amino acids 70 and 104 and does not include the NLS1.

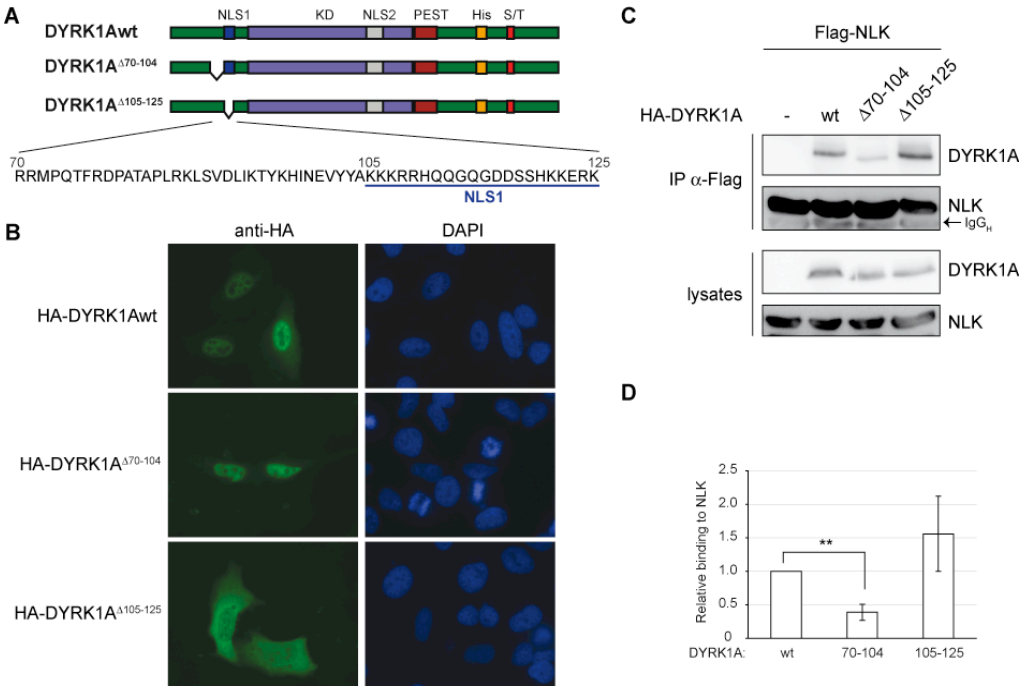

Figure R7: A binding site for NLK is present within amino acids 70-104 in DYRK1A. (A) Schematic representation of DYRK1A wt and the N-terminal deletion mutants. The amino acid sequence of the deleted regions is shown. **(B)** U2-OS cells were transfected with expression plasmids for HA-DYRK1A wt or the deletion mutants indicated. The localization of the HA-fusions was detected by indirect immunofluorescence staining with anti-HA. DNA was counterstained with DAPI. **(C)** Soluble extracts from HEK-293T cells expressing Flag-NLK and HA-tagged DYRK1A wt or the indicated deletion mutants were immunoprecipitated with anti-Flag followed by Western blot with anti-HA or anti-Flag. Cell lysates representing 5% of inpus are shown. **(D)** Quantification of the relative binding of DYRK1A wt or deletion mutants to NLK. The graph represents the average (± SEM) of four independent experiments in which the binding of DYRK1Awt was set as 1. (**p<0.01).

NLK interacts with DYRK1A through its C-terminal region

The C-terminal part of NLK has been suggested to contribute to the interaction of this kinase with specific substrates or targets such as TCF-4, HMG2L1 and NARF (Ishitani et al., 1999; Yamada et al., 2003; Yamada et al., 2006). For this reason and to define the region in NLK necessary for the interaction with DYRK1A, an NLK mutant with a deletion of the C-terminal part of NLK, from the end of the kinase domain and including the last 100 amino acids, was generated (Fig. R8A). As shown in Figure R8B, HA-DYRK1A was not present in NLK-specific immunoprecipitates, indicating that this region of NLK is required for the interaction with DYRK1A.

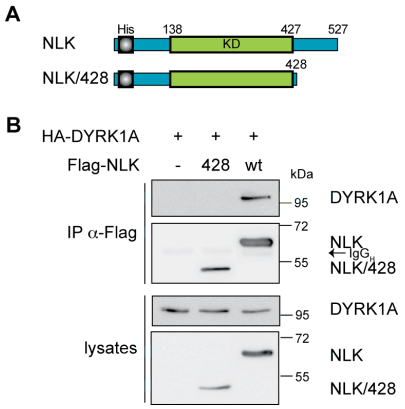

Figure R8: The C-terminal region of NLK harbours a DYRK1A binding domain. (A) Schematic representation of the NLK C-terminal deletion mutant. **(B)** Soluble extracts from HEK-293T cells expressing HA-DYRK1A and Flag-NLK wild type (wt) or the C-terminal deletion mutant as indicated were immunoprecipitated with anti-Flag followed by Western blot with anti-HA or anti-Flag. Cell lysates representing 5% of input are shown.

Members of the MAPK family have a conserved domain that is used for docking to their activators, inhibitors and substrates (Tanoue et al., 2000). This domain, known as CD-domain, is located C-terminally to the subdomain XI outside the catalytic domain (Fig. R9A). No CD-domain has been reported yet for NLK, and a comparison of the NLK sequence C-terminal to the catalytic domain with those of the CD-domains of ERK, JNK o p38 did not revealed any homology (Fig. R9A). To test whether this region was important for DYRK1A interaction, a deletion mutant covering the region was generated (Fig. R9B). The deletion results in the loss of NLK autophosphorylation capability (Fig. R9C), and it does not seem to affect its subcellular localization (Fig. R9D). As Figure R9E shows, the interaction of DYRK1A with this mutant was almost completely abolished, suggesting that this region of NLK is required for the formation of complexes with DYRK1A.

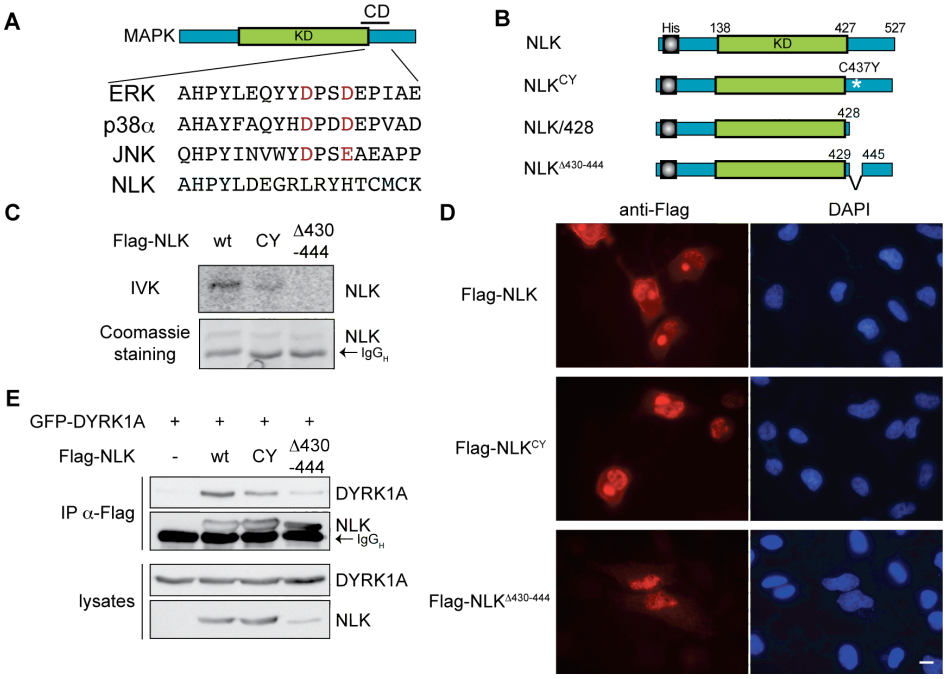

Figure R9: NLK interacts with DYRK1A via a putative CD-domain. (A) Amino acid sequence comparison of the CD-domains of classical MAPKs with NLK. **(B)** Schematic representation of the NLK mutants used in these experiments. **(C)** HEK-293T cells were transfected with plasmids expresssing Flag-NLK wt or the indicated mutants. Anti-Flag-immunoprecipitated complexes were incubated with [γ^{32}P-ATP] in an *IVK* assay. Phosphorylated proteins were separated by SDS-PAGE and analyzed by autoradiography. A Coomassie staining of the gel shows that comparable amounts of proteins were used. **(D)** U2-OS cells were transfected with expression plasmids for Flag-NLK wt or the indicated mutants, and the localization of the Flag-fusions was detected by indirect immunofluorescence with anti-Flag. DNA was counterstained with DAPI. Scale bars, 10 μm. **(E)** Soluble extracts from HEK-293T cells expressing GFP-DYRK1A and Flag-NLK wt or the mutants indicated were immunoprecipitated with anti-Flag followed by Western blot with anti-GFP or anti-Flag. Cell lysates representing 5% of input are shown.

A LIT-1, the NLK orthologous *C. elegans,* loss-of-function mutant has been described in which the cysteine residue 541, within the putative CD-domain, is mutated to tyrosine (Meneghini et al., 1999). When the analogous mutation (cysteine residue 437 to tyrosine) was introduced into human NLK, this mutant was unable to associate with TCF-4 (Ishitani et al., 1999). The cysteine residue is included within the region defined as important for DYRK1A interaction (Fig. R9A and B). To test whether this residue contributes to DYRK1A interaction, the same mutation was introduced to generate the NLK^{CY} mutant. The mutation reduces the NLK catalytic activity (Fig. R9C) and does not change its subcellular localization (Fig. R9D). As Fig. 9E shows, DYRK1A protein levels were slightly decreased in the NLK^{CY} immunocomplexes when compared with the NLK wt ones, suggesting that Cys437 located within the DYRK1A interacting region participates in the binding.

NLK phosphorylates DYRK1A

Given that DYRK1A interacts with NLK through a region previously shown to be involved in the interaction with NLK substrates (Ishitani et al., 1999; Yamada et al., 2003; Yamada et al., 2006), we wondered whether DYRK1A could be a NLK substrate. To address whether NLK can phosphorylate DYRK1A, we performed *IVK* assays using anti-GFP immunocomplexes prepared from soluble extracts of cells expressing the kinase active or inactive forms of GFP-NLK as the enzyme source, and the kinase-inactive form of DYRK1A K179R fused to GFP as the substrate. The DYRK1A kinase-dead form is the appropriate tool for this type of experiments, because DYRK1A autophosphorylates (Kentrup et al., 1996). As shown in Figure R10, DYRK1A was phosphorylated when the wild type form of NLK was present in the immunocomplexes, but not in the presence of comparable amounts of an NLK kinase-dead version, indicating that NLK phosphorylates DYRK1A.

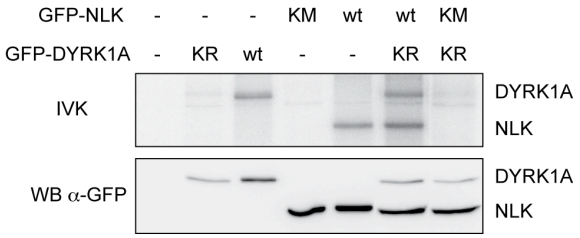

Figure R10: NLK phosphorylates DYRK1A. HEK-293T cells were transfected with plasmids expressing GFP-DYRK1A wt or the DYRK1A catalytically inactive mutant K179R (KR) and GFP-NLK wt or the NLK kinase-dead mutant K167M (KM) as indicated. Anti-GFP-immunocomplexes were incubated with [γ^{32}P-ATP] in an *IVK* assay. Phosphorylated proteins were separated by SDS-PAGE and analyzed by autoradiography. The presence of comparable amount of GFP-fusion proteins was analyzed by Western blot with anti-GFP.

NLK phosphorylation of DYRK1A affects neither enzymatic activity nor subcellular localization

Post-translational modification by protein kinases may modify several activities of their substrates, including enzymatic activity, cellular location, and/or association with other proteins. DYRK1A is a phosphoprotein and several tyrosine, serine and threonine residues have been identified as phosphorylated (Alvarez et al., 2007; Himpel et al., 2001; www.phosphosite.org). Given that DYRK1A is synthesized as constitutively active kinase, it is proposed that other mechanisms might regulate its cellular activity (see *Introduction*). One of these mechanisms could be

phosphorylation, similar to what has been shown for DYRK2, which is regulated by MAP3K10 phosphorylation (Varjosalo et al., 2008). To check whether NLK-dependent phosphorylation could alter the intrinsic kinase activity of DYRK1A, DYRK1A *IVK* assays were performed using as substrate a peptide, DYRKtide, which contains the consensus phosphorylation sequence of DYRK1A (Himpel et al., 2000). Given that DYRK1A and NLK phosphorylate serine/threonine residues with a preference for a proline at P+1 (see *Introduction*), we first checked whether NLK kinase activity was interfering with the DYRK1A-specific assay by phosphorylating the DYRK1A substrate and found that, whereas ^{32}P incorporation into the peptide was clearly detected in the presence of DYRK1A, no incorporation above the control levels was detected in the presence of NLK, confirming that the assay was adequate (Fig. R11A and B). Next, we examined whether phosphorylation by NLK would affect DYRK1A kinase activity. To this end, increasing amounts of NLK were mixed with DYRK1A and an *IVK* assay on DYRKtide was performed (Fig. R11C and D). The presence of NLK did not alter the enzymatic activity of DYRK1A (Fig. R11D).

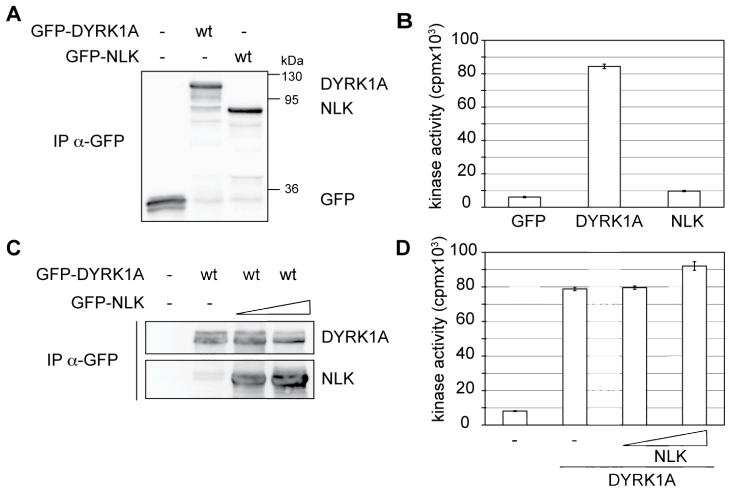

Figure R11: DYRK1A kinase activity is not affected by NLK phosphorylation. (A, B) NLK cannot phosphorylate the DYRK1A specific peptide, DYRKtide. HEK-293T soluble cell extracts expressing unfused GFP, GFP-DYRK1A or GFP-NLK were immunoprecipitated with anti-GFP and subjected to an *IVK* assay with DYRKtide as substrate **(B)**. The presence of equal amounts of GFP-tagged proteins was checked by Western blot with anti-GFP **(A)**. **(C, D)** NLK does not alter DYRK1A enzymatic activity. Soluble extracts from cells expressing GFP-DYRK1A were mixed with increasing amounts of GFP-NLK or GFP as control (-) and immunoprecipitated with anti-GFP in the presence of cold ATP to allow DYRK1A phosphorylation. The GFP-fusion protein levels in the immunocomplexes were analyzed by immunoblot with anti-GFP **(C)**. DYRK1A kinase activity was determined in the immunocomplexes using DYRKtide as substrate in a radioactive *IVK* assay **(D)**. In **(B)** and **(D)**, the graph shows a representative experiment in which each data point was determined in triplicate; data are represented as the means ± SEM.

DYRK1A is a shuttling protein, although it is not known how its nuclear import or export is regulated (see *Introduction*). Given that protein phosphorylation can contribute to the control of NLS or NES accessability (for a recent review Sorokin et al., 2007), we check whether NLK-dependent phosphorylation could alter the subcellular localization of DYRK1A. For that, the subcellular localization of GFP-DYRK1A was determined in the absence or presence of Flag-NLK, both the wild type or the kinase-inactive mutant. As shown in Figure R12A, co-expression of NLK did not affect the subcellular distribution of DYRK1A. In the nucleus, both DYRK1A and NLK accumulate in the splicing factor compartment when they are expressed exogenously (Alvarez et al., 2003; Salichs et al., 2009). The subnuclear localization of both DYRK1A and NLK was analyzed by confocal microscope that showed co-localization of both proteins in the nuclear speckles (Fig. R12B), and indicating that their interaction does not induce any change in their nuclear localization.

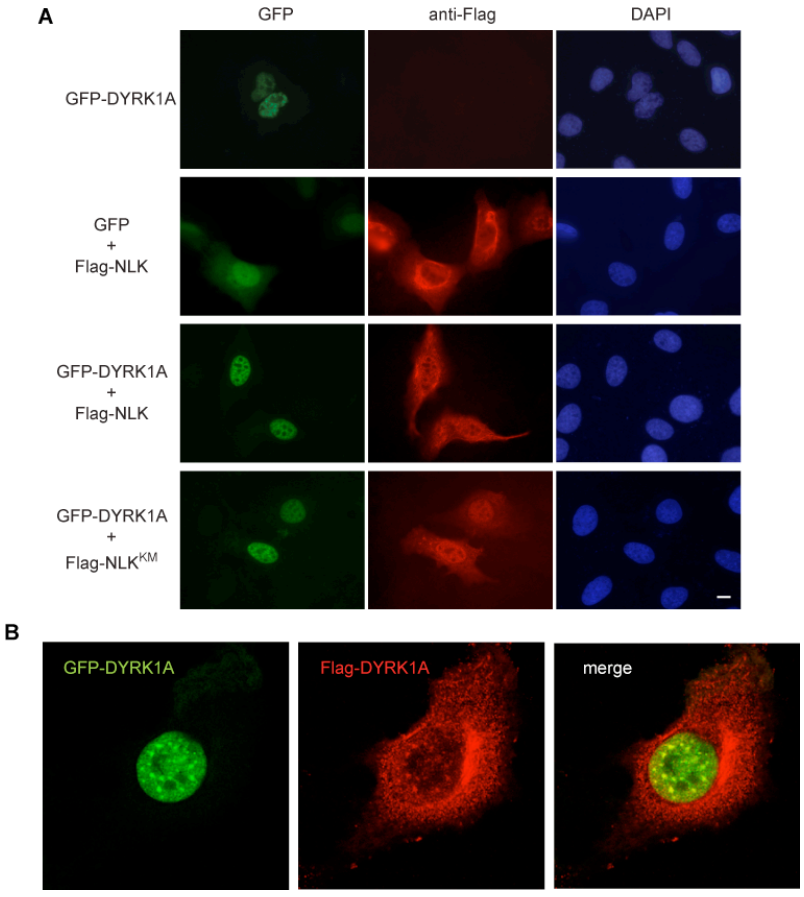

Figure R12: The subcellular localization of DYRK1A is not affected by NLK co-expression. (A, B) U2-OS cells were transfected with plasmids to express unfused GFP or GFP-DYRK1A together with Flag-NLK wt or Flag-NLK^{KM}. The localization of the GFP-fusions was assessed by direct fluorescence, whereas the Flag-fusions were detected by indirect immunofluorescence with anti-Flag. DNA was counterstained with DAPI. Scales bars, 10 μm. Images were taken either by conventional microscopy **(A)** or by confocal microscopy **(B)**.

NLK co-expression induces a decrease in the accumulation of DYRK1A

When analyzing the results of the DYRK1A and NLK co-transfection experiments, we noticed that DYRK1A protein levels were repeatedly decreased when it was co-expressed with NLK. This could be the result of differences in the transfection efficiency or due to a direct effect of NLK on DYRK1A accumulation. To check these possibilities, we analyzed total cell extracts from cells transfected with combinations of plasmids expressing both proteins. A *Renilla* luciferase reporter vector was used as an internal control for transfection efficiency. Whereas Renilla activity was not affected by the co-expression of any of the protein combinations (Fig. R13A), excluding thus a transfection effect, a decrease in DYRK1A protein levels, both wild type and null-mutant, was observed when it was co-expressed with NLK (Fig. R13A and B). Notably, this effect was not apparent when the NLK kinase inactive mutant was used (Fig. R13B).

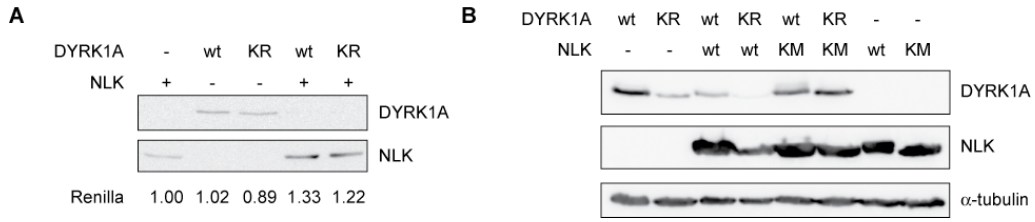

Figure R13: NLK affects DYRK1A accumulation in cells. Total cell extracts from HEK-293T cells expressing HA-DYRK1A wt or the kinase-inactive mutant version K179R (KR) together with Flag-NLK wt or the kinase-dead version K167M (KM), as indicated, were analyzed by immunoblot with anti-HA and anti-Flag. In **(A)**, extracts were co-transfected with a Renilla luciferase reporter to confirm equal transfection; relative luciferase values are shown at the bottom of the panels. In (B), membranes were re-blotted with anti-α-tubulin to confirm equal loading.

All these findings suggested that NLK could be regulating the accumulation of DYRK1A in cells. To confirm this hypothesis, we decided to analyze DYRK1A levels in the absence of NLK. To deplete NLK from cells we use lentivirus-derived vectors that express shRNAs against NLK mRNA, and that were tested for their ability to knock down NLK expression in co-transfection experiments (data not shown). When cells were infected with the combination of two shNLK-lentiviruses, NLK protein levels were decreased (Fig. R14). Notably, endogenous DYRK1A protein levels were increased when compared to the levels in control cells infected with a non-target shRNA (Fig. R14).

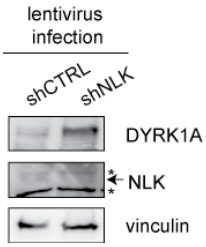

Figure R14: NLK affects DYRK1A accumulation in cells. HEK-293T cells were infected with pLKO-derived lentivirus expressing a shRNA targeting NLK mRNA or a non-target sequence, as a control (CTRL). Total cell extracts were analyzed by immunoblot with anti-DYRK1A and anti-NLK. Membranes were re-blotted with anti-vinculin to confirm equal loading.

Next, we analyzed whether the detected effect was dependent of DYRK1A interaction with NLK. For this, we tested accumulation of the DYRK1A$^{\Delta 70\text{-}104}$ deletion mutant that had showed a reduced interaction (Fig. R7). No significant decrease in the protein levels of DYRK1A$^{\Delta 70\text{-}104}$ was observed when it was co-expressed with NLKwt (Fig. R15A; quantification of independent experiments in Fig. R15B). These results suggest that the interaction with NLK modifies the accumulation of DYRK1A protein either at the transcriptional, translational and/or post-translational levels.

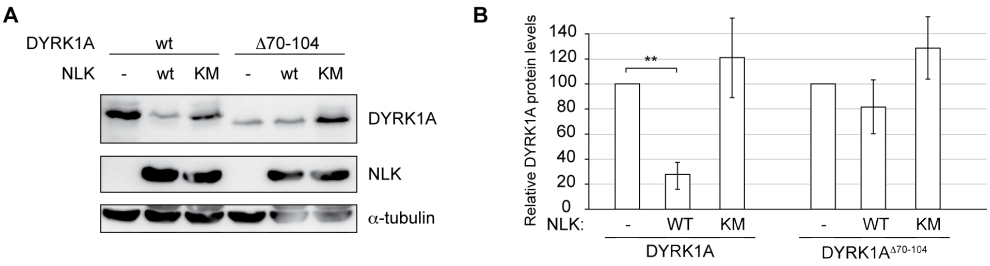

Figure R15: The interaction with NLK reduces the accumulation of DYRK1A protein. (A) Total cell extracts from HEK-293T cells expressing HA-DYRK1A wt or the non-interacting mutant HA-DYRK1A$^{\Delta 70\text{-}104}$ together with Flag-NLK wt or the kinase-inactive version K167M (KM) were analyzed by immunoblot with anti-HA and anti-Flag. Membranes were immunoblotted with anti-α-tubulin to confirm equal loading. **(B)** Quantification of DYRK1A protein levels (wild type or deletion mutant) as a percentage of the value obtained when the DYRK1A proteins were expressed alone, which was set at 100. Values correspond to the means ± SEM of at least three independent experiments (**p<0.01).

NLK induces DYRK1A proteasome-dependent degradation

NLK has been shown to induce the degradation of some of its substrates such as c-Myb and TCF/LEF (Kanei-Ishii et al., 2004; Yamada et al., 2006). To determine whether the NLK effects on DYRK1A protein levels were due to enhanced degradation, the half-life of DYRK1A was estimated by radioactive pulse-chase experiments and immunoprecipitation. As shown in Figure R16A, the presence of the active kinase NLK decreased DYRK1A half-life by approximately 1.5-fold, while the inactive-kinase mutant NLK^{KM} slightly increased DYRK1A half-life by around 0.5-fold.

These results suggest that NLK-dependent phosphorylation may affect the half-life of the DYRK1A protein, inducing its degradation.

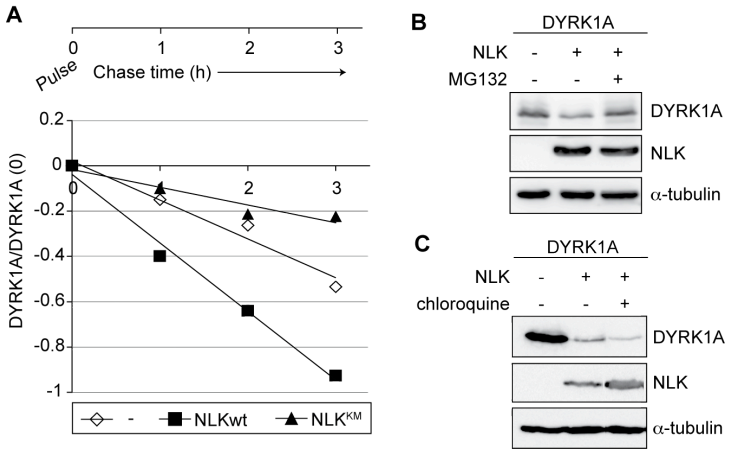

Figure R16: NLK induces the proteasome-mediated degradation of DYRK1A. (A) HEK-293T cells were transfected with the pHA-DYRK1A expression plasmid alone or together with pFlag-NLK wild type (wt) or the kinase-inactive version K167M (KM) and pulse-chase labelled with [^{35}S]-methionine according to the scheme. At the pulse and at the indicated times after the chase, DYRK1A protein levels were examined by immunoprecipitation and autoradiography. The plot shows the natural log of the ratio DYRK1A at the pulse/DYRK1A at the chase period. Results correspond to the average of two independent sets of experiments. **(B, C)** HEK-293T cells expressing HA-DYRK1A with or without Flag-NLK were treated with 50 μM MG132 for 7 h **(B)** or 100 μM chloroquine for 8 h **(C)** or the corresponding control vehicles, and total cell lysates were prepared and analyzed by immunoblot with anti-HA and anti-Flag. Membranes were re-blotted with anti-α-tubulin to confirm equal loading.

In eukaryotic cells, degradation of most intracellular proteins is carried out by the proteasome or the lysosome compartment (for a recent review Knecht et al., 2009). To find out whether NLK-dependent phosphorylation marks DYRK1A for either the proteasome- or the lysosome-mediated degradation, total cell lysates of cells treated with specific inhibitors of these degradation pathways, MG132 and chloroquine, respectively, were analyzed. The results suggest that NLK-dependent phosphorylation marks DYRK1A for proteasome-mediated degradation, but not for lysosome-mediated degradation (Fig. R16B and C).

A PEST region can be predicted within the C-terminal region of DYRK1A (amino acids 472-517) according to ePESTFIND. In general, these domains are linked to the control of protein stability (Rogers et al., 1986); in some cases, phosphorylation of the PEST domains marks proteins for proteasomal-mediated degradation (Rechsteiner, 1990). Interestingly, the accumulation of DYRK1A^{522} deletion mutant, which is the shortest C-terminal deletion mutant that is stable when expressed in cells by transfection and still contains the PEST region (Fig. R17A), is affected by co-expression of NLK (Fig. R17B), and the protein levels were recovered

when the co-transfected cells were treated with the proteasome inhibitor MG132 (Fig. R17C). These results suggest that NLK target residues that are important to induce DYRK1A degradation are among the first 522 amino acids.

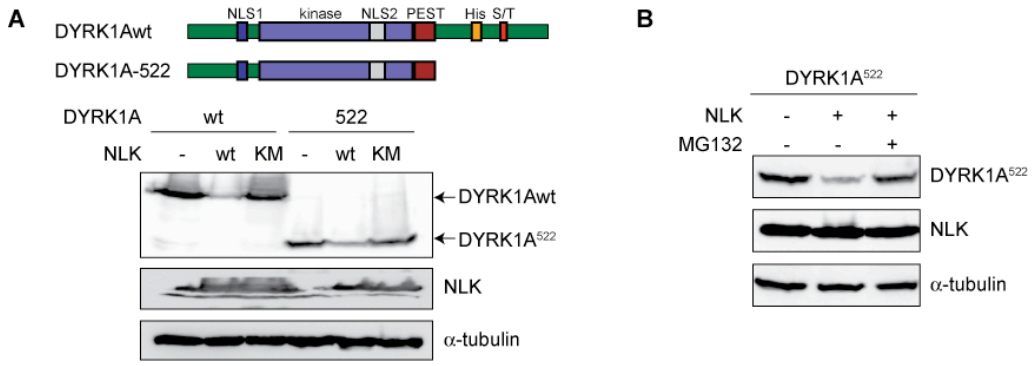

Figure R17: NLK affects the accumulation of DYRK1A^{522} deletion mutant. (A) Total cell extracts from HEK-293T cells expressing HA-DYRK1A wt or HA-DYRK1A^{522} (see scheme) together with Flag-NLK wt or the kinase-inactive mutant K167M (KM) were analyzed by immunoblot with anti-HA and anti-Flag. **(B)** HEK-293T cells expressing HA-DYRK1A^{522} alone or together with Flag-NLK were treated with 50 μM MG132 for 7 h or with control vehicle, and total cell lysates were prepared and analyzed by immunoblot with anti-HA and anti-Flag. Membranes were re-blotted with anti-α-tubulin to confirm equal loading.

NLK affects DYRK1A half-life through phosphorylation of multiple sites

Taking into account all the previous results, we considered the possibility of NLK inducing DYRK1A degradation by phosphorylating the PEST region. To check this possibility, we took advantage of the existence of a GFP-tagged DYRK1A fragment available in the group from amino acid 378 to 522, which contains the PEST region and the C-terminal part of the kinase domain (Fig. R18A). As Fig. 18B shows, the DYRK1A$^{378\text{-}522}$ fragment was phosphorylated by NLK in *IVK* assays, indicating the presence of residues that can be phosphorylated by NLK.

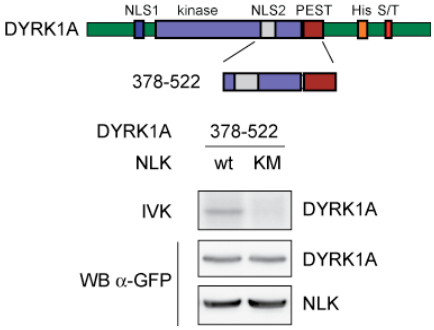

Figure R18: NLK phosphorylates DYRK1A at multiple sites close to the PEST region. Soluble extracts from HEK-293T cells expressing GFP-NLK and the GFP-tagged DYRK1A fragments indicated (see scheme) were immunoprecipitated with anti-GFP. Immunoprecipitated complexes were incubated with [γ^{32}P-ATP] in an *IVK* assay. Phosphorylated proteins were separated by SDS-PAGE and analyzed by autoradiography. Comparable amount of proteins were used as detected by Western blot analysis with anti-GFP.

The identification of the phosphorylatable sites was approached by using mass spectrometry analysis at the CRG/UPF Proteomics Facility. To this end, *IVK* assays were carried out and the phosphorylated bands were separated by SDS-PAGE. The putative phosphoresidues identified are listed in Fig. 19A: threonine 393, threonine 422, serine 433, threonine 436, threonine 457 and serine 468. All of them are located N-terminal from the PEST region, and are conserved when DYRK1A proteins from different organisms are compared (Fig. R19B). These results suggest that NLK phosphorylates multiple sites in DYRK1A.

A

Phosphopeptide sequence	Mass observed	Mass calculated	Mass error	Charge	MASCOT Score	ΔScore
LPDGpTWNLKK	1250.6062	1250.6060	0.18	2	31	22
KLHNILGVEpTGGPGGR	1683.8451	1683.8458	- 1.60	3	62	56
AGEpSGHTVADYLK	1426.6106	1426.6130	- 1.62	2	67	20
AGESGHpTVADYLK	1426.6118	1426.6130	- 0.78	2	69	11
MLDYDPKTR	1217.5142	1217.5152	- 0.74	2	26	7
IQPYYALQHpSFFK	1720.8000	1720.8014	- 0.80	2	65	40

B

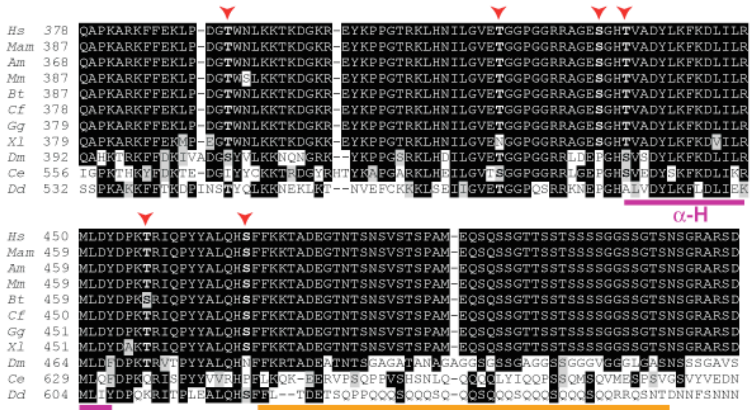

Figure R19: Identification of the residues phosphorylated by NLK by mass spectrometry. (A) The identification of the phosphorylated residues by NLK in the DYRK1A fragment 378-522 by mass spectrometry was carried out as explained in Materials and Methods. The table shows only those sites that appeared in two independent experiments. **(B)** Alignment of the equivalent regions to human (Hs) DYRK1A 378-522 in other DYRK1A proteins from several organisms (see Annex 2 in Material and Methods for Accession numbers), with the invariant residues in black and the conserved ones in grey. The predicted PEST region is underlined in orange and the α-helix H of the catalytic domain in purple. NLK-phosphorylated amino acids detected in human DYRK1A are shown with red arrows.

To confirm the mass spectrometry data, all the six phosphorylatable sites were mutated into alanine in the fragment DYRK1A$^{378\text{-}522}$ and found that the phosphorylation by NLK of this mutant was heavily decreased (Fig. R20A). More importantly, a similar result was observed when the full-length protein DYRK1A^{KR} with

all the residues mutated to alanine was used in the *IVK* assays (Fig. R20B), strongly suggesting that these six amino acids are the major NLK phosphorylatable sites.

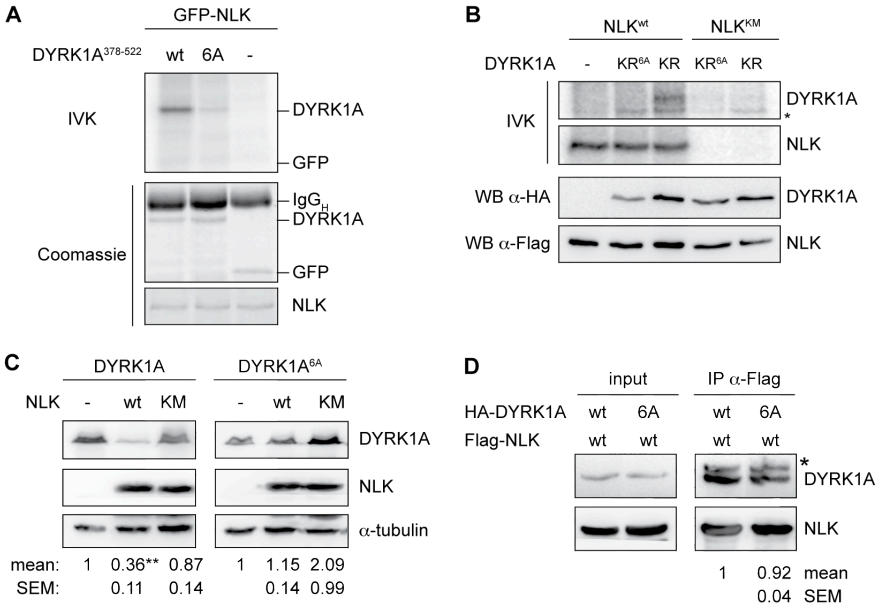

Figure R20: NLK affects DYRK1A half-life through phosphorylation of multiple sites. (A) Soluble extracts from HEK-293T cells expressing GFP-NLK and GFP-DYRK1A$^{378-522}$ (wt), the equivalent fragment with the 6 phosphorylatable residues mutated to alanine (6A) or unfused GFP as a control (-) were immunoprecipitated with anti-GFP and subjected to an *IVK* assay with [γ^{32}P-ATP]. Phosphorylated proteins were separated by SDS-PAGE, stained with Coomassie to confirm equal loading, and analyzed by autoradiography. **(B)** Soluble extracts from HEK-293T cells expressing Flag-NLK (wt) or its kinase-inactive version (KM) and HA-DYRK1A^{KR} or the equivalent fragment with the 6 phosphorylatable residues mutated to alanine (6A) were immunoprecipitated with anti-Flag and anti-HA antibodies, and processed as described in (**A**). Comparable amounts of proteins were used as detected by Western blot with anti-HA or anti-Flag. **(C)** Total cell extracts from HEK-293T cells expressing HA-DYRK1A wt or HA-DYRK1A^{6A} and Flag-NLK wt or its kinase-inactive version (KM), as indicated, were analyzed by immunoblot with anti-HA and anti-Flag. Membranes were re-blotted with anti-α-tubulin to confirm equal loading. The quantification of DYRK1A accumulation is shown with the data corresponding to means ± SEM of two independent experiments in which the values for DYRK1A (wt or 6A) in the absence of NLK were set as 1. (**p<0.01) (**D**) Soluble cell extracts from HEK-293T cells expressing HA-DYRK1A wild type (wt) or the mutant with the 6 phosphorylatable residues mutated to alanine (6A) and Flag-NLK were immunoprecipitated with anti-Flag antibody. Immunoprecipitated proteins (IP) and cell lysates (5% of input) were analyzed by Western blot with anti-Flag and anti-HA. The quantification of the relative binding to NLK is shown (DYRK1A in the immunoprecipitated/DYRK1A in the lysate) with the data corresponding to means ± SEM of two independent experiments in which the values of DYRK1Awt were set as 1.

Finally, the accumulation of the non-phosphorylatable DYRK1A^{6A} mutant protein in response to NLK was analyzed in comparison the wild-type protein. No significative changes were observed in the amount of accumulated DYRK1A^{6A} protein when expressed alone or in the presence of NLK (Fig. R20C), indicating that the DYRK1A mutant is resistant to the NLK effect. One possibility to consider when interpreting these results is that NLK does not affect the accumulation of DYRK1A^{6A}

because the mutations have altered the interaction DYRK1A-NLK, something that we have previously proven to be required for the effect. To test this possibility, immunoprecipitation experiments using HA-DYRK1Awt or HA-DYRK1A^{6A} and Flag-NLK were performed. As Figure R20D shows, the relative binding to NLK of the DYRK1A^{6A} deletion mutant was similar to that of DYRK1Awt, suggesting that the interaction was not affected by the mutations. Altogether, these results suggest that the six amino acids described above represent the major sites by which NLK affects DYRK1A half-life through phosphorylation.

The Wnt1/Wnt3a-Fzd1-HIPK2-NLK signaling cascade affects DYRK1A half-life

Another substrate of NLK, c-Myb, is phosphorylated and degraded by the proteasome upon Wnt1 signal via the pathway involving Fzd1, HIPK2 and NLK (Kanei-Ishii et al., 2004; Kanei-Ishii et al., 2008). Based on the similarity between NLK-induced DYRK1A and c-Myb phosphorylation and degradation, it is possible that upon specific stimuli, this signaling cascade has a role in the regulation of DYRK1A protein degradation. To test this hypothesis, we analyzed total cell extracts from HEK-293T cells transfected with DYRK1A alone or together with plasmids expressing different members of the Wnt1-Fzd1-HIPK2-NLK signaling cascade. To check whether the HIPK2-NLK cascade can be activated by other Wnt ligands, the effect of Wnt3a or Wnt5a was also analyzed. A decrease in DYRK1A protein levels was observed when it was co-expressed with Wnt1, Wnt3a, Fzd1, HIPK2 and NLK (Fig. R21), while Wnt5a signal, which activates Ca^{2+}/CAMKII/TAK1/NLK signaling pathway (Ishitani et al., 2003), does not seem to affect DYRK1A protein stability. These results suggest that Wnt1 and Wnt3a, the main activators of Wnt/β-catenin signaling pathway, induce DYRK1A degradation via the pathway involving Fzd1, HIPK2 and NLK.

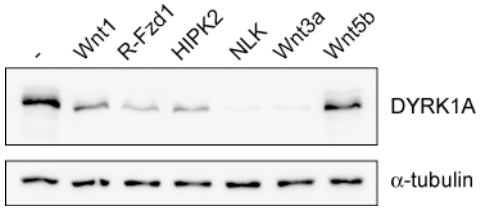

Figure R21: The Wnt1/Wnt3a-Fzd1-HIPK2-NLK signaling cascade affects DYRK1A half-life. Total cell extracts from HEK-293T cells expressing HA-DYRK1A wt alone or together with the indicated proteins, were analyzed by immunoblot with anti-HA antibody. Membranes were re-blotted with anti-α-tubulin to confirm equal loading.

DYRK1A is a positive regulator of the transcriptional activity of a β-catenin-dependent reporter

Given that DYRK1A seems to be an NLK target and Wnt1/Wnt3a is able to regulate DYRK1A protein stability, we decided to investigate whether DYRK1A can influence Wnt signaling. As a starting point, the effect of DYRK1A on the transcriptional activity of a β-catenin/TCF-dependent reporter was analyzed. The analysis was based on a reporter plasmid in which the luciferase gene is under the control of TCF/LEF-binding sites (Korinek et al., 1997). The transcriptional activity was induced by exogenous expression of a β-catenin mutant -S33Y- a natural mutant that has a substitution of one of the GSK-3 phosphorylated residues by an unphosphorylatable residue resulting in the stabilization of β-catenin (Kolligs et al., 1999). The system is controlled by the use of a modified reporter, FOPFLASH, in which the TCF/LEF binding sites are mutated (Veeman et al., 2003).

DYRK1A co-expression with suboptimal levels of β-catenin^{S33Y} resulted in a dose-dependent increase on the transcriptional activity (Fig. R22). Notably, co-expression of the DYRK1A kinase-inactive form did not altered the β-catenin-dependent transcriptional activity (Fig. R22), suggesting that DYRK1A can enhance β-catenin-dependent transcriptional activity in a kinase-dependent and dose-dependent manner.

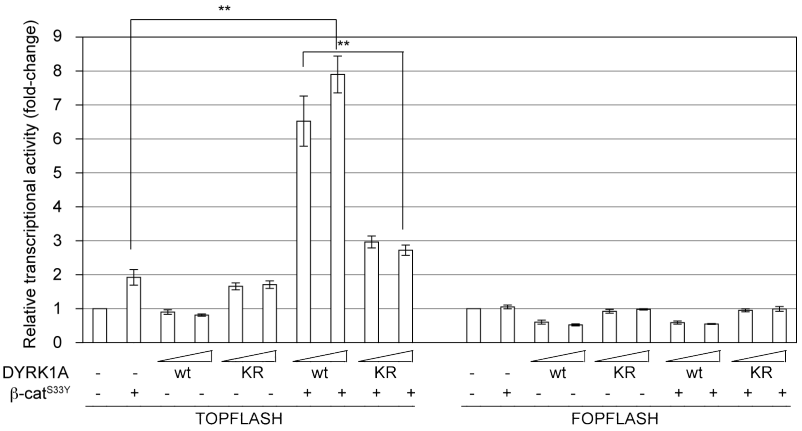

Figure R22: DYRK1A induces the transcriptional activity of β-catenin-dependent reporter. HEK-293 cells were co-transfected with pTOPFLASH reporter or with pFOPFLASH reporter, pβCat^{S33Y} and pCMV-RNL plasmids together with expression plasmids encoding DYRK1A wild type (WT: 1 μg, 2 μg) or mutant K179R (KR: 1 μg, 2 μg) as indicated. Luciferase activity was measured in triplicate plates and values were corrected for transfection efficiency as measured by Renilla activity. Data are represented as the mean of three independent experiments ± SEM in which the value corresponding to the basal activation was arbitrarily set as 1. (**p<0.01)

Next, we wondered whether DYRK1A could directly act on TCF-4/LEF-1, the other component of the TCF/β-catenin transcription complex. Thus, the cooperation of DYRK1A with TCF-4 was tested in the transcriptional assay, but no effect was detected (Fig. R23). Moreover, we observed in these experiments that DYRK1A exogenous expression results in a dose-dependent and kinase-dependent decrease on the transcriptional activity on the reporter (Fig. R22 and R23). These results would indicate that DYRK1A needs the presence of a nuclear β-catenin to act as a positive regulator of β-catenin-dependent transcriptional activity.

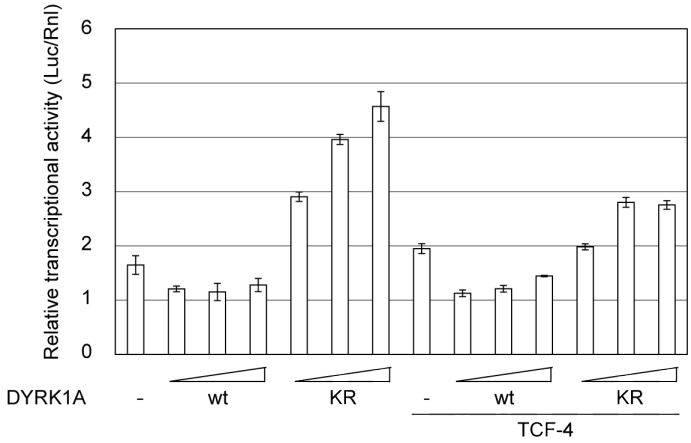

Figure R23: DYRK1A needs β-catenin to enhance the transcriptional activity of TCF-4/LEF-1. HEK-293 cells were co-transfected with the TOPFLASH reporter, pCMV-TCF-4 and pCMV-RNL plasmids together with expression plasmids encoding DYRK1A wild type (WT) or the kinase-inactive mutant K179R (KR) as indicated. Luciferase activity was measured in triplicate plates. Values were corrected for transfection efficiency as measured by Renilla activity, and data are represented as the means ± SEM. The graph corresponds to a representative experiment of several performed.

To confirm the role of DYRK1A in the enhancement of β-catenin-dependent transcriptional activity, we took advantage of harmine, an inhibitor of DYRK1A kinase activity (Bain et al., 2007). Our group has shown that harmine acts as an ATP-competitive inhibitor for DYRK1A and inhibits DYRK1A kinase activity *in vivo* (Laguna et al., 2008). First, the ability of harmine to inhibit the DYRK1A enhancement in overexpressing conditions was tested. As shown in Figure R24A, the DYRK1A enhancement on β-catenin-dependent transcriptional activity was decreased when cells were treated with harmine. In agreement with this, when luciferase activity was induced by exogenous expression of β-catenin/S33Y, treatment of cells with increasing amount of the inhibitor (2-20μM) decreases the β-catenin-dependent transcriptional activity (Fig. R24B).

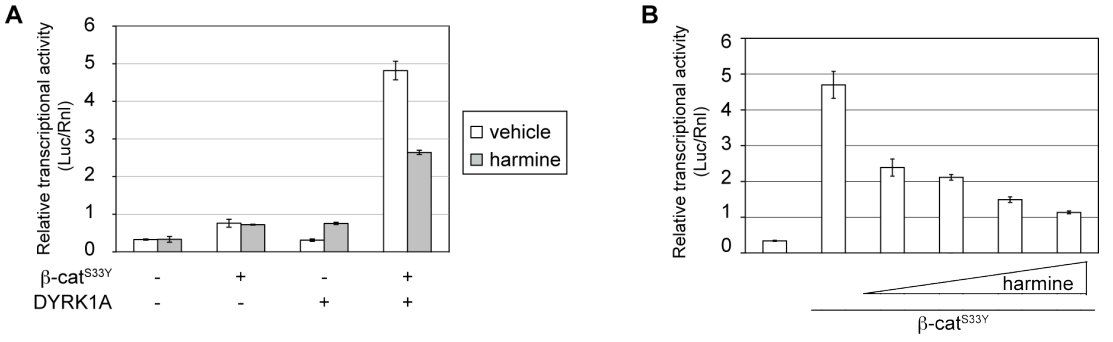

Figure R24: Harmine blocks DYRK1A enhancement on β-catenin-dependent transcriptional activity. (A) HEK-293 cells were co-transfected with pTOPFLASH reporter, pβCat^{S33Y} and pCMV-RNL plasmids together with an expression plasmid encoding DYRK1A as indicated. Cells were incubated with 10 μM harmine or DMSO as vehicle for 16 h at 24 h after transfection. Luciferase activity was measured in triplicate plates and values were corrected for transfection efficiency as measured by Renilla activity. Data are represented as the means ± SD. **(B)** HEK-293 cells were co-transfected with pTOPFLASH reporter, pβCat^{S33Y} and pCMV-RNL plasmids as indicated. Cells were incubated with harmine at different concentrations (2-20 μM) for 16 h at 24 h after transfection. Luciferase activity was measured in triplicate plates. Values were corrected for transfection efficiency as measured by Renilla activity, and data are represented as the means ± SEM. The graphs correspond to representative experiments of several performed.

DYRK1A interacts with β-catenin

An explanation for the findings presented above could rely on DYRK1A able to bind to the β-catenin/TCF complex. To address this possibility, co-immunprecipitation experiments were performed using cell extracts expressing different combinations of HA-DYRK1A, β-catenin^{S33Y} and/or TCF-4. As Figure R25A shows, both TCF-4 and β-catenin were present in the anti-DYRK1A immunocomplexes when these proteins were singly expressed with DYRK1A. These results would suggest that DYRK1A might interact with β-catenin and TCF-4 independently. Additionally, the two proteins were detected when they were both co-expressed with DYRK1A (Fig. R25A), indicating that none of them displaced the binding of the other and, moreover, that DYRK1A could form a ternary complex with the β-catenin/TCF transcriptional complex. This together with the fact that endogenous β-catenin appeared in the DYRK1A immunoprecipitation when TCF-4 was overexpressed suggest the possibility that this protein may recruit β-catenin to DYRK1A. To rule out this possibility, pull-down experiments were performed using bacterially expressed and purified proteins: unfused β-catenin and a GST-DYRK1A fusion protein. β-catenin was pulled down by the GST-DYRK1A fusion protein, but not by unfused GST (Fig. R25B), confirming that DYRK1A is able to directly bind to β-catenin.

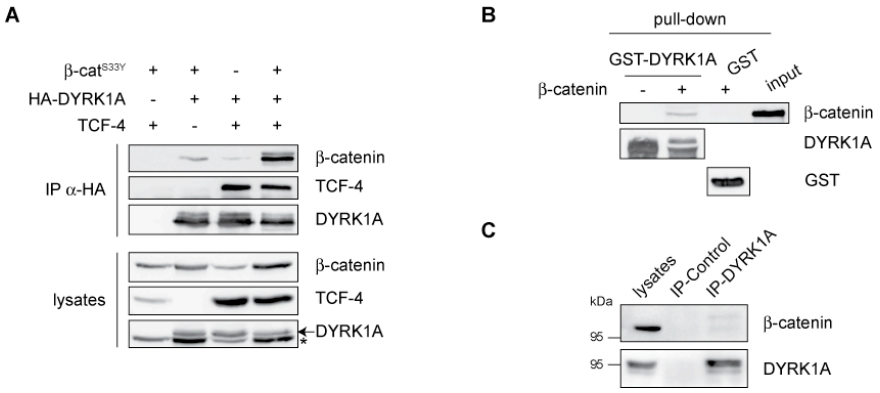

Figure R25: DYRK1A interacts with β–catenin. (A) Soluble extracts from HEK-293T cells expressing different combinations of HA-DYRK1A, TCF-4 and β-Cat^{S33Y} as indicated were immunoprecipitated with anti-HA. Immunoprecipitated proteins (IP) and cell lysates (5% of input) were analyzed by Western blot with anti-β-catenin, anti-TCF-4 and anti-HA. The asterisk indicates the signal of the re-blotting with β–catenin antibody. Note the presence of the endogenous β-catenin in the DYRK1A immunocomplexes. **(B)** Bacterially expressed and purified β-catenin was incubated with unfused GST or GST-DYRK1A immobilized on gluthatione-Sepharose beads. Bound protein was detected by Western blot with anti-β–catenin or anti-GST. Input β-catenin (10%) is shown. **(C)** HeLa nuclear lysates were immunoprecipitated with anti-DYRK1A or mouse IgG as a control antibody. Immunoprecipitated proteins (IP) and nuclear lysates (5% of input) were analyzed by Western blot with anti-DYRK1A and anti-β-catenin. The position of protein markers (in kDa) is shown.

β-catenin is a multifunctional protein, acting in cell adhesion, cytoskeletal regulation, and Wnt signaling (reviewed in Brembeck et al., 2006). The fact that DYRK1A enhances the transcriptional activity mediated by a constitutively stable, and therefore nuclear, β-catenin mutant suggests that the two proteins might interact in the nucleus. To test this, nuclear extracts from HeLa cells, in which both proteins were present (Fig. R25C) were used for immunoprecipitation experiments. Antibodies recognizing the endogenous proteins were used. As shown in Figure R25C, β-catenin was immunoprecipitated with DYRK1A in anti-DYRK1A immunocomplexes, but it was not precipitated by a control mouse IgG, confirming that β-catenin and DYRK1A can form complexes, at least in the nucleus.

DYRK1A forms a ternary complex with the β-catenin/TCF transcriptional complex

When analyzed the co-immunoprecipitation experiments in detail, we observed an increase in the amount of β-catenin in the DYRK1A immunocomplexes when TCF-4 was co-expressed (Fig. R25A). This was apparent even for the endogenous β-catenin recruited to the complexes. This observation suggests that DYRK1A may

increase the interaction between β-catenin and TCF-4. To support this idea, co-immunoprecipitation experiments were performed, but this time anti-TCF-4 immunocomplexes were subjected to analysis. In this case, both endogenous and overexpressed levels of β-catenin were increased when DYRK1A was co-expressed (Fig. R26A). Remarkably, the increment in β-catenin recruitment was not observed when the kinase inactive form of DYRK1A was co-expressed (Fig. R26B). This was not due to the inability of the inactive form to be recruited to the β-catenin-TCF-4 complexes because the mutant protein was present in the immunocomplexes (Fig. R26B). In conclusion, DYRK1A directly binds to at least β-catenin in the β-catenin/TCF transcriptional complex and enhances the interaction between the transcriptional co-activator β-catenin and the DNA-binding unit TCF-4, the latter effect depending on the kinase activity of DYRK1A.

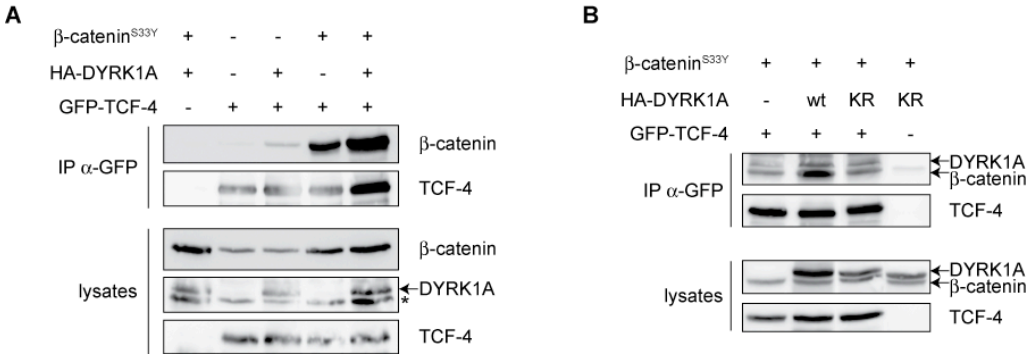

Figure R26: DYRK1A enhances the formation of TFC-4/β–catenin complexes through a phosphorylation event. (A) Soluble extracts from HEK-293T cells expressing HA-DYRK1A, GFP-TCF-4 and βCatenin^{S33Y} as indicated were immunoprecipitated with anti-GFP. Immunoprecipitated proteins (IP) and cell lysates (5% of input) were analyzed by Western blot with anti-β-catenin, anti-GFP and anti-HA. The asterisk indicates the signal of the re-blotting with the β–catenin antibody. **(B)** Soluble cell extracts from HEK-293T cells expressing HA-DYRK1A wt or its inactive-kinase mutant K179R (KR) together with GFP-TCF-4 and βCatenin^{S33Y} were immunoprecipitated with anti-GFP. Immunoprecipitated proteins (IP) and cell lysates (5% of input) were analyzed by Western blot with anti-HA, anti-GFP and anti-β-catenin.

DYRK1A phosphorylates β-catenin at multiple sites

The dependence of the β-catenin-transcriptional enhancement on DYRK1A kinase activity leads to the question of whether DYRK1A is able to phosphorylate any member of the β-catenin/TCF complex. To this aim, *in vitro* kinase experiments were performed using TCF-4 as substrate. Given that DYRK1A and TCF-4 have similar molecular weights, a catalytically active DYRK1A C-terminal deletion mutant - DYRK1A^{522}- was used, which allows to clearly distinguish the two protein in gels. As

shown in Fig. 27A, TCF-4 was phosphorylated in the presence of catalytically active DYRK1A, but not in the presence of the kinase inactive mutant, suggesting that TCF-4 is a DYRK1A substrate.

Next, we tested whether DYRK1A was able to phosphorylate β-catenin. For this purpose, *IVK* experiments were performed with bacterially expressed, purified GST-β-catenin and GST-DYRK1A. Incorporation of radioactive ATP in β-catenin was clearly detected by incubation with catalytically active DYRK1A, but not with the kinase inactive form (Fig. R27B). It is worthy to note that a slower-migrating band of β-catenin was observed when DYRK1A wild type was present both using soluble extracts (Fig. R25A and C) or bacterially expressed, purified proteins (Fig. R27B), suggesting that DYRK1A very likely phosphorylates β-catenin at several sites.

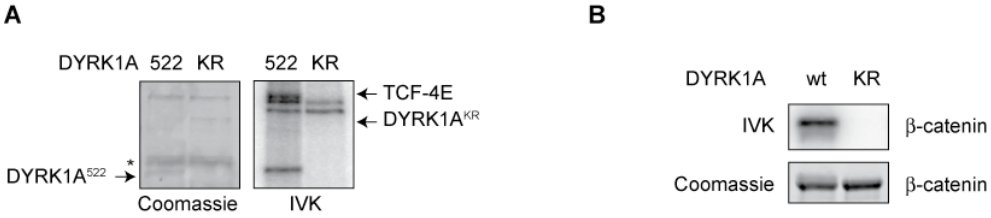

Figure R27: DYRK1A phosphorylates β–catenin and TCF-4. (A) Soluble extracts from HEK-293T cells expressing GFP-TCF-4 together with GFP-DYRK1A^{522} or GFP-DYRK1A^{KR} were subjected to immunoprecipitation with anti-GFP and incubated with [γ^{32}P-ATP] in an *in vitro* kinase assay. **(B)** Bacterially expressed, purified GST-β–catenin together with GST-DYRK1A wt or its inactive kinase version K179R (KR) were incubated with [γ^{32}P-ATP] in an *in vitro* kinase assay. In A and B, phosphorylated proteins were separated by SDS-PAGE, stained with Coomassie Blue to confirm equal loading, and analyzed by autoradiography.

To find the sites that are phosphorylated by DYRK1A in β-catenin, *in vitro* kinase assays were performed under cold conditions using bacterially expressed, purified DYRK1A as source of enzyme and β-catenin as substrate. Phosphorylated proteins were separated by SDS-PAGE, the band corresponding to β-catenin excised from the gel, and the phosphorylation sites identified by mass spectrometry. As shown in Figure R28A, four phosphorylated peptides were repeatedly found in independent experiments, and the mass spectrometry results indicated that some of these peptides could be phosphorylated in one or two residues, although the exact residue could not be accurately assigned.

A

Residue	exp1	exp2	exp3	exp4	Peptide
S29, S33, S37, T41	+	+	+	+	KAAVSHWQQQSYLDSGIHSGATTTAPSLSGK
S129	+		+		RLAEPSQMLK
T551, S552, T556	+	+	+	+	RTSMGGTQQQFVEGVR
S675, S679, S680, S681	+		+	+	RLSVELTSSLFR

B

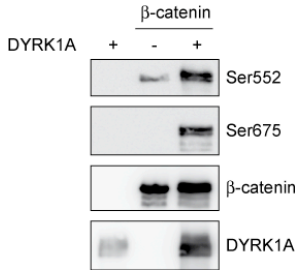

Figure R28: DYRK1A phosphorylates β–catenin at multiple sites. (A) The identification of the phosphorylated residues by DYRK1A in β–catenin by mass spectrometry was carried out as explained in Materials and Methods using bacterially expressed, purified GST-β–catenin and GST-DYRK1A. The table shows the summary of four independent experiments. The sequence of the phosphorylated peptides and the residue number are shown. **(B)** Bacterially expressed GST-β–catenin and GST-DYRK1A were immobilized on gluthatione-Sepharose beads and bound proteins were used in an *in vitro* kinase assay. Unfused GST (-) was used as control. Samples were analyzed by Western blot with the anti-phospho-β-catenin antibodies indicated to detect the phosphorylated residues, with anti-β-catenin as a loading control, and with anti-HA to detect the presence of DYRK1A. Note that anti-phosphoSer552 shows cross-reaction with non-phosphorylated β-catenin.

One of the peptides identified in the analysis contains Ser33, Ser37 and Thr41, the residues known to be phosphorylated by GSK-3β that trigger β-catenin proteasome-dependent degradation. Given that a constitutively stable form of β-catenin in which Ser33 is mutated was used in the transcription assays, these sites, if phosphorylated, should not be relevant for the DYRK1A effect observed in the transcription assays. For this reason, they were not further analyzed.

Two other peptides were located in the C-terminal part of the β-catenin armadillo repeats, in a region to which regulatory functions on the transcriptional activity have been associated (see *Introduction*). To validate the mass spectrometry analysis, we took advantage of the existence of commercial antibodies that specifically recognize phosphoSer552 and phosphoSer675 residues. Thus, bacterially expressed, purified β-catenin was phosphorylated by bacterially expressed DYRK1A and analyzed by Western blot with these antibodies. As Figure R28B shows, the phosphospecific antibodies detected β-catenin only when GST-DYRK1A was present in the experiment, but not when unfused GST was added. These results confirmed that DYRK1A phosphorylates β-catenin in, at least, Ser552 and Ser675.

DYRK1A enhances β-catenin-dependent transcriptional activity through phosphorylation of serine residues 552 and 675

Based on their similarity to the DYRK1A consensus phosphorylation sequence and according to their functional roles described by other groups (Fang et al., 2007; Hino et al., 2005; Taurin et al., 2006), we focused on Ser129, Ser552 and Ser675 as putative DYRK1A target sites. To find out which of them are responsible for the DYRK1A-dependent enhancement of the β-catenin-dependent transcriptional activity, Ser-to-Ala mutations were introduced into β-catenin/S33Y in these residues and the ability of DYRK1A to enhance the transcriptional activity of these β-catenin mutant forms was analyzed. For β-catenin serine residue 129, the increase in transcriptional activity mediated by DYRK1A was comparable to the non-mutated β-catenin (Fig. R29A), suggesting that DYRK1A phosphorylation on this residue is not responsible for the transcriptional enhancement. However, when a β-catenin protein with mutations in Ser552 or Ser675 was assayed, DYRK1A enhanced transcription to a considerably lesser extent than to the corresponding non-mutated β-catenin, although statistical analysis of four independent experiments suggests that the observed differences are significant only for the data obtained with the Ser675-to-Ala mutant (Fig. R29B). Notably, the DYRK1A-dependent enhancement was even lesser when a β-catenin protein with the two residues mutated to alanine was assayed. All these data together suggest, that DYRK1A enhances β-catenin-dependent transcriptional activity through phosphorylation of serine residue 675.

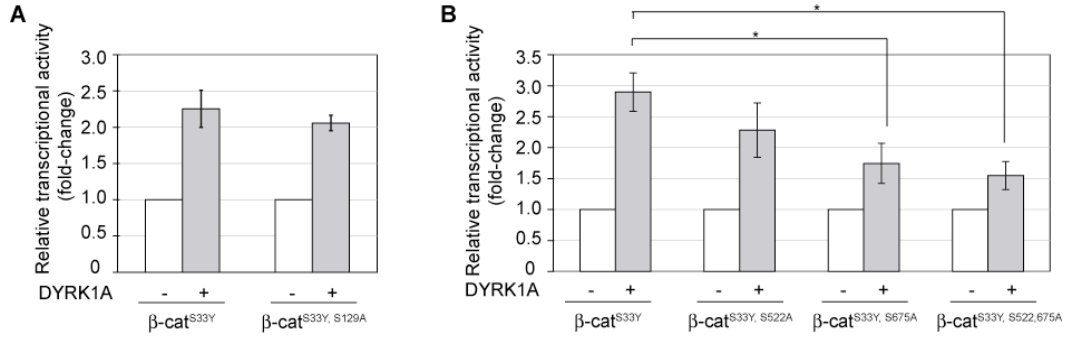

Figure R29: DYRK1A enhances β-catenin-dependent transcriptional activity through phosphorylation of serine residue 675. HEK-293 cells were co-transfected with pTOPFLASH, pCMV-RNL, pβCat-S33Y or the indicated mutants in the absence (white bars) or presence (grey bars) of HA-DYRK1A expression plasmid as indicated. Values were corrected for transfection efficiency as measured by Renilla activity. Histograms show DYRK1A enhancement of β–catenin transcriptional activity where the basal transcriptional activity of each β–catenin mutant was set as 1. Data show means ± SEM of three independent experiments in which each value was measured in triplicate plates.

NLK inhibits the DYRK1A enhancement on the β-catenin-dependent transcriptional activity.

Finally, given that DYRK1A and NLK have opposite effects on β-catenin-dependent transcriptional activity and that NLK negatively regulates DYRK1A protein stability, we analyzed how NLK affects DYRK1A enhancement of the TOPFLASH β-catenin-dependent transcriptional activation. Co-transfected NLK inhibited the DYRK1A-dependent enhancement of the transcriptional activity in a kinase-dependent and dose-dependent manner (Fig. R30).

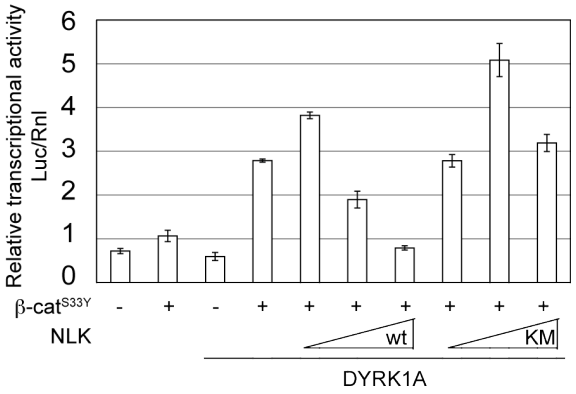

Figure R30: NLK inhibits the DYRK1A enhancement on the β-catenin-dependent transcriptional activity. HEK-293 cells were co-transfected with the TOPFLASH reporter, pβCat^{S33Y} and pCMV-RNL plasmids together with expression plasmids encoding NLK wt or mutant K167M (KM) and DYRK1A as indicated. Luciferase activity was measured in triplicate plates. Values were corrected for transfection efficiency as measured by Renilla activity, and data are represented as the means ± SEM. The graph corresponds to a representative experiment of several performed.

As a final summary, all the data presented strongly suggest that nuclear DYRK1A acts as a positive effector of Wnt/β-catenin signaling, while NLK interferes with the co-activating ability of DYRK1A by changing the half-life of this protein. The Wnt1/Wnt3a-Fzd1-HIPK2 signaling cascade is responsible for NLK-mediated DYRK1A degradation, which suggest the existence of a negative regulatory feed-back loop to switch off β-catenin-mediated transcription.

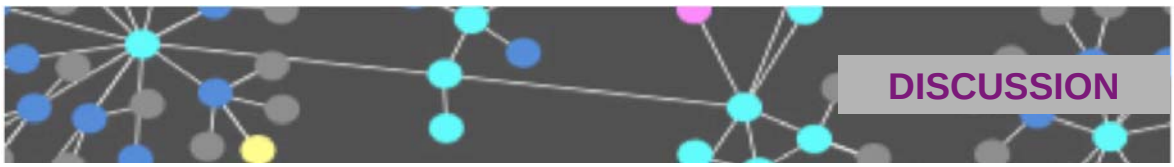

DISCUSSION

The protein kinases DYRK1A and NLK interact

In this thesis work, the interaction between the protein kinases DYRK1A and NLK has been demonstrated. The two proteins have been found in complexes not only when overexpressed by transfection but also in HeLa nuclear extracts confirming therefore that the interaction exists in physiological conditions. The interaction is independent of the kinase activity of each of the proteins. Furthermore, the fact that the two proteins interact in pull-down experiments with NLK expressed in bacteria and DYRK1A in rabbit reticulocyte extracts support that DYRK1A and NLK interact directly.

The region in DYRK1A involved in the interaction with NLK has been defined between amino acids 70-104 at the N-terminus of the protein. This region consists of a group of hydrophobic residues and it putatively overlaps with a 14-3-3 interacting region identified in the first 125 N-terminal amino acids (Alvarez et al., 2007). We do not know whether the two interacting domains really overlap or whether the DYRK1A interaction with 14-3-3 has any implication for the DYRK1A/NLK interaction. Furthermore, based on the fact that the deletion of the N-terminal binding region does not completely abrogate the interaction, we cannot exclude that other regions in DYRK1A are involved in the interaction and suggest that the kinase domain could be one of them (see below). Given that not many binding regions in DYRK1A with other partners have been defined to date, this work also contributes to define a novel protein-protein interacting surface in DYRK1A (Fig. D1).

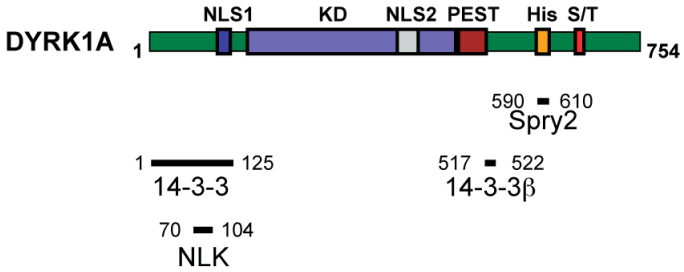

Figure D1: Interacting domains in DYRK1A. Schematic representation of DYRK1A regions important for the interaction with other molecules: 14-3-3 (Alvarez et al., 2007; Kim et al., 2004); Spry2 (Aranda et al., 2008). Position for the first and last amino acid for each region is shown.

The NLK-binding region at the N-terminus of DYRK1A is located at close vicinity to the NLS1. However, our results suggest that DYRK1A NLS1 is not involved in the interaction, and immunostaining experiments in cells overexpressing the two proteins supported the idea that the binding of NLK does not affect the intracellular localization of DYRK1A.

Our data indicate that NLK can interact with all human DYRK kinases, although with different efficiency. The NLK-interacting domain located at the DYRK1A N-terminus shows sequence similarity with the corresponding region in its closest paralogous DYRK1B, and the sequence homology would therefore account for the similar binding efficiency shown by the two proteins. However, the other DYRK family members do not share sequence similarity within this region. The homology among them is restricted to the conserved catalytic domain. Thus, the fact that they all bind NLK suggests that there should be another common interacting region, possibly within the kinase domain, that could also represent a secondary binding site for DYRK1A. As the DYRK family members differ in their expression levels in different tissues and cell lines, it is plausible to think that this may contribute to the physiological function associated to the interaction with NLK.

A region in NLK required for DYRK1A interaction has been defined between amino acids 430-444 at the C-terminus of the protein. This region, which is highly convserved in all NLK orthologs, is located downstream the subdomain XI outside the catalytic domain (Fig. D2).

```
Homo sapiens          402 HLLCRMLVFDPSKRISAKDALAHPYLDEGRLRYHTCMCKCCFSTSTG--RVYT 452
Pan troglodytes       402 HLLCRMLVFDPSKRISAKDALAHPYLDEGRLRYHTCMCKCCFSTSTG--RVYT 452
Bos taurus            402 HLLCRMLVFDPSKRISAKDALAHPYLDEGRLRYHTCMCKCCFSTSTG--RVYT 452
Canis familiaris      402 HLLCRMLVFDPSKRISAKDALAHPYLDEGRLRYHTCMCKCCFSTSTG--RVYT 452
Mus musculus          402 HLLCRMLVFDPSKRISAKDALAHPYLDEGRLRYHTCMCKCCFSTSTG--RVYT 452
Gallus gallus         402 HLLCRMLVFDPSKRISAKDALAHPYLDEGRLRYHTCMCKCCFSTSTG--RVYT 452
Takifugu rubripes     317 HILCRMLVFDPSKRISAKDALAHPYLDEGRLRYHTCMCKCCYTTSSG--RVYT 368
Danio rerio           352 HLLCRMLVFDPAKRISGSDALSHPYLDEGRLRYHTCMCKCCYSVPSG--RVYT 402
D. melanogaster       305 HLLCQMLVFDPDKRISVTDALAHPYLDEGRLRYHSCMCKCCFTTSAGM-RQYT 355
C. elegans            473 DLLQKLLHFDPDKRISVEEALQHRYLEEGRLRFHSCMCSCCYTKPNMPSRLFA 525
                              Subdomain XI              Δ430-444
```

Figure D2: Sequence alignment of NLK orthologs. Amino acid sequence alignment of NLK proteins from different species. The corresponding Accession numbers are listed in Annex 2 in Materials and Methods. The position of subdomain XI in the catalytic domain and the deleted region in $NLK^{\Delta 430-444}$ is shown. The cysteine residue 541 in *C. elegans* LIT-1 that when mutated rendered a null mutant (Meneghini et al., 1999) is in red.

Furthermore, considering that the interaction with DYRK1A was not completely abolished when $NLK^{\Delta 430-444}$ was used, it is thus possible that a second binding domain may exist. For instance, ERK2 binds its regulators and substrates by two distinct protein-protein interaction sites, one the CD-domain and a second region overlapping with the N-lobe within the kinase domain (Zhang et al., 2003). The presence of two interacting sites in NLK would increase binding affinity for DYRK1A. As in the case of DYRK1A, very few interacting domains have been defined in NLK to date and the one identified in this thesis work represents a novel one (Fig. D3).

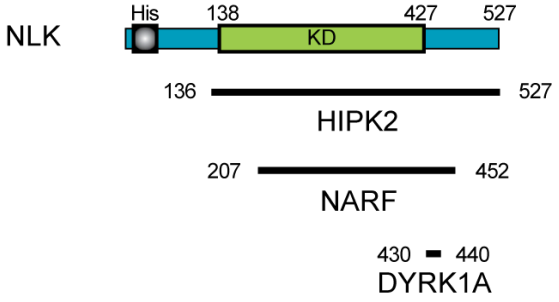

Figure D3: Summary of binding domains in NLK. Schematic representation of NLK regions important for the interaction with other molecules such as HIPK2 (Kanei-Ishii et al., 2004) and NARF (Yamada et al., 2006). The position of the first and last amino acid numbers is shown. As the interacting domains in HIPK2 and NARF have been defined roughly, it is difficult to predict whether they overlap with the defined DYRK1A binding region or not.

The interacting region in NLK would be located similarly to the CD-domain of MAPKs (Fig. D4) (Tanoue et al., 2000). The CD-domain is used for docking MAPKs to their activators, inhibitors and substrates and whose deletion of the CD-domain in MAPKs renders these kinases inactive due to inefficient activation (reviewed in Murphy and Blenis, 2006). The amino acid sequence of NLK in this region does not show any homology to other CD-domain sequences (Fig. D4). However, in the NLK orthologue in *C. elegans*, LIT-1, the cysteine residue 541, located in the middle of the DYRK1A interacting region, was found to be important for LIT-1 activity during embryo development (Meneghini et al., 1999). Interestingly, we found that the NLK mutant lacking this region, $NLK^{\Delta 430\text{-}444}$, is catalytically inactive (data not shown). Although we cannot exclude that the deletion could have altered the proper folding of the adjacent kinase domain, two plausible situations can account for the result. One possibility is that NLK requires the phosphorylation of residues within this domain to be active, since the region includes a highly conserved tyrosine and threonine residue (Fig. D2). Alternatively, the mutant protein lacks the binding domain for the upstream activating kinase. It is worthwhile to mention that the lack of activity of the bacterially expressed protein confirms that NLK needs to be phosphorylated by an upstream kinase for full activation, as suggested by others (Brott et al., 1998; Kanei-Ishii et al., 2004). It has been also reported that an NLK mutated on the cysteine residue 437, equivalent to LIT-1 Cys541, loses its ability of interacting with TCF-4 (Ishitani et al., 1999). All these observations lead us to propose that the identified region in NLK may act as a CD-domain, in the sense that this protein region may act as a recruitment platform for NLK activators, inhibitors or substrates. Thus, it could be also hypothesized that DYRK1A and TCF-4 binding domains in NLK overlap or are close and that the two proteins may compete for binding to NLK.

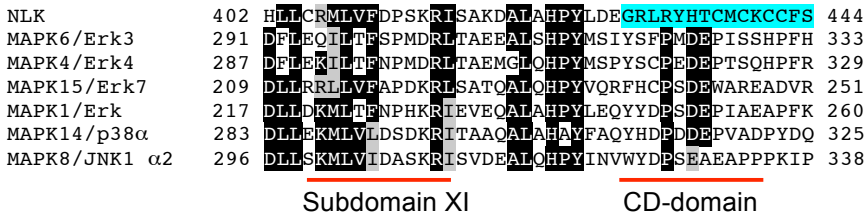

Figure D4: Sequence alignment of MAPKs. Amino sequence alignment of different human MAPKs in the region indicated. The corresponding accession numbers are listed in Annex 2 in Materials and Methods. The locations of subdomain XI in the catalytic domain and CD-domain are indicated. The amino acid region deleted in NLK mutant Δ430-444 is boxed in blue.

To organize the specific signaling cascades, MAPKs usually interact with their upstream MAPKKs by using the CD-domain and MAPKKs interact with their downstream MAPKs by using a region known as the D-site that is located outside the catalytic domain in the N-terminal region of the kinases (Fig. D5). It is worthwhile to note that the interacting region in NLK would correspond to the CD domain in MAPKs and the interacting region in DYRK1A locates similarly to the D-site in MAPKKs (Fig. D5) opening the possibility that DYRK1A might be an upstream kinase for NLK, a possibility that needs to be further explored.

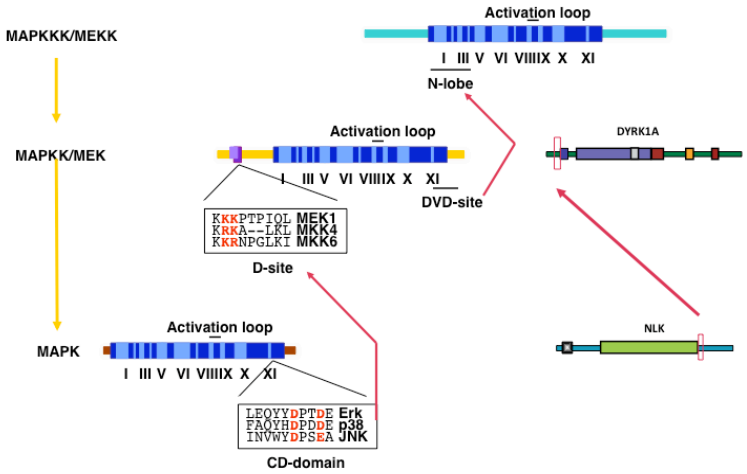

Figure D5: Physical relationship in MAPK signaling cascades. Schematic representation of docking domains in the MAPK modules and the binding sites in DYRK1A and NLK defined in this work. The amino acid sequences of the docking domains in classical MAPKs are highlighted. Key amino acids for the interaction are in red.

DYRK1A is a substrate of NLK

We propose that DYRK1A is phosphorylated by NLK, based in the fact that DYRK1A is phosphorylated by immunocomplexes prepared from cell extracts that contain an active NLK and not when a catalytically inactive mutant is present in the complexes.

However, we cannot exclude the possibility that DYRK1A is not phosphorylated directly by NLK, but by another kinase present in the immunocomplexes and activated by NLK. This possibility could be tested using purified proteins. However, NLK expressed in *E. coli* is catalytically inactive (data not shown), precluding these experiments.

We have found that NLK co-expression induces a decrease in the accumulation of DYRK1A in a kinase-dependent manner. In agreement, and supporting that the effect is not an artifact resulting from the overexpression of both proteins, down-regulation of NLK endogenous protein levels by using a specific shRNA leads to an increase in the accumulation of endogenous DYRK1A protein. Moreover, NLK does not affect accumulation of a DYRK1A deletion mutant that is not able to interact with NLK. All these results indicate that the interaction of DYRK1A with NLK and its subsequent phosphorylation controls DYRK1A accumulation.

The effect of NLK on DYRK1A protein accumulation could be the result of either NLK repressing DYRK1A expression and/or accelerating degradation of the protein. The results obtained with pulse-chase experiments show that NLK-dependent phosphorylation affects the half-life of DYRK1A protein. It is worth to note that NLK is involved in the proteasome-mediated degradation of some of its target molecules, such as c-Myb (Kanei-Ishii et al., 2004), TCF-4 and LEF-1 (Yamada et al., 2006). Using proteasome inhibitors we have found that NLK-induced phosphorylation also marks DYRK1A for proteasome-mediated degradation. In the case of TCF-4/LEF-1 and c-Myb, NLK phosphorylation targets these proteins for binding to the E3 ubiquitin ligases NARF (Yamada et al., 2006) and Fbxw7, respectively (Kanei-Ishii et al., 2008). It is therefore possible that NLK-induced phosphorylation also triggers ubiquitination of DYRK1A by a yet unknown E3 ubiquitin ligase (Fig. D6). Alternatively, either DYRK1A/NLK interaction or DYRK1A phosphorylation by NLK could induce changes in the interaction of DYRK1A with other binding partners that might lead to changes in its half-life.

The phosphorylation sites responsible for DYRK1A degradation have been identified by mass spectrometry analysis and further validated by mutation. At least, six serine and threonine residues in DYRK1A are phosphorylated by NLK. A consensus phosphorylation sequence has not been described yet for NLK. Although many of its substrates show a proline residue at the +1 position, other substrates do not comply with this rule, as is the case for Paxillin (KQK<u>S</u>A) (Ishitani et al., 2009) and the twenty-two sites identified in FOXO4 (Szypowska et al., 2010). Thus, the fact

that none of the DYRK1A phosphorylated sites have a proline at P+1 is not so surprising, and we should consider that in some cases other mechanisms might exist to direct the specificity of NLK towards its substrates. One such mechanism could be a tight interaction with its substrates through docking sites, as described above. The phosphorylated sites in DYRK1A are located just N-terminal to the PEST region. In general, PEST sequences are potentially involved in the regulation of protein stability (Rogers et al., 1986); in some cases, phosphorylation of the PEST domains marks proteins for proteasome-mediated degradation (Rechsteiner and Rogers, 1996; Garcia-Alai et al., 2006). The mass spectrometry analysis did not completely cover the PEST region sequence, and therefore, we cannot exclude that NLK phosphorylates sites within the PEST region of DYRK1A. If this were the case, they would be not critical for the NLK-dependent regulation of DYRK1A half-life, because mutation of the six phosphorylatable sites in DYRK1A makes it resistant against NLK-induced degradation. Nonetheless, it is possible that NLK phosphorylates other sites in DYRK1A, and that phosphorylation at a minimum number of sites or a combination of specific sites may be sufficient to induce the degradation of DYRK1A.

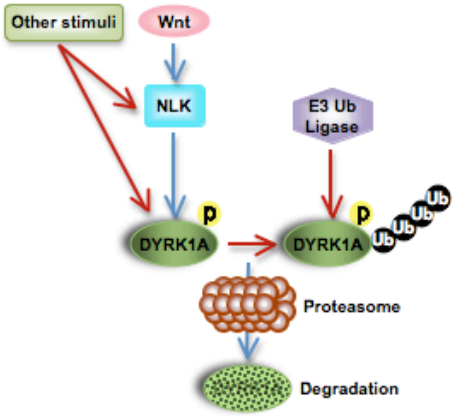

Figure D6: Mechanism to regulate DYRK1A protein stability. Schematic representation of the findings of this work on the regulation of DYRK1A protein stability by NLK. The functional relationships found in this work are depicted with blue arrows. Hypothetical relationships or to-be-identified links are depicted with red arrows.

Most importantly, we have shown that NLK-dependent DYRK1A degradation can be induced by the Wnt1/Wnt3a-Fzd1-HIPK2 signaling cascade (Fig. D6). Another substrate of NLK, c-Myb, is phosphorylated and degraded by the proteasome upon Wnt1 signal via the pathway involving Fzd1, HIPK2 and NLK contributing thus to the inhibition of the undifferentiated state in hematopoietic cells (Kanei-Ishii et al., 2004; Kanei-Ishii et al., 2008). Thus, it is possible that DYRK1A could interact with Wnt signaling in some physiological contexts and furthermore, that Wnt-activated NLK would regulate the protein levels of several proteins involved in cellular responses to Wnt. Unfortunately, we have not yet identified a cellular context for the Wnt-DYRK1A

functional interaction and this would surely deserve future research. In addition to Wnt, other activators of NLK could also work in controlling DYRK1A activity. This could be the case of p38 (Ohnishi et al., 2010), which has been suggested to cross-talk with DYRK1A in other context (Seifert and Clarke, 2009) (Fig. D6).

In summary, this thesis work describes for the first time a mechanism for the regulation of the stability of the protein kinase DYRK1A. DYRK1A effects are sensitive to gene dosage, because both gain-of-copy and loss-of-copy of *Dyrk1A* leads to alterations in the development and function of the CNS (Ahn et al., 2006; Altafaj et al., 2001; Benavides-Piccione et al., 2005; Branchi et al., 2004; Fotaki et al., 2002; Martinez de Lagran et al., 2004; Smith et al., 1997). Any change in the regulation of DYRK1A kinase activity or DYRK1A protein amounts, might therefore lead to severe physiological dysfunctions. To date, binding of the 14-3-3β or the SPRED1/2 proteins have been shown to regulate positively and negatively the catalytic activity of DYRK1A, respectively. The regulation of DYRK1A protein stability had not been studied yet and we propose that it could be one of the mechanisms contributing to regulate appropriate DYRK1A levels. Results from our lab suggest that DYRK1A protein levels change during the cell cycle (C. di Vona, S. de la Luna, unpublished results) and during the differentiation of mesenchymal precursor cells into adipocytes (K. Arato, S. de la Luna, unpublished results). We do not know yet whether these effects depend on NLK phosphorylation, although it could be possible that DYRK1A protein levels could be regulated by other signals depending on the cellular context.

DYRK1A plays a positive role on β-catenin-dependent transcriptional activity

This thesis work describes that DYRK1A enhances β-catenin-dependent transcriptional activity. DYRK1A must carry out this activity through phosphorylation events, because inhibition of DYRK1A catalytic activity by mutation on the ATP-binding lysine residue or incubation with the DYRK1A inhibitor harmine abolishes its ability to enhance β-catenin-dependent transcription. Moreover, as the β-catenin form used along this work was undegradable by the destruction complex, DYRK1A should be acting downstream of β-catenin stabilization events. This proposal is supported by our findings that endogenous DYRK1A and β-catenin can be found in complexes in

HeLa nuclear extracts. In the β-catenin/TCF transcription complex, whereas β-catenin contributes by recruiting co-activators and the general transcriptional machinery, TCF provides the DNA-binding activity (recently reviewed in for instance MacDonald et al., 2009). Importantly, we have found that DYRK1A does not induce transcriptional activation when only TCF-4 is overexpressed. Therefore, DYRK1A cannot substitute the trans-activating activity of β-catenin, but it enhances the transcriptional activity of existing β-catenin/TCF complexes.

Our results indicate that both β-catenin and TCF-4 are substrates of DYRK1A. We have identified several peptides in β-catenin, clustered in the N-terminal and C-terminal regions, that are phosphorylated by DYRK1A (Fig. D7). Two of the phosphosites, Ser552 and Ser675, have been further validated. Moreover, phosphorylation of Ser552 and, more likely, Ser675 seems to be responsible for DYRK1A enhancement on β-catenin-dependent transcriptional activity.

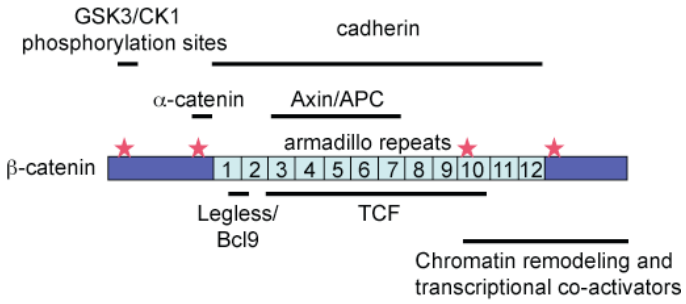

Figure D7: Schematic representation of β-catenin. The regions identified as important for the interaction with other molecules are shown. Red stars indicate the location of the DYRK1A peptides phosphorylated by NLK and identified by mass spectrometry.

The regulation of the β-catenin-dependent transcriptional activity is a complex process, which is regulated at multiple levels. With this in mind, there are several possibilities to explain how DYRK1A can enhance β-catenin/TCF transcriptional activity.

i.- DYRK1A might stabilize β-catenin levels independently of Wnt, as described for 14-3-3ζ, which binds β-catenin and induces its stabilization (Tian et al., 2004). As in all the experiments of this Thesis work a constitutively stable form of β-catenin was used, we cannot provide conclusive proofs on whether DYRK1A affects β-catenin protein levels. However, one of the β-catenin peptides identified as phosphorylated by DYRK1A *in vitro* contains Ser33, Ser37 and Ser41, which are the well-known target sites of GSK3β. Phosphorylation of these sites triggers recruitment of the

destruction complex to cytosolic β-catenin and subsequent degradation by the proteasome. DYRK1A has been suggested to act as a classical priming kinase of GSK3 for several proteins such as eI2Fβ, tau, MAP1B or CRY2 (Kurabayashi et al., 2010; Scales et al., 2009; Woods et al., 2001). Therefore, the possibility of DYRK1A targeting a cytosolic pool of β-catenin is still open (see below).

ii.- DYRK1A might increase β-catenin nuclear entry, as described for the PTEN-Akt pathway, in which Akt phosphorylates β-catenin on Ser552, which results in its nuclear localization (He et al., 2007a). In this regard, although DYRK1A is able to phosphorylate Ser552 in β-catenin, we have not been able to detect any changes in the intracellular localization of β-catenin when coexpressed with DYRK1A (data not shown).

iii.- DYRK1A might help β-catenin to recruit the co-activators that mediate the transcriptional response. It has been reported that phosphorylation of Ser675 by PKA enhances β-catenin transcriptional activity by promoting association with CBP (Taurin et al., 2006). Phosphorylation of Ser552 by AKT has also been found to enhance nuclear signaling (Fang et al., 2007; Tian et al., 2004), although the precise mechanism remains unclear. It can be predicted therefore that DYRK1A-dependent phosphorylation of β-catenin in these two sites might increase its interaction with CBP or other co-activators, a possibility that needs to be tested.

iv.- DYRK1A might work to protect TCF-4 from proteasome-mediated degradation. Our results show that TCF-4 is also a substrate of DYRK1A. Moreover, we have observed that DYRK1A increased the protein levels of a specific isoform of TCF-4, which lacks the LVPQ motif, the SxxSS motif and the C-terminal tail (Fig. 25), but did not affect the protein levels of the TCF-4E isoform (Fig. 26). These results suggest that DYRK1A might interfere with the Wnt signaling pathway not only at the level of β-catenin, but also at the level of TCF-4 and that sequence differences in TCF-4 isoforms might offer specificity for the DYRK1A regulatory abilities in different cellular contexts.

v.- DYRK1A might enhance the TCF transcriptional activity by increasing DNA binding efficiency or abrogating repressors binding.

vi.- DYRK1A might facilitate β-catenin/TCF interaction. In this regard, we have shown that DYRK1A-dependent phosphorylation is able to facilitate the interaction between TCF-4 and β-catenin. As DYRK1A is able to phosphorylate both β-catenin and TCF-

4, it is possible that DYRK1A facilitate β-catenin/TCF interaction through phosphorylation events that involve both members of the heterodimer. Moreover, DYRK1A interacts both with TCF-4 and with β-catenin, therefore, it might serve as an adaptor protein, as it has been suggested for the members of the signaling cascade RAS-BRaf-MEK1 (Kelly and Rahmani, 2005).

All these events, alone or in combination may explain how DYRK1A is able to enhance β-catenin-dependent transcription. We have to mention, nonetheless, that the results obtained in the presence of a constitutively stable β-catenin are not in concordance with those obtained in its absence. Thus, overexpressed DYRK1A slightly represses the TOPFLASH reporter and knock-down of DYRK1A protein by expression of a specific shRNA enhances the activity of the reporter when the pathway is activated by incubation with Wnt (data not shown). These results suggest that DYRK1A might also regulate the Wnt signaling pathway upstream or at the level of β-catenin stabilization. As mentioned above, the possibility of DYRK1A phosphorylating one or several of the priming sites for GSK3 at the β-catenin N-terminus exists, and this would result in DYRK1A acting as an inhibitor of the pathway. As in the reporter assays we used the β-catenin^{S33Y} form that is undegradable by the destruction complex, the effect of DYRK1A on β-catenin transcription is restricted to a nuclear fraction of β-catenin that is already stabilized. This observation is supported by our findings that DYRK1A and β-catenin interact, under physiological conditions, in nuclear extracts of cells that express both proteins. Further research would be needed to shed light on all the aspects that are not clear yet on the functional interaction of DYRK1A with the Wnt signaling pathway.

Finally, a functional link can be established between the two experimental blocks of this Thesis work. NLK expression inhibits β-catenin-mediated transcriptional activity by phosphorylating TCF-4 on two residues (Ishitani et al., 2003). This phosphorylation event prevents β-catenin/TCF-4 complex from binding to DNA and targets TCF-4 for proteasome-mediated degradation (Yamada et al., 2006). We have found that NLK also inhibits DYRK1A-dependent enhancement of β-catenin/TCF transcriptional activity in a kinase dependent manner. Given that NLK affects DYRK1A protein levels, we speculate that NLK not only induces TCF-4 degradation, but at the same time it interferes with the co-activating ability of DYRK1A by reducing the half-life of this protein. As NLK-mediated DYRK1A and TCF/LEF degradation are

activated by Wnt stimuli, NLK would act as a negative feed-back regulator of Wnt/β-catenin signaling by targeting two of the positive effectors of the pathway (Fig. D8).

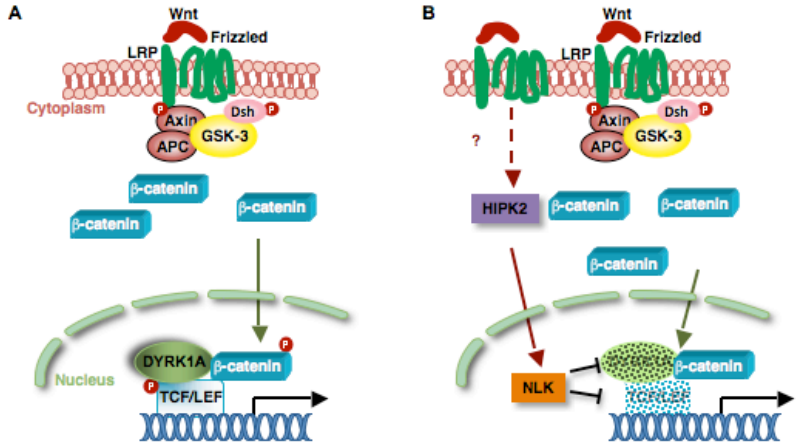

Figure D8: Schematic representation of DYRK1A involvement in the Wnt signaling pathway. (A) In the proposed model, DYRK1A acts as a positive factor in the Wnt-β-catenin signaling pathway at a point downstream stabilization of β-catenin. **(B)** Upon high levels of Wnt signal, the Wnt1/Wnt3a-Fzd1-HIPK2-NLK cascade is activated and NLK acts as a negative regulator by targeting both DYRK1A and TCF/LEF transcription factors for proteasome-mediated degradation.

Final remarks and future prospects

Finally, I would like to finish this Discussion section presenting several aspects that could be important for the functional interaction of DYRK1A with the Wnt signaling pathway and that, at this stage, are only matter of speculation. This section intends to highlight DYRK1A as a molecule able to connect several signaling pathways.

In contrast to β-catenin/TCF, ***FOXO*** transcription factors inhibit cell cycle progression and this function is enhanced by ***β-catenin*** (Kops et al., 2002; Medema et al., 2000). Thus, β-catenin appears to play a role in balancing positive (through TCF) and negative (through FOXO) regulation of cell cycle progression (Essers et al., 2005). DYRK1A has been reported as a FOXO kinase (Woods et al., 2001). Moreover, experiments using the DYRK1A inhibitor harmine suggested that DYRK1A stimulates FOXO nuclear exclusion and inhibits its DNA binding activity, thus acting as an inhibitor of the pathway (Bartholome et al., 2010). As our results suggest that DYRK1A can positively modulate β-catenin/TCF-dependent transcription, it is therefore possible that DYRK1A may function similarly as β-catenin and participate in the cross-talk between FOXO and TCF signaling.

Wnt and ***FGF*** signaling pathways cross-talk during a variety of cellular processes, such as human colorectal carcinogenesis, embryogenesis and neurogenesis, among others (reviewed in Dailey et al., 2005; Katoh, 2006). This cross-talk results from specific interactions between molecules within the pathways, and the convergence and divergence of the gene expression programs activated by each pathway. We have recently shown that DYRK1A potentiates FGF signaling by two mechanisms. First, it phosphorylates an antagonist of FGF signaling, Sprouty2, resulting in the inhibition of its negative regulatory functions (Aranda et al., 2008). Second, DYRK1A appears to enhance FGF-dependent responses independently of its kinase activity, very likely by acting as a scaffold protein for members of the FGF signaling pathway (Aranda et al., 2008). It is tempting to propose therefore that DYRK1A may contribute to the cross-talk between Wnt and FGF signaling pathways.

There are several examples on both synergistic and antagonistic cross-talk between ***Wnt*** and ***Notch*** signaling pathways in cell fate decision events. Examples for antagonistic cross-talk between Wnt and Notch pathways are the activation or inhibition, respectively, of neurogenesis and intestinal differentiation in mammals (for a recent review Johnson et al., 2009). In contrast, Wnt-β-catenin signaling has been placed upstream of the Notch pathway in vertebrate somitogenesis (Galceran et al., 2004; Greco et al., 1996; Ikeya and Takada, 2001) and they also act synergistically in *Drosophila* wing formation (Hing et al., 1994). DYRK1A has been shown to repress the transcriptional activity of NICD and, moreover, the negative role of Notch on neuronal maturation is reverted by the presence of DYRK1A (Fernandez-Martinez et al., 2009). Therefore, it is tempting to speculate that during some cell fate decision events DYRK1A may contribute to the cross-talk between Wnt and Notch pathways, although it might not be the case for all type of cellular contexts.

Activation of the ***Wnt***-Ca^{2+} signaling pathway induces the release of intracellular calcium and the subsequent activation of PKC and CAMKII. As a result, the NFAT family of transcription factors translocate to the nucleus where activate their target genes (Kohn and Moon, 2005; Kuhl et al., 2000). ***NFAT*** nuclear localization is countered by distinct NFAT kinases, being one of them DYRK1A (Arron et al., 2006; Gwack et al., 2006; Lee et al., 2009). Therefore, DYRK1A might also have a role in non-canonical Wnt signaling.

Based on the idea that DYRK1A is able to both promote and antagonize Wnt signaling pathway in a context-specific manner, a regulatory mechanism by which DYRK1A may regulate transcription at TCF/LEF promoter sites can be suggested.

Results in our group indicate that DYRK1A binds the transcription factor Yin Yang 1 (YY1) (Salichs, 2008). This protein acts as a repressor of the transcription of TCF-4, as part of the mechanisms that regulate oligodendrocyte differentiation (He et al., 2007b). YY1 is also recruited to the promoter region of LEF-1 responsible for the production of a dominant negative LEF-1 isoform. In this case, YY1-mediated target gene repression is linked to progression of colon cancer (Yokoyama et al., 2010). Thus, DYRK1A might indirectly control TCF/LEF transcriptional programs, if able to modulate YY1 activity.

Association of deregulated Wnt/β-catenin signaling with cancer has been well documented, particularly with colorectal cancer (Polakis, 2007). Constitutively activated β-catenin signaling, leads to excessive stem cell renewal/proliferation that predisposes cells to tumorigenesis. As DYRK1A behaves as a protective kinase against apoptosis acting through several molecular targets (caspase-9 (Laguna et al., 2008; Seifert et al., 2008), p53 (Guo et al., 2010), FOXO (Chang et al., 2007), Hip-1 (Kang et al., 2005)), it might contribute to immortalization and tumorigenesis by acting as a survival factor for tumor cells. In fact, DYRK1A has been associated to HPV16 virus-related cervical oncogenesis and keratinocyte proliferation (Chang et al., 2007; Liang et al., 2008). DYRK1A enhancement on Wnt/β-catenin signaling might account as a novel mechanism by which DYRK1A could initiate transformation of Wnt responding cells. In this context, a link between the tight regulation of DYRK1A protein levels mediated by NLK and prostate cancer development can be established. Androgen receptor (AR) signaling plays a critical role in prostatic tumor growth. NLK has been shown to inhibit AR-mediated transcription through inducing the degradation of AR mRNA and protein, and in prostate cancer metastases the expression of NLK is decreased in comparison to normal prostate epithelium (Emami et al., 2009). By contrast, DYRK1A enhances AR-mediated transcription through interaction with AR-interacting protein 4 (Arip4) (Sitz et al., 2004). Therefore, it is likely, that any change in the regulation of NLK and DYRK1A protein levels may cause alterations in the homeostasis of steroid hormone-controlled cellular events.

DYRK1A is dynamically expressed in the developing and adult CNS (Hammerle et al., 2008; Marti et al., 2003). Deficiencies in any developmental phases of the CNS may be due to altered signaling mediated by growth factors. Several scenarios, in which DYRK1A would interact with the Wnt signaling pathway, can be envisaged. Early during development (E10.5 in mice), β-catenin signals are essential for the proliferation of neuronal progenitors, controlling the size of the progenitor pool

(Zechner et al., 2003). Moreover, cell-cell contact between neural stem cells in the developing cerebral cortex has been shown to induce phosphorylation of β-catenin at Ser552, which results in stabilization of and increased transcriptional activation (Zhang et al., 2010). At a later stage (E13.5 in mice), Wnt signaling inhibits the self-renewal capacity of neural precursor cells of the neocortex and promotes their neuronal differentiation (Hirabayashi et al., 2004). It has been proposed that DYRK1A defines a transition step between proliferating and neurogenic divisions of neuroepithelial progenitor cells (Hammerle et al., 2002; Yabut et al., 2010), although it is not known yet whether it does so in response to specific signals. Moreover, DYRK1A positively impacts on the persistence of adult neural stem cells in the subependymal zone niche (Ferron et al., 2010), however its role in embryonic neural stem cell maintenance needs further investigation.

Finally, Dyrk1A is persistently expressed in differentiated neurons (Hammerle et al., 2008; Marti et al., 2003; Wegiel et al., 2004), where structural changes at synapses are thought to underpin long-term memory formation. The Wnt/β-catenin signaling pathway has been shown to be involved in the regulation of synaptic plasticity in the hippocampus (Chen et al., 2006) and in long-term memory formation in the amygdala (Maguschak and Ressler, 2008). In this regard, mouse models of overexpression of DYRK1A show impairment in synaptic plasticity and deficiencies in learning and memory through mechanisms that are not well understood yet (Ahn et al., 2006; Altafaj et al., 2001; Branchi et al., 2004; Martinez de Lagran et al., 2004; Smith et al., 1997). Therefore, DYRK1A could play an important role in several aspects of the development and homeostasis of CNS through modulating signal transduction pathways mediated by Wnts.

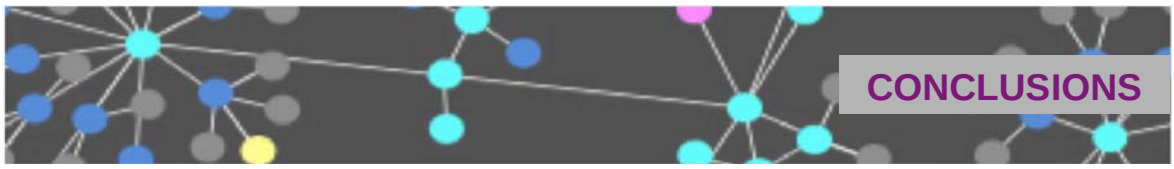

CONCLUSIONS

1. The two protein kinases DYRK1A and NLK interact independently of their kinase activity. The interaction might occur in the nucleus under physiological conditions.
2. An N-terminal region, amino acids 70-104, in DYRK1A is involved in the interaction. NLK binds through a region just C-terminal from the kinase domain, amino acids 430-444, which is located similarly to the CD-domain used for docking interactions in other MAPKs.
3. NLK interacts with other members of the DYRK family of protein kinases.
4. NLK phosphorylates DYRK1A at multiple sites including Thr393, Thr422, Ser433, Thr436, Thr457 and Ser468.
5. NLK-induced DYRK1A phosphorylation does not affect DYRK1A subcellular localization or catalytic activity.
6. NLK-induced phosphorylation marks DYRK1A for proteasome-mediated degradation, and therefore, NLK acts as a negative regulator of DYRK1A.
7. DYRK1A interacts with β-catenin and TCF-4, the components of the transcriptional unit responsible of transducing the nuclear responses in the Wnt signaling pathway.
8. DYRK1A and β-catenin are found in complexes in HeLa nuclear extracts, supporting that their functional interaction might occur in the nucleus under physiological conditions.
9. DYRK1A enhances β-catenin-dependent transcriptional activity by, at least, phosphorylating β-catenin at Ser552 and Ser675.
10. DYRK1A-mediated β-catenin and TCF-4 phosphorylation facilitates the interaction between these two proteins, which also might contribute to the DYRK1A-induced enhancement of β-catenin-dependent transcription.
11. The Wnt1/Wnt3a-Fzd1-HIPK2 signaling cascade enhances NLK-induced DYRK1A degradation.
12. A model is proposed, in which DYRK1A acts as a positive factor in the Wnt/β-catenin signaling pathway at a point downstream of β-catenin stabilization. As a negative feed-back loop, Wnt signals through NLK to target both DYRK1A and TCF transcription factors for degradation.

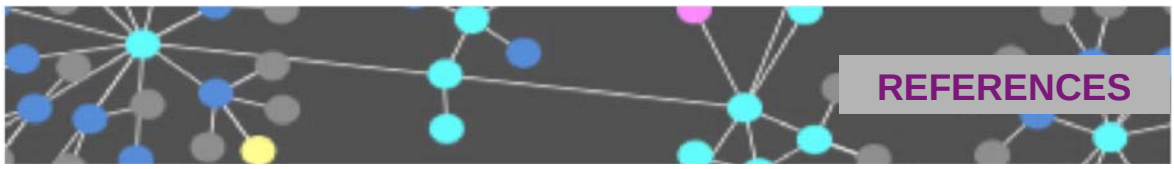

REFERENCES

Ahn, K.J., Jeong, H.K., Choi, H.S., Ryoo, S.R., Kim, Y.J., Goo, J.S.*, et al.* (2006). DYRK1A BAC transgenic mice show altered synaptic plasticity with learning and memory defects. Neurobiol Dis *22*, 463-472.

Aikin, R.A., Ayers, K.L., and Therond, P.P. (2008). The role of kinases in the Hedgehog signalling pathway. EMBO Rep *9*, 330-336.

Altafaj, X., Dierssen, M., Baamonde, C., Marti, E., Visa, J., Guimera, J.*, et al.* (2001). Neurodevelopmental delay, motor abnormalities and cognitive deficits in transgenic mice overexpressing Dyrk1A (minibrain), a murine model of Down's syndrome. Hum Mol Genet *10*, 1915-1923.

Alvarez, M. (2004). Localización subcelular de la proteína quinasa DYRK1A: compartimentos, señales y regulación (Doctoral Thesis, Universitat de Barcelona).

Alvarez, M., Altafaj, X., Aranda, S., and de la Luna, S. (2007). DYRK1A autophosphorylation on serine residue 520 modulates its kinase activity via 14-3-3 binding. Mol Biol Cell *18*, 1167-1178.

Alvarez, M., Estivill, X., and de la Luna, S. (2003). DYRK1A accumulates in splicing speckles through a novel targeting signal and induces speckle disassembly. J Cell Sci *116*, 3099-3107.

Amit, S., Hatzubai, A., Birman, Y., Andersen, J.S., Ben-Shushan, E., Mann, M.*, et al.* (2002). Axin-mediated CKI phosphorylation of beta-catenin at Ser 45: a molecular switch for the Wnt pathway. Genes Dev *16*, 1066-1076.

Angers, S., and Moon, R.T. (2009). Proximal events in Wnt signal transduction. Nat Rev Mol Cell Biol *10*, 468-477.

Arai, T., Haze, K., Iimura-Morita, Y., Machida, T., Iida, M., Tanaka, K.*, et al.* (2008). Identification of beta-catenin as a novel substrate of Polo-like kinase 1. Cell Cycle *7*, 3556-3563.

Aranda, S. (2007). DYRK1A: Implicación en vías de señalización intracelular (Doctoral Thesis, Universitat de Barcelona).

Aranda, S., Alvarez, M., Turro, S., Laguna, A., and de la Luna, S. (2008). Sprouty2-mediated inhibition of fibroblast growth factor signaling is modulated by the protein kinase DYRK1A. Mol Cell Biol *28*, 5899-5911.

Aranda, S., Laguna, A., and de la Luna, S. (2010). DYRK family of protein kinases: evolutionary relationships, biochemical properties and functional roles. FASEB J *in press*.

Arce, L., Yokoyama, N.N., and Waterman, M.L. (2006). Diversity of LEF/TCF action in development and disease. Oncogene *25*, 7492-7504.

Arron, J.R., Winslow, M.M., Polleri, A., Chang, C.P., Wu, H., Gao, X.*, et al.* (2006). NFAT dysregulation by increased dosage of DSCR1 and DYRK1A on chromosome 21. Nature *441*, 595-600.

Ayers, K.L., and Therond, P.P. (2010). Evaluating Smoothened as a G-protein-coupled receptor for Hedgehog signalling. Trends Cell Biol *20*, 287-298.

Baek, K.H., Zaslavsky, A., Lynch, R.C., Britt, C., Okada, Y., Siarey, R.J.*, et al.* (2009). Down's syndrome suppression of tumour growth and the role of the calcineurin inhibitor DSCR1. Nature *459*, 1126-1130.

Bain, J., Plater, L., Elliott, M., Shpiro, N., Hastie, C.J., McLauchlan, H.*, et al.* (2007). The selectivity of protein kinase inhibitors: a further update. Biochem J *408*, 297-315.

Bartholome, A., Kampkotter, A., Tanner, S., Sies, H., and Klotz, L.O. (2010). Epigallocatechin gallate-induced modulation of FoxO signaling in mammalian cells and C. elegans: FoxO stimulation is masked via PI3K/Akt activation by hydrogen peroxide formed in cell culture. Arch Biochem Biophys *501*, 58-64.

Bartscherer, K., and Boutros, M. (2008). Regulation of Wnt protein secretion and its role in gradient formation. EMBO Rep *9*, 977-982.

Beals, C.R., Sheridan, C.M., Turck, C.W., Gardner, P., and Crabtree, G.R. (1997). Nuclear export of NF-ATc enhanced by glycogen synthase kinase-3. Science *275*, 1930-1934.

Becker, W., and Joost, H.G. (1999). Structural and functional characteristics of Dyrk, a novel subfamily of protein kinases with dual specificity. Prog Nucleic Acid Res Mol Biol *62*, 1-17.

Becker, W., Weber, Y., Wetzel, K., Eirmbter, K., Tejedor, F.J., and Joost, H.G. (1998). Sequence characteristics, subcellular localization, and substrate specificity of DYRK-related kinases, a novel family of dual specificity protein kinases. J Biol Chem *273*, 25893-25902.

Benavides-Piccione, R., Dierssen, M., Ballesteros-Yanez, I., Martinez de Lagran, M., Arbones, M.L., Fotaki, V.*, et al.* (2005). Alterations in the phenotype of neocortical pyramidal cells in the Dyrk1A+/- mouse. Neurobiol Dis *20*, 115-122.

Bogacheva, O., Bogachev, O., Menon, M., Dev, A., Houde, E., Valoret, E.I.*, et al.* (2008). DYRK3 dual-specificity kinase attenuates erythropoiesis during anemia. J Biol Chem *283*, 36665-36675.

Braid, L.R., Lee, W., Uetrecht, A.C., Swarup, S., Papaianni, G., Heiler, A.*, et al.* (2010). Nemo phosphorylates Even-skipped and promotes Eve-mediated repression of odd-skipped in even parasegments during Drosophila embryogenesis. Dev Biol *343*, 178-189.

Branchi, I., Bichler, Z., Minghetti, L., Delabar, J.M., Malchiodi-Albedi, F., Gonzalez, M.C.*, et al.* (2004). Transgenic mouse in vivo library of human Down syndrome critical region 1: association between DYRK1A overexpression, brain development abnormalities, and cell cycle protein alteration. J Neuropathol Exp Neurol *63*, 429-440.

Brembeck, F.H., Rosario, M., and Birchmeier, W. (2006). Balancing cell adhesion and Wnt signaling, the key role of beta-catenin. Curr Opin Genet Dev *16*, 51-59.

Brembeck, F.H., Schwarz-Romond, T., Bakkers, J., Wilhelm, S., Hammerschmidt, M., and Birchmeier, W. (2004). Essential role of BCL9-2 in the switch between beta-catenin's adhesive and transcriptional functions. Genes Dev *18*, 2225-2230.

Briscoe, J. (2009). Making a grade: Sonic Hedgehog signalling and the control of neural cell fate. EMBO J *28*, 457-465.

Brott, B.K., Pinsky, B.A., and Erikson, R.L. (1998). Nlk is a murine protein kinase related to Erk/MAP kinases and localized in the nucleus. Proc Natl Acad Sci U S A *95*, 963-968.

Buratti, E., De Conti, L., Stuani, C., Romano, M., Baralle, M., and Baralle, F. (2010). Nuclear factor TDP-43 can affect selected microRNA levels. FEBS J *277*, 2268-2281.

Castano, J., Raurell, I., Piedra, J.A., Miravet, S., Dunach, M., and Garcia de Herreros, A. (2002). Beta-catenin N- and C-terminal tails modulate the coordinated binding of adherens junction proteins to beta-catenin. J Biol Chem *277*, 31541-31550.

Chang, H.S., Lin, C.H., Yang, C.H., Yen, M.S., Lai, C.R., Chen, Y.R.*, et al.* (2007). Increased expression of Dyrk1a in HPV16 immortalized keratinocytes enable evasion of apoptosis. Int J Cancer *120*, 2377-2385.

Chen, J., Park, C.S., and Tang, S.J. (2006). Activity-dependent synaptic Wnt release regulates hippocampal long term potentiation. J Biol Chem *281*, 11910-11916.

Choi, K.W., and Benzer, S. (1994). Rotation of photoreceptor clusters in the developing Drosophila eye requires the nemo gene. Cell *78*, 125-136.

Ciani, L., Krylova, O., Smalley, M.J., Dale, T.C., and Salinas, P.C. (2004). A divergent canonical WNT-signaling pathway regulates microtubule dynamics: dishevelled signals locally to stabilize microtubules. J Cell Biol *164*, 243-253.

Clevers, H. (2006). Wnt/beta-catenin signaling in development and disease. Cell *127*, 469-480.

Coluccia, A.M., Vacca, A., Dunach, M., Mologni, L., Redaelli, S., Bustos, V.H.*, et al.* (2007). Bcr-Abl stabilizes beta-catenin in chronic myeloid leukemia through its tyrosine phosphorylation. EMBO J *26*, 1456-1466.

Cong, F., and Varmus, H. (2004). Nuclear-cytoplasmic shuttling of Axin regulates subcellular localization of beta-catenin. Proc Natl Acad Sci U S A *101*, 2882-2887.

Coudreuse, D.Y., Roel, G., Betist, M.C., Destree, O., and Korswagen, H.C. (2006). Wnt gradient formation requires retromer function in Wnt-producing cells. Science *312*, 921-924.

Coulombe, P., and Meloche, S. (2007). Atypical mitogen-activated protein kinases: structure, regulation and functions. Biochim Biophys Acta *1773*, 1376-1387.

Cox, R.T., Pai, L.M., Kirkpatrick, C., Stein, J., and Peifer, M. (1999). Roles of the C terminus of Armadillo in Wingless signaling in Drosophila. Genetics *153*, 319-332.

D'Souza, B., Miyamoto, A., and Weinmaster, G. (2008). The many facets of Notch ligands. Oncogene *27*, 5148-5167.

Dahmane, N., Charron, G., Lopes, C., Yaspo, M.L., Maunoury, C., Decorte, L.*, et al.* (1995). Down syndrome-critical region contains a gene homologous to Drosophila sim expressed during rat and human central nervous system development. Proc Natl Acad Sci U S A *92*, 9191-9195.

Dailey, L., Ambrosetti, D., Mansukhani, A., and Basilico, C. (2005). Mechanisms underlying differential responses to FGF signaling. Cytokine Growth Factor Rev *16*, 233-247.

Deng, X., Ewton, D.Z., Li, S., Naqvi, A., Mercer, S.E., Landas, S.*, et al.* (2006). The kinase Mirk/Dyrk1B mediates cell survival in pancreatic ductal adenocarcinoma. Cancer Res *66*, 4149-4158.

Dowjat, W.K., Adayev, T., Kuchna, I., Nowicki, K., Palminiello, S., Hwang, Y.W.*, et al.* (2007). Trisomy-driven overexpression of DYRK1A kinase in the brain of subjects with Down syndrome. Neurosci Lett *413*, 77-81.

Ebisuya, M., Kondoh, K., and Nishida, E. (2005). The duration, magnitude and compartmentalization of ERK MAP kinase activity: mechanisms for providing signaling specificity. J Cell Sci *118*, 2997-3002.

Emami, K.H., Brown, L.G., Pitts, T.E., Sun, X., Vessella, R.L., and Corey, E. (2009). Nemo-like kinase induces apoptosis and inhibits androgen receptor signaling in prostate cancer cells. Prostate *69*, 1481-1492.

Epstein, C.J. (2006). Down's syndrome: critical genes in a critical region. Nature *441*, 582-583.

Espinosa, L., Ingles-Esteve, J., Aguilera, C., and Bigas, A. (2003). Phosphorylation by glycogen synthase kinase-3 beta down-regulates Notch activity, a link for Notch and Wnt pathways. J Biol Chem *278*, 32227-32235.

Essers, M.A., de Vries-Smits, L.M., Barker, N., Polderman, P.E., Burgering, B.M., and Korswagen, H.C. (2005). Functional interaction between beta-catenin and FOXO in oxidative stress signaling. Science *308*, 1181-1184.

Fang, D., Hawke, D., Zheng, Y., Xia, Y., Meisenhelder, J., Nika, H.*, et al.* (2007). Phosphorylation of beta-catenin by AKT promotes beta-catenin transcriptional activity. J Biol Chem *282*, 11221-11229.

Fernandez-Martinez, J., Vela, E.M., Tora-Ponsioen, M., Ocana, O.H., Nieto, M.A., and Galceran, J. (2009). Attenuation of Notch signalling by the Down-syndrome-associated kinase DYRK1A. J Cell Sci *122*, 1574-1583.

Ferron, S.R., Pozo, N., Laguna, A., Aranda, S., Porlan, E., Moreno, M.*, et al.* (2010). Regulated segregation of kinase Dyrk1A during asymmetric neural stem cell division is critical for EGFR-mediated biased signaling. Cell Stem Cell *7*, 367-379.

Fiol, C.J., Haseman, J.H., Wang, Y.H., Roach, P.J., Roeske, R.W., Kowalczuk, M.*, et al.* (1988). Phosphoserine as a recognition determinant for glycogen synthase kinase-3: phosphorylation of a synthetic peptide based on the G-component of protein phosphatase-1. Arch Biochem Biophys *267*, 797-802.

Foltz, D.R., and Nye, J.S. (2001). Hyperphosphorylation and association with RBP of the intracellular domain of Notch1. Biochem Biophys Res Commun *286*, 484-492.

Foltz, D.R., Santiago, M.C., Berechid, B.E., and Nye, J.S. (2002). Glycogen synthase kinase-3beta modulates notch signaling and stability. Curr Biol *12*, 1006-1011.

Fortini, M.E. (2009). Notch signaling: the core pathway and its posttranslational regulation. Dev Cell *16*, 633-647.

Fortini, M.E., and Bilder, D. (2009). Endocytic regulation of Notch signaling. Curr Opin Genet Dev *19*, 323-328.

Fotaki, V., Dierssen, M., Alcantara, S., Martinez, S., Marti, E., Casas, C.*, et al.* (2002). Dyrk1A haploinsufficiency affects viability and causes developmental delay and abnormal brain morphology in mice. Mol Cell Biol *22*, 6636-6647.

Fradkin, L.G., Dura, J.M., and Noordermeer, J.N. (2010). Ryks: new partners for Wnts in the developing and regenerating nervous system. Trends Neurosci *33*, 84-92.

Fu, Z., and Tindall, D.J. (2008). FOXOs, cancer and regulation of apoptosis. Oncogene *27*, 2312-2319.

Fujita, H., Torii, C., Kosaki, R., Yamaguchi, S., Kudoh, J., Hayashi, K.*, et al.* (2010). Microdeletion of the Down syndrome critical region at 21q22. Am J Med Genet A *152A*, 950-953.

Fukuda, M., Gotoh, Y., and Nishida, E. (1997). Interaction of MAP kinase with MAP kinase kinase: its possible role in the control of nucleocytoplasmic transport of MAP kinase. EMBO J *16*, 1901-1908.

Galceran, J., Sustmann, C., Hsu, S.C., Folberth, S., and Grosschedl, R. (2004). LEF1-mediated regulation of Delta-like1 links Wnt and Notch signaling in somitogenesis. Genes Dev *18*, 2718-2723.

Gao, C., and Chen, Y.G. (2010). Dishevelled: The hub of Wnt signaling. Cell Signal *22*, 717-727.

Garcia-Alai, M.M., Gallo, M., Salame, M., Wetzler, D.E., McBride, A.A., Paci, M.*, et al.* (2006). Molecular basis for phosphorylation-dependent, PEST-mediated protein turnover. Structure *14*, 309-319.

Gockler, N., Jofre, G., Papadopoulos, C., Soppa, U., Tejedor, F.J., and Becker, W. (2009). Harmine specifically inhibits protein kinase DYRK1A and interferes with neurite formation. FEBS J *276*, 6324-6337.

Greco, T.L., Takada, S., Newhouse, M.M., McMahon, J.A., McMahon, A.P., and Camper, S.A. (1996). Analysis of the vestigial tail mutation demonstrates that Wnt-3a gene dosage regulates mouse axial development. Genes Dev *10*, 313-324.

Guimera, J., Casas, C., Estivill, X., and Pritchard, M. (1999). Human minibrain homologue (MNBH/DYRK1): characterization, alternative splicing, differential tissue expression, and overexpression in Down syndrome. Genomics *57*, 407-418.

Guimera, J., Casas, C., Pucharcos, C., Solans, A., Domenech, A., Planas, A.M.*, et al.* (1996). A human homologue of Drosophila minibrain (MNB) is expressed in the neuronal regions affected in Down syndrome and maps to the critical region. Hum Mol Genet *5*, 1305-1310.

Guo, X., Williams, J.G., Schug, T.T., and Li, X. (2010). DYRK1A and DYRK3 promote cell survival through phosphorylation and activation of SIRT1. J Biol Chem *285*, 13223-13232.

Guy, G.R., Jackson, R.A., Yusoff, P., and Chow, S.Y. (2009). Sprouty proteins: modified modulators, matchmakers or missing links? J Endocrinol *203*, 191-202.

Gwack, Y., Sharma, S., Nardone, J., Tanasa, B., Iuga, A., Srikanth, S.*, et al.* (2006). A genome-wide Drosophila RNAi screen identifies DYRK-family kinases as regulators of NFAT. Nature *441*, 646-650.

Hammerle, B., Carnicero, A., Elizalde, C., Ceron, J., Martinez, S., and Tejedor, F.J. (2003). Expression patterns and subcellular localization of the Down syndrome candidate protein MNB/DYRK1A suggest a role in late neuronal differentiation. Eur J Neurosci *17*, 2277-2286.

Hammerle, B., Elizalde, C., and Tejedor, F.J. (2008). The spatio-temporal and subcellular expression of the candidate Down syndrome gene Mnb/Dyrk1A in the developing mouse

brain suggests distinct sequential roles in neuronal development. Eur J Neurosci *27*, 1061-1074.

Hammerle, B., Vera-Samper, E., Speicher, S., Arencibia, R., Martinez, S., and Tejedor, F.J. (2002). Mnb/Dyrk1A is transiently expressed and asymmetrically segregated in neural progenitor cells at the transition to neurogenic divisions. Dev Biol *246*, 259-273.

Harada, H., Yoshida, S., Nobe, Y., Ezura, Y., Atake, T., Koguchi, T.*, et al.* (2002). Genomic structure of the human NLK (nemo-like kinase) gene and analysis of its promoter region. Gene *285*, 175-182.

Hausmann, G., Banziger, C., and Basler, K. (2007). Helping Wingless take flight: how WNT proteins are secreted. Nat Rev Mol Cell Biol *8*, 331-336.

He, X.C., Yin, T., Grindley, J.C., Tian, Q., Sato, T., Tao, W.A.*, et al.* (2007a). PTEN-deficient intestinal stem cells initiate intestinal polyposis. Nat Genet *39*, 189-198.

He, Y., Dupree, J., Wang, J., Sandoval, J., Li, J., Liu, H.*, et al.* (2007b). The transcription factor Yin Yang 1 is essential for oligodendrocyte progenitor differentiation. Neuron *55*, 217-230.

Henderson, B.R., and Fagotto, F. (2002). The ins and outs of APC and beta-catenin nuclear transport. EMBO Rep *3*, 834-839.

Hendrickx, M., and Leyns, L. (2008). Non-conventional Frizzled ligands and Wnt receptors. Dev Growth Differ *50*, 229-243.

Hendriksen, J., Fagotto, F., van der Velde, H., van Schie, M., Noordermeer, J., and Fornerod, M. (2005). RanBP3 enhances nuclear export of active (beta)-catenin independently of CRM1. J Cell Biol *171*, 785-797.

Hermann, G.J., Leung, B., and Priess, J.R. (2000). Left-right asymmetry in C. elegans intestine organogenesis involves a LIN-12/Notch signaling pathway. Development *127*, 3429-3440.

Himpel, S., Panzer, P., Eirmbter, K., Czajkowska, H., Sayed, M., Packman, L.C.*, et al.* (2001). Identification of the autophosphorylation sites and characterization of their effects in the protein kinase DYRK1A. Biochem J *359*, 497-505.

Himpel, S., Tegge, W., Frank, R., Leder, S., Joost, H.G., and Becker, W. (2000). Specificity determinants of substrate recognition by the protein kinase DYRK1A. J Biol Chem *275*, 2431-2438.

Hing, H.K., Sun, X., and Artavanis-Tsakonas, S. (1994). Modulation of wingless signaling by Notch in Drosophila. Mech Dev *47*, 261-268.

Hino, S., Tanji, C., Nakayama, K.I., and Kikuchi, A. (2005). Phosphorylation of beta-catenin by cyclic AMP-dependent protein kinase stabilizes beta-catenin through inhibition of its ubiquitination. Mol Cell Biol *25*, 9063-9072.

Hirabayashi, Y., Itoh, Y., Tabata, H., Nakajima, K., Akiyama, T., Masuyama, N.*, et al.* (2004). The Wnt/beta-catenin pathway directs neuronal differentiation of cortical neural precursor cells. Development *131*, 2791-2801.

Hogan, P.G., Chen, L., Nardone, J., and Rao, A. (2003). Transcriptional regulation by calcium, calcineurin, and NFAT. Genes Dev *17*, 2205-2232.

Hoppler, S., and Kavanagh, C.L. (2007). Wnt signalling: variety at the core. J Cell Sci *120*, 385-393.

Huang, H., and He, X. (2008). Wnt/beta-catenin signaling: new (and old) players and new insights. Curr Opin Cell Biol *20*, 119-125.

Huang, Y., Chen-Hwang, M.C., Dolios, G., Murakami, N., Padovan, J.C., Wang, R.*, et al.* (2004). Mnb/Dyrk1A phosphorylation regulates the interaction of dynamin 1 with SH3 domain-containing proteins. Biochemistry *43*, 10173-10185.

Hubbard, S.R., and Miller, W.T. (2007). Receptor tyrosine kinases: mechanisms of activation and signaling. Curr Opin Cell Biol *19*, 117-123.

Hyodo-Miura, J., Urushiyama, S., Nagai, S., Nishita, M., Ueno, N., and Shibuya, H. (2002). Involvement of NLK and Sox11 in neural induction in Xenopus development. Genes Cells *7*, 487-496.

Ikeya, M., and Takada, S. (2001). Wnt-3a is required for somite specification along the anteroposterior axis of the mouse embryo and for regulation of cdx-1 expression. Mech Dev *103*, 27-33.

Ille, F., and Sommer, L. (2005). Wnt signaling: multiple functions in neural development. Cell Mol Life Sci *62*, 1100-1108.

Impey, S., McCorkle, S.R., Cha-Molstad, H., Dwyer, J.M., Yochum, G.S., Boss, J.M.*, et al.* (2004). Defining the CREB regulon: a genome-wide analysis of transcription factor regulatory regions. Cell *119*, 1041-1054.

Ingles-Esteve, J., Espinosa, L., Milner, L.A., Caelles, C., and Bigas, A. (2001). Phosphorylation of Ser2078 modulates the Notch2 function in 32D cell differentiation. J Biol Chem *276*, 44873-44880.

Ishitani, T., Hirao, T., Suzuki, M., Isoda, M., Ishitani, S., Harigaya, K.*, et al.* (2010). Nemo-like kinase suppresses Notch signalling by interfering with formation of the Notch active transcriptional complex. Nat Cell Biol *12*, 278-285.

Ishitani, T., Ishitani, S., Matsumoto, K., and Itoh, M. (2009). Nemo-like kinase is involved in NGF-induced neurite outgrowth via phosphorylating MAP1B and paxillin. J Neurochem *111*, 1104-1118.

Ishitani, T., Kishida, S., Hyodo-Miura, J., Ueno, N., Yasuda, J., Waterman, M.*, et al.* (2003). The TAK1-NLK mitogen-activated protein kinase cascade functions in the Wnt-5a/Ca(2+) pathway to antagonize Wnt/beta-catenin signaling. Mol Cell Biol *23*, 131-139.

Ishitani, T., Ninomiya-Tsuji, J., Nagai, S., Nishita, M., Meneghini, M., Barker, N.*, et al.* (1999). The TAK1-NLK-MAPK-related pathway antagonizes signalling between beta-catenin and transcription factor TCF. Nature *399*, 798-802.

Ji, J., Yamashita, T., Budhu, A., Forgues, M., Jia, H.L., Li, C.*, et al.* (2009). Identification of microRNA-181 by genome-wide screening as a critical player in EpCAM-positive hepatic cancer stem cells. Hepatology *50*, 472-480.

Jiang, J., and Hui, C.C. (2008). Hedgehog signaling in development and cancer. Dev Cell *15*, 801-812.

Johnson, M.A., Ables, J.L., and Eisch, A.J. (2009). Cell-intrinsic signals that regulate adult neurogenesis in vivo: insights from inducible approaches. BMB Rep *42*, 245-259.

Jung, K.H., Kim, J.K., Noh, J.H., Eun, J.W., Bae, H.J., Xie, H.J.*, et al.* (2010). Targeted disruption of Nemo-like kinase inhibits tumor cell growth by simultaneous suppression of cyclin D1 and CDK2 in human hepatocellular carcinoma. J Cell Biochem *110*, 687-696.

Kageyama, R., Ohtsuka, T., Shimojo, H., and Imayoshi, I. (2009). Dynamic regulation of Notch signaling in neural progenitor cells. Curr Opin Cell Biol *21*, 733-740.

Kaletta, T., Schnabel, H., and Schnabel, R. (1997). Binary specification of the embryonic lineage in Caenorhabditis elegans. Nature *390*, 294-298.

Kanei-Ishii, C., Ninomiya-Tsuji, J., Tanikawa, J., Nomura, T., Ishitani, T., Kishida, S.*, et al.* (2004). Wnt-1 signal induces phosphorylation and degradation of c-Myb protein via TAK1, HIPK2, and NLK. Genes Dev *18*, 816-829.

Kanei-Ishii, C., Nomura, T., Takagi, T., Watanabe, N., Nakayama, K.I., and Ishii, S. (2008). Fbxw7 acts as an E3 ubiquitin ligase that targets c-Myb for nemo-like kinase (NLK)-induced degradation. J Biol Chem *283*, 30540-30548.

Kang, J.E., Choi, S.A., Park, J.B., and Chung, K.C. (2005). Regulation of the proapoptotic activity of huntingtin interacting protein 1 by Dyrk1 and caspase-3 in hippocampal neuroprogenitor cells. J Neurosci Res *81*, 62-72.

Katanaev, V.L., Solis, G.P., Hausmann, G., Buestorf, S., Katanayeva, N., Schrock, Y.*, et al.* (2008). Reggie-1/flotillin-2 promotes secretion of the long-range signalling forms of Wingless and Hedgehog in Drosophila. EMBO J *27*, 509-521.

Katoh, M. (2005). Comparative genomics on nemo-like kinase gene. Int J Oncol *26*, 1715-1719.

Katoh, M. (2006). Cross-talk of WNT and FGF signaling pathways at GSK3beta to regulate beta-catenin and SNAIL signaling cascades. Cancer Biol Ther *5*, 1059-1064.

Kelly, P.A., and Rahmani, Z. (2005). DYRK1A enhances the mitogen-activated protein kinase cascade in PC12 cells by forming a complex with Ras, B-Raf, and MEK1. Mol Biol Cell *16*, 3562-3573.

Kentrup, H., Becker, W., Heukelbach, J., Wilmes, A., Schurmann, A., Huppertz, C.*, et al.* (1996). Dyrk, a dual specificity protein kinase with unique structural features whose activity is dependent on tyrosine residues between subdomains VII and VIII. J Biol Chem *271*, 3488-3495.

Kim, D., Won, J., Shin, D.W., Kang, J., Kim, Y.J., Choi, S.Y.*, et al.* (2004). Regulation of Dyrk1A kinase activity by 14-3-3. Biochem Biophys Res Commun *323*, 499-504.

Kim, E.J., Sung, J.Y., Lee, H.J., Rhim, H., Hasegawa, M., Iwatsubo, T.*, et al.* (2006a). Dyrk1A phosphorylates alpha-synuclein and enhances intracellular inclusion formation. J Biol Chem *281*, 33250-33257.

Kim, M.Y., Jeong, B.C., Lee, J.H., Kee, H.J., Kook, H., Kim, N.S.*, et al.* (2006b). A repressor complex, AP4 transcription factor and geminin, negatively regulates expression of target genes in nonneuronal cells. Proc Natl Acad Sci U S A *103*, 13074-13079.

Kim, S., Kim, Y., Lee, J., and Chung, J. (2010). Regulation of FOXO1 by TAK1-Nemo-like kinase pathway. J Biol Chem *285*, 8122-8129.

Kimura, R., Kamino, K., Yamamoto, M., Nuripa, A., Kida, T., Kazui, H.*, et al.* (2007). The DYRK1A gene, encoded in chromosome 21 Down syndrome critical region, bridges between beta-amyloid production and tau phosphorylation in Alzheimer disease. Hum Mol Genet *16*, 15-23.

Kinstrie, R., Luebbering, N., Miranda-Saavedra, D., Sibbet, G., Han, J., Lochhead, P.A.*, et al.* (2010). Characterization of a domain that transiently converts class 2 DYRKs into intramolecular tyrosine kinases. Sci Signal *3*, ra16.

Knecht, E., Aguado, C., Carcel, J., Esteban, I., Esteve, J.M., Ghislat, G.*, et al.* (2009). Intracellular protein degradation in mammalian cells: recent developments. Cell Mol Life Sci *66*, 2427-2443.

Kohn, A.D., and Moon, R.T. (2005). Wnt and calcium signaling: beta-catenin-independent pathways. Cell Calcium *38*, 439-446.

Kojima, H., Sasaki, T., Ishitani, T., Iemura, S., Zhao, H., Kaneko, S.*, et al.* (2005). STAT3 regulates Nemo-like kinase by mediating its interaction with IL-6-stimulated TGFbeta-activated kinase 1 for STAT3 Ser-727 phosphorylation. Proc Natl Acad Sci U S A *102*, 4524-4529.

Kolligs, F.T., Hu, G., Dang, C.V., and Fearon, E.R. (1999). Neoplastic transformation of RK3E by mutant beta-catenin requires deregulation of Tcf/Lef transcription but not activation of c-myc expression. Mol Cell Biol *19*, 5696-5706.

Kopan, R., and Ilagan, M.X. (2009). The canonical Notch signaling pathway: unfolding the activation mechanism. Cell *137*, 216-233.

Kops, G.J., Medema, R.H., Glassford, J., Essers, M.A., Dijkers, P.F., Coffer, P.J.*, et al.* (2002). Control of cell cycle exit and entry by protein kinase B-regulated forkhead transcription factors. Mol Cell Biol *22*, 2025-2036.

Korinek, V., Barker, N., Morin, P.J., van Wichen, D., de Weger, R., Kinzler, K.W.*, et al.* (1997). Constitutive transcriptional activation by a beta-catenin-Tcf complex in APC-/- colon carcinoma. Science *275*, 1784-1787.

Kortenjann, M., Wehrle, C., Nehls, M.C., and Boehm, T. (2001). Only one nemo-like kinase gene homologue in invertebrate and mammalian genomes. Gene *278*, 161-165.

Kovall, R.A. (2008). More complicated than it looks: assembly of Notch pathway transcription complexes. Oncogene *27*, 5099-5109.

Krishnan, V., Bryant, H.U., and Macdougald, O.A. (2006). Regulation of bone mass by Wnt signaling. J Clin Invest *116*, 1202-1209.

Kuhl, M., Sheldahl, L.C., Malbon, C.C., and Moon, R.T. (2000). Ca(2+)/calmodulin-dependent protein kinase II is stimulated by Wnt and Frizzled homologs and promotes ventral cell fates in Xenopus. J Biol Chem *275*, 12701-12711.

Kuhn, C., Frank, D., Will, R., Jaschinski, C., Frauen, R., Katus, H.A., *et al.* (2009). DYRK1A is a novel negative regulator of cardiomyocyte hypertrophy. J Biol Chem *284*, 17320-17327.

Kurabayashi, N., Hirota, T., Sakai, M., Sanada, K., and Fukada, Y. (2010). DYRK1A and glycogen synthase kinase 3beta, a dual-kinase mechanism directing proteasomal degradation of CRY2 for circadian timekeeping. Mol Cell Biol *30*, 1757-1768.

Kurahashi, T., Nomura, T., Kanei-Ishii, C., Shinkai, Y., and Ishii, S. (2005). The Wnt-NLK signaling pathway inhibits A-Myb activity by inhibiting the association with coactivator CBP and methylating histone H3. Mol Biol Cell *16*, 4705-4713.

Laguna, A., Aranda, S., Barallobre, M.J., Barhoum, R., Fernandez, E., Fotaki, V., *et al.* (2008). The protein kinase DYRK1A regulates caspase-9-mediated apoptosis during retina development. Dev Cell *15*, 841-853.

Lauth, M., Bergstrom, A., Shimokawa, T., Tostar, U., Jin, Q., Fendrich, V., *et al.* (2010). DYRK1B-dependent autocrine-to-paracrine shift of Hedgehog signaling by mutant RAS. Nat Struct Mol Biol *17*, 718-725.

Lee, K., Deng, X., and Friedman, E. (2000). Mirk protein kinase is a mitogen-activated protein kinase substrate that mediates survival of colon cancer cells. Cancer Res *60*, 3631-3637.

Lee, Y., Ha, J., Kim, H.J., Kim, Y.S., Chang, E.J., Song, W.J., *et al.* (2009). Negative feedback Inhibition of NFATc1 by DYRK1A regulates bone homeostasis. J Biol Chem *284*, 33343-33351.

Lemmon, M.A., and Schlessinger, J. (2010). Cell signaling by receptor tyrosine kinases. Cell *141*, 1117-1134.

Li, D., Jackson, R.A., Yusoff, P., and Guy, G.R. (2010a). The direct association of Sprouty-related protein with an EVH1 domain (SPRED) 1 or SPRED2 with DYRK1A modifies substrate/kinase interactions. J Biol Chem.

Li, K., Zhao, S., Karur, V., and Wojchowski, D.M. (2002). DYRK3 activation, engagement of protein kinase A/cAMP response element-binding protein, and modulation of progenitor cell survival. J Biol Chem *277*, 47052-47060.

Li, M., Wang, H., Huang, T., Wang, J., Ding, Y., Li, Z., *et al.* (2010b). TAB2 scaffolds TAK1 and NLK in repressing canonical Wnt signaling. J Biol Chem *285*, 13397-13404.

Liang, Y.J., Chang, H.S., Wang, C.Y., and Yu, W.C. (2008). DYRK1A stabilizes HPV16E7 oncoprotein through phosphorylation of the threonine 5 and threonine 7 residues. Int J Biochem Cell Biol *40*, 2431-2441.

Lim, S., Jin, K., and Friedman, E. (2002). Mirk protein kinase is activated by MKK3 and functions as a transcriptional activator of HNF1alpha. J Biol Chem *277*, 25040-25046.

Liu, C., Li, Y., Semenov, M., Han, C., Baeg, G.H., Tan, Y., *et al.* (2002). Control of beta-catenin phosphorylation/degradation by a dual-kinase mechanism. Cell *108*, 837-847.

Liu, F., Liang, Z., Wegiel, J., Hwang, Y.W., Iqbal, K., Grundke-Iqbal, I., *et al.* (2008). Overexpression of Dyrk1A contributes to neurofibrillary degeneration in Down syndrome. FASEB J *22*, 3224-3233.

Liu, G., Bafico, A., and Aaronson, S.A. (2005). The mechanism of endogenous receptor activation functionally distinguishes prototype canonical and noncanonical Wnts. Mol Cell Biol *25*, 3475-3482.

Lo, M.C., Gay, F., Odom, R., Shi, Y., and Lin, R. (2004). Phosphorylation by the beta-catenin/MAPK complex promotes 14-3-3-mediated nuclear export of TCF/POP-1 in signal-responsive cells in C. elegans. Cell *117*, 95-106.

Lochhead, P.A., Sibbet, G., Morrice, N., and Cleghon, V. (2005). Activation-loop autophosphorylation is mediated by a novel transitional intermediate form of DYRKs. Cell *121*, 925-936.

Logan, C.Y., and Nusse, R. (2004). The Wnt signaling pathway in development and disease. Annu Rev Cell Dev Biol *20*, 781-810.

Lord, K.A., Creasy, C.L., King, A.G., King, C., Burns, B.M., Lee, J.C., *et al.* (2000). REDK, a novel human regulatory erythroid kinase. Blood *95*, 2838-2846.

Lorenowicz, M.J., and Korswagen, H.C. (2009). Sailing with the Wnt: charting the Wnt processing and secretion route. Exp Cell Res *315*, 2683-2689.

MacDonald, B.T., Tamai, K., and He, X. (2009). Wnt/beta-catenin signaling: components, mechanisms, and diseases. Dev Cell *17*, 9-26.

Macian, F. (2005). NFAT proteins: key regulators of T-cell development and function. Nat Rev Immunol *5*, 472-484.

MacKeigan, J.P., Murphy, L.O., and Blenis, J. (2005). Sensitized RNAi screen of human kinases and phosphatases identifies new regulators of apoptosis and chemoresistance. Nat Cell Biol *7*, 591-600.

Maenz, B., Hekerman, P., Vela, E.M., Galceran, J., and Becker, W. (2008). Characterization of the human DYRK1A promoter and its regulation by the transcription factor E2F1. BMC Mol Biol *9*, 30.

Maguschak, K.A., and Ressler, K.J. (2008). Beta-catenin is required for memory consolidation. Nat Neurosci *11*, 1319-1326.

Mancini, M., and Toker, A. (2009). NFAT proteins: emerging roles in cancer progression. Nat Rev Cancer *9*, 810-820.

Manning, G., Whyte, D.B., Martinez, R., Hunter, T., and Sudarsanam, S. (2002). The protein kinase complement of the human genome. Science *298*, 1912-1934.

Mao, J., Maye, P., Kogerman, P., Tejedor, F.J., Toftgard, R., Xie, W.*, et al.* (2002). Regulation of Gli1 transcriptional activity in the nucleus by Dyrk1. J Biol Chem *277*, 35156-35161.

Marti, E., Altafaj, X., Dierssen, M., de la Luna, S., Fotaki, V., Alvarez, M.*, et al.* (2003). Dyrk1A expression pattern supports specific roles of this kinase in the adult central nervous system. Brain Res *964*, 250-263.

Martinez de Lagran, M., Altafaj, X., Gallego, X., Marti, E., Estivill, X., Sahun, I.*, et al.* (2004). Motor phenotypic alterations in TgDyrk1a transgenic mice implicate DYRK1A in Down syndrome motor dysfunction. Neurobiol Dis *15*, 132-142.

Matus, D.Q., Li, X.Y., Durbin, S., Agarwal, D., Chi, Q., Weiss, S.J.*, et al.* (2010). In vivo identification of regulators of cell invasion across basement membranes. Sci Signal *3*, ra35.

McKay, M.M., and Morrison, D.K. (2007). Integrating signals from RTKs to ERK/MAPK. Oncogene *26*, 3113-3121.

Medema, R.H., Kops, G.J., Bos, J.L., and Burgering, B.M. (2000). AFX-like Forkhead transcription factors mediate cell-cycle regulation by Ras and PKB through p27kip1. Nature *404*, 782-787.

Meneghini, M.D., Ishitani, T., Carter, J.C., Hisamoto, N., Ninomiya-Tsuji, J., Thorpe, C.J.*, et al.* (1999). MAP kinase and Wnt pathways converge to downregulate an HMG-domain repressor in Caenorhabditis elegans. Nature *399*, 793-797.

Mercer, S.E., Ewton, D.Z., Shah, S., Naqvi, A., and Friedman, E. (2006). Mirk/Dyrk1b mediates cell survival in rhabdomyosarcomas. Cancer Res *66*, 5143-5150.

Merino, C., Penney, J., Gonzalez, M., Tsurudome, K., Moujahidine, M., O'Connor, M.B.*, et al.* (2009). Nemo kinase interacts with Mad to coordinate synaptic growth at the Drosophila neuromuscular junction. J Cell Biol *185*, 713-725.

Minami, Y., Oishi, I., Endo, M., and Nishita, M. (2010). Ror-family receptor tyrosine kinases in noncanonical Wnt signaling: their implications in developmental morphogenesis and human diseases. Dev Dyn *239*, 1-15.

Mirkovic, I., Charish, K., Gorski, S.M., McKnight, K., and Verheyen, E.M. (2002). Drosophila nemo is an essential gene involved in the regulation of programmed cell death. Mech Dev *119*, 9-20.

Molkentin, J.D. (2004). Calcineurin-NFAT signaling regulates the cardiac hypertrophic response in coordination with the MAPKs. Cardiovasc Res *63*, 467-475.

Moller, R.S., Kubart, S., Hoeltzenbein, M., Heye, B., Vogel, I., Hansen, C.P.*, et al.* (2008). Truncation of the Down syndrome candidate gene DYRK1A in two unrelated patients with microcephaly. Am J Hum Genet *82*, 1165-1170.

Moon, R.T., Kohn, A.D., De Ferrari, G.V., and Kaykas, A. (2004). WNT and beta-catenin signalling: diseases and therapies. Nat Rev Genet *5*, 691-701.

Mosimann, C., Hausmann, G., and Basler, K. (2009). Beta-catenin hits chromatin: regulation of Wnt target gene activation. Nat Rev Mol Cell Biol *10*, 276-286.

Munoz, J.P., Huichalaf, C.H., Orellana, D., and Maccioni, R.B. (2007). cdk5 modulates beta- and delta-catenin/Pin1 interactions in neuronal cells. J Cell Biochem *100*, 738-749.

Murakami, N., Bolton, D., and Hwang, Y.W. (2009). Dyrk1A binds to multiple endocytic proteins required for formation of clathrin-coated vesicles. Biochemistry *48*, 9297-9305.

Murphy, L.O., and Blenis, J. (2006). MAPK signal specificity: the right place at the right time. Trends Biochem Sci *31*, 268-275.

Ninomiya-Tsuji, J., Kishimoto, K., Hiyama, A., Inoue, J., Cao, Z., and Matsumoto, K. (1999). The kinase TAK1 can activate the NIK-I kappaB as well as the MAP kinase cascade in the IL-1 signalling pathway. Nature *398*, 252-256.

Nusse, R. (2008). Wnt signaling and stem cell control. Cell Res *18*, 523-527.

Oh-hora, M., and Rao, A. (2008). Calcium signaling in lymphocytes. Curr Opin Immunol *20*, 250-258.

Ohkawara, B., Shirakabe, K., Hyodo-Miura, J., Matsuo, R., Ueno, N., Matsumoto, K.*, et al.* (2004). Role of the TAK1-NLK-STAT3 pathway in TGF-beta-mediated mesoderm induction. Genes Dev *18*, 381-386.

Ohnishi, E., Goto, T., Sato, A., Kim, M.S., Iemura, S., Ishitani, T.*, et al.* (2010). Nemo-like kinase, an essential effector of anterior formation, functions downstream of p38 mitogen-activated protein kinase. Mol Cell Biol *30*, 675-683.

Okui, M., Ide, T., Morita, K., Funakoshi, E., Ito, F., Ogita, K.*, et al.* (1999). High-level expression of the Mnb/Dyrk1A gene in brain and heart during rat early development. Genomics *62*, 165-171.

Ortiz-Abalia, J., Sahun, I., Altafaj, X., Andreu, N., Estivill, X., Dierssen, M.*, et al.* (2008). Targeting Dyrk1A with AAVshRNA attenuates motor alterations in TgDyrk1A, a mouse model of Down syndrome. Am J Hum Genet *83*, 479-488.

Palka-Hamblin, H.L., Gierut, J.J., Bie, W., Brauer, P.M., Zheng, Y., Asara, J.M.*, et al.* (2010). Identification of beta-catenin as a target of the intracellular tyrosine kinase PTK6. J Cell Sci *123*, 236-245.

Panakova, D., Sprong, H., Marois, E., Thiele, C., and Eaton, S. (2005). Lipoprotein particles are required for Hedgehog and Wingless signalling. Nature *435*, 58-65.

Papadopoulos, C., Arato, K., Lilienthal, E., Zerweck, J., Schutkowski, M., Chatain, N.*, et al.* (2010). Alternative splicing regulates the catalytic activiy and subcellular localization of the Dual-Specificity Tyrosine Phosphorylation-Regulated Kinase 4 (DYRK4). J Biol Chem *in press*.

Park, J., Song, W.J., and Chung, K.C. (2009). Function and regulation of Dyrk1A: towards understanding Down syndrome. Cell Mol Life Sci *66*, 3235-3240.

Phng, L.K., and Gerhardt, H. (2009). Angiogenesis: a team effort coordinated by notch. Dev Cell *16*, 196-208.

Poellinger, L., and Lendahl, U. (2008). Modulating Notch signaling by pathway-intrinsic and pathway-extrinsic mechanisms. Curr Opin Genet Dev *18*, 449-454.

Polakis, P. (2000). Wnt signaling and cancer. Genes Dev *14*, 1837-1851.

Polakis, P. (2007). The many ways of Wnt in cancer. Curr Opin Genet Dev *17*, 45-51.

Prasad, B.C., and Clark, S.G. (2006). Wnt signaling establishes anteroposterior neuronal polarity and requires retromer in C. elegans. Development *133*, 1757-1766.

Raaf, L., Noll, C., Cherifi, M., Benazzoug, Y., Delabar, J.M., and Janel, N. (2009). Hyperhomocysteinemia-induced Dyrk1a downregulation results in cardiomyocyte hypertrophy in rats. Int J Cardiol. *Epub*.

Rabiller, M., Getlik, M., Kluter, S., Richters, A., Tuckmantel, S., Simard, J.R., *et al.* (2010). Proteus in the world of proteins: conformational changes in protein kinases. Arch Pharm (Weinheim) *343*, 193-206.

Rechsteiner, M. (1990). PEST sequences are signals for rapid intracellular proteolysis. Semin Cell Biol *1*, 433-440.

Rechsteiner, M., and Rogers, S.W. (1996). PEST sequences and regulation by proteolysis. Trends Biochem Sci *21*, 267-271.

Reya, T., and Clevers, H. (2005). Wnt signalling in stem cells and cancer. Nature *434*, 843-850.

Rhee, J., Buchan, T., Zukerberg, L., Lilien, J., and Balsamo, J. (2007). Cables links Robo-bound Abl kinase to N-cadherin-bound beta-catenin to mediate Slit-induced modulation of adhesion and transcription. Nat Cell Biol *9*, 883-892.

Roca, C., and Adams, R.H. (2007). Regulation of vascular morphogenesis by Notch signaling. Genes Dev *21*, 2511-2524.

Rocheleau, C.E., Yasuda, J., Shin, T.H., Lin, R., Sawa, H., Okano, H., *et al.* (1999). WRM-1 activates the LIT-1 protein kinase to transduce anterior/posterior polarity signals in C. elegans. Cell *97*, 717-726.

Rogers, S., Wells, R., and Rechsteiner, M. (1986). Amino acid sequences common to rapidly degraded proteins: the PEST hypothesis. Science *234*, 364-368.

Rottinger, E., Croce, J., Lhomond, G., Besnardeau, L., Gache, C., and Lepage, T. (2006). Nemo-like kinase (NLK) acts downstream of Notch/Delta signalling to downregulate TCF during mesoderm induction in the sea urchin embryo. Development *133*, 4341-4353.

Ruiz i Altaba, A., Mas, C., and Stecca, B. (2007). The Gli code: an information nexus regulating cell fate, stemness and cancer. Trends Cell Biol *17*, 438-447.

Ruiz i Altaba, A., Palma, V., and Dahmane, N. (2002). Hedgehog-Gli signalling and the growth of the brain. Nat Rev Neurosci *3*, 24-33.

Ryoo, S.R., Cho, H.J., Lee, H.W., Jeong, H.K., Radnaabazar, C., Kim, Y.S., *et al.* (2008). Dual-specificity tyrosine(Y)-phosphorylation regulated kinase 1A-mediated phosphorylation of amyloid precursor protein: evidence for a functional link between Down syndrome and Alzheimer's disease. J Neurochem *104*, 1333-1344.

Ryoo, S.R., Jeong, H.K., Radnaabazar, C., Yoo, J.J., Cho, H.J., Lee, H.W., *et al.* (2007). DYRK1A-mediated hyperphosphorylation of Tau. A functional link between Down syndrome and Alzheimer disease. J Biol Chem *282*, 34850-34857.

Saijo, K., Winner, B., Carson, C.T., Collier, J.G., Boyer, L., Rosenfeld, M.G., *et al.* (2009). A Nurr1/CoREST pathway in microglia and astrocytes protects dopaminergic neurons from inflammation-induced death. Cell *137*, 47-59.

Salichs, E. (2008). PolyHistidine repeats and DYRK1A: from the localization to the function (Doctoral Thesis, Universitat Pompeu Fabra).

Salichs, E., Ledda, A., Mularoni, L., Alba, M.M., and de la Luna, S. (2009). Genome-wide analysis of histidine repeats reveals their role in the localization of human proteins to the nuclear speckles compartment. PLoS Genet *5*, e1000397.

Satoh, K., Ohnishi, J., Sato, A., Takeyama, M., Iemura, S., Natsume, T., *et al.* (2007). Nemo-like kinase-myocyte enhancer factor 2A signaling regulates anterior formation in Xenopus development. Mol Cell Biol *27*, 7623-7630.

Scales, T.M., Lin, S., Kraus, M., Goold, R.G., and Gordon-Weeks, P.R. (2009). Nonprimed and DYRK1A-primed GSK3 beta-phosphorylation sites on MAP1B regulate microtubule dynamics in growing axons. J Cell Sci *122*, 2424-2435.

Schulte, G., and Bryja, V. (2007). The Frizzled family of unconventional G-protein-coupled receptors. Trends Pharmacol Sci *28*, 518-525.

Schulz, R.A., and Yutzey, K.E. (2004). Calcineurin signaling and NFAT activation in cardiovascular and skeletal muscle development. Dev Biol *266*, 1-16.

Seifert, A., Allan, L.A., and Clarke, P.R. (2008). DYRK1A phosphorylates caspase 9 at an inhibitory site and is potently inhibited in human cells by harmine. FEBS J *275*, 6268-6280.

Seifert, A., and Clarke, P.R. (2009). p38alpha- and DYRK1A-dependent phosphorylation of caspase-9 at an inhibitory site in response to hyperosmotic stress. Cell Signal *21*, 1626-1633.

Seifert, J.R., and Mlodzik, M. (2007). Frizzled/PCP signalling: a conserved mechanism regulating cell polarity and directed motility. Nat Rev Genet *8*, 126-138.

Shi, J., Zhang, T., Zhou, C., Chohan, M.O., Gu, X., Wegiel, J.*, et al.* (2008). Increased dosage of Dyrk1A alters alternative splicing factor (ASF)-regulated alternative splicing of tau in Down syndrome. J Biol Chem *283*, 28660-28669.

Shi, Y., Ye, K., Wu, H., Sun, Y., Shi, H., and Huo, K. (2010). Human SMAD4 is phosphorylated at Thr9 and Ser138 by interacting with NLK. Mol Cell Biochem *333*, 293-298.

Shimokawa, T., Tostar, U., Lauth, M., Palaniswamy, R., Kasper, M., Toftgard, R.*, et al.* (2008). Novel human glioma-associated oncogene 1 (GLI1) splice variants reveal distinct mechanisms in the terminal transduction of the hedgehog signal. J Biol Chem *283*, 14345-14354.

Shin, T.H., Yasuda, J., Rocheleau, C.E., Lin, R., Soto, M., Bei, Y.*, et al.* (1999). MOM-4, a MAP kinase kinase kinase-related protein, activates WRM-1/LIT-1 kinase to transduce anterior/posterior polarity signals in C. elegans. Mol Cell *4*, 275-280.

Sitz, J.H., Baumgartel, K., Hammerle, B., Papadopoulos, C., Hekerman, P., Tejedor, F.J.*, et al.* (2008). The Down syndrome candidate dual-specificity tyrosine phosphorylation-regulated kinase 1A phosphorylates the neurodegeneration-related septin 4. Neuroscience *157*, 596-605.

Sitz, J.H., Tigges, M., Baumgartel, K., Khaspekov, L.G., and Lutz, B. (2004). Dyrk1A potentiates steroid hormone-induced transcription via the chromatin remodeling factor Arip4. Mol Cell Biol *24*, 5821-5834.

Skurat, A.V., and Dietrich, A.D. (2004). Phosphorylation of Ser640 in muscle glycogen synthase by DYRK family protein kinases. J Biol Chem *279*, 2490-2498.

Smit, L., Baas, A., Kuipers, J., Korswagen, H., van de Wetering, M., and Clevers, H. (2004). Wnt activates the Tak1/Nemo-like kinase pathway. J Biol Chem *279*, 17232-17240.

Smith, D.J., Stevens, M.E., Sudanagunta, S.P., Bronson, R.T., Makhinson, M., Watabe, A.M.*, et al.* (1997). Functional screening of 2 Mb of human chromosome 21q22.2 in transgenic mice implicates minibrain in learning defects associated with Down syndrome. Nat Genet *16*, 28-36.

Song, D.H., Dominguez, I., Mizuno, J., Kaut, M., Mohr, S.C., and Seldin, D.C. (2003). CK2 phosphorylation of the armadillo repeat region of beta-catenin potentiates Wnt signaling. J Biol Chem *278*, 24018-24025.

Sorkin, A., and von Zastrow, M. (2009). Endocytosis and signalling: intertwining molecular networks. Nat Rev Mol Cell Biol *10*, 609-622.

Sorokin, A.V., Kim, E.R., and Ovchinnikov, L.P. (2007). Nucleocytoplasmic transport of proteins. Biochemistry (Mosc) *72*, 1439-1457.

Staal, F.J., Luis, T.C., and Tiemessen, M.M. (2008). WNT signalling in the immune system: WNT is spreading its wings. Nat Rev Immunol *8*, 581-593.

Su, Y., Fu, C., Ishikawa, S., Stella, A., Kojima, M., Shitoh, K.*, et al.* (2008). APC is essential for targeting phosphorylated beta-catenin to the SCFbeta-TrCP ubiquitin ligase. Mol Cell *32*, 652-661.

Suh, E.K., and Gumbiner, B.M. (2003). Translocation of beta-catenin into the nucleus independent of interactions with FG-rich nucleoporins. Exp Cell Res *290*, 447-456.

Szypowska, A., de Ruiter, H., Meijer, L., Smits, L., and Burgering, B. (2010). Oxidative stress dependent regulation of Forkhead box O4 activity by Nemo-like kinase. Antioxid Redox Signal.

Taira, N., Nihira, K., Yamaguchi, T., Miki, Y., and Yoshida, K. (2007). DYRK2 is targeted to the nucleus and controls p53 via Ser46 phosphorylation in the apoptotic response to DNA damage. Mol Cell *25*, 725-738.

Taira, N., Yamamoto, H., Yamaguchi, T., Miki, Y., and Yoshida, K. (2010). ATM augments nuclear stabilization of DYRK2 by inhibiting MDM2 in the apoptotic response to DNA damage. J Biol Chem *285*, 4909-4919.

Takada, I., Mihara, M., Suzawa, M., Ohtake, F., Kobayashi, S., Igarashi, M.*, et al.* (2007). A histone lysine methyltransferase activated by non-canonical Wnt signalling suppresses PPAR-gamma transactivation. Nat Cell Biol *9*, 1273-1285.

Takada, R., Satomi, Y., Kurata, T., Ueno, N., Norioka, S., Kondoh, H.*, et al.* (2006). Monounsaturated fatty acid modification of Wnt protein: its role in Wnt secretion. Dev Cell *11*, 791-801.

Tanoue, T., Adachi, M., Moriguchi, T., and Nishida, E. (2000). A conserved docking motif in MAP kinases common to substrates, activators and regulators. Nat Cell Biol *2*, 110-116.

Taurin, S., Sandbo, N., Qin, Y., Browning, D., and Dulin, N.O. (2006). Phosphorylation of beta-catenin by cyclic AMP-dependent protein kinase. J Biol Chem *281*, 9971-9976.

Tejedor, F., Zhu, X.R., Kaltenbach, E., Ackermann, A., Baumann, A., Canal, I.*, et al.* (1995). minibrain: a new protein kinase family involved in postembryonic neurogenesis in Drosophila. Neuron *14*, 287-301.

Thorpe, C.J., and Moon, R.T. (2004). nemo-like kinase is an essential co-activator of Wnt signaling during early zebrafish development. Development *131*, 2899-2909.

Tian, Q., Feetham, M.C., Tao, W.A., He, X.C., Li, L., Aebersold, R.*, et al.* (2004). Proteomic analysis identifies that 14-3-3zeta interacts with beta-catenin and facilitates its activation by Akt. Proc Natl Acad Sci U S A *101*, 15370-15375.

Tien, A.C., Rajan, A., and Bellen, H.J. (2009). A Notch updated. J Cell Biol *184*, 621-629.

van Amerongen, R., Mikels, A., and Nusse, R. (2008). Alternative wnt signaling is initiated by distinct receptors. Sci Signal *1*, re9.

van Amerongen, R., and Nusse, R. (2009). Towards an integrated view of Wnt signaling in development. Development *136*, 3205-3214.

Varjosalo, M., Bjorklund, M., Cheng, F., Syvanen, H., Kivioja, T., Kilpinen, S.*, et al.* (2008). Application of active and kinase-deficient kinome collection for identification of kinases regulating hedgehog signaling. Cell *133*, 537-548.

Varjosalo, M., and Taipale, J. (2008). Hedgehog: functions and mechanisms. Genes Dev *22*, 2454-2472.

Veeman, M.T., Slusarski, D.C., Kaykas, A., Louie, S.H., and Moon, R.T. (2003). Zebrafish prickle, a modulator of noncanonical Wnt/Fz signaling, regulates gastrulation movements. Curr Biol *13*, 680-685.

Verheyen, E.M., Mirkovic, I., MacLean, S.J., Langmann, C., Andrews, B.C., and MacKinnon, C. (2001). The tissue polarity gene nemo carries out multiple roles in patterning during Drosophila development. Mech Dev *101*, 119-132.

Vlad, A., Rohrs, S., Klein-Hitpass, L., and Muller, O. (2008). The first five years of the Wnt targetome. Cell Signal *20*, 795-802.

Wang, C., Deng, L., Hong, M., Akkaraju, G.R., Inoue, J., and Chen, Z.J. (2001). TAK1 is a ubiquitin-dependent kinase of MKK and IKK. Nature *412*, 346-351.

Wang, H.Y., Liu, T., and Malbon, C.C. (2006). Structure-function analysis of Frizzleds. Cell Signal *18*, 934-941.

Wang, Y., and Nathans, J. (2007). Tissue/planar cell polarity in vertebrates: new insights and new questions. Development *134*, 647-658.

Wegiel, J., Dowjat, K., Kaczmarski, W., Kuchna, I., Nowicki, K., Frackowiak, J.*, et al.* (2008). The role of overexpressed DYRK1A protein in the early onset of neurofibrillary degeneration in Down syndrome. Acta Neuropathol *116*, 391-407.

Wegiel, J., Kuchna, I., Nowicki, K., Frackowiak, J., Dowjat, K., Silverman, W.P., *et al.* (2004). Cell type- and brain structure-specific patterns of distribution of minibrain kinase in human brain. Brain Res *1010*, 69-80.

Willert, K., and Jones, K.A. (2006). Wnt signaling: is the party in the nucleus? Genes Dev *20*, 1394-1404.

Wong, S.Y., and Reiter, J.F. (2008). The primary cilium at the crossroads of mammalian hedgehog signaling. Curr Top Dev Biol *85*, 225-260.

Woods, Y.L., Rena, G., Morrice, N., Barthel, A., Becker, W., Guo, S., *et al.* (2001). The kinase DYRK1A phosphorylates the transcription factor FKHR at Ser329 in vitro, a novel in vivo phosphorylation site. Biochem J *355*, 597-607.

Wu, H., Symes, K., Seldin, D.C., and Dominguez, I. (2009). Threonine 393 of beta-catenin regulates interaction with Axin. J Cell Biochem *108*, 52-63.

Xing, Y., Takemaru, K., Liu, J., Berndt, J.D., Zheng, J.J., Moon, R.T., *et al.* (2008). Crystal structure of a full-length beta-catenin. Structure *16*, 478-487.

Xu, W., and Kimelman, D. (2007). Mechanistic insights from structural studies of beta-catenin and its binding partners. J Cell Sci *120*, 3337-3344.

Yabut, O., Domogauer, J., and D'Arcangelo, G. (2010). Dyrk1A overexpression inhibits proliferation and induces premature neuronal differentiation of neural progenitor cells. J Neurosci *30*, 4004-4014.

Yamada, M., Ohkawara, B., Ichimura, N., Hyodo-Miura, J., Urushiyama, S., Shirakabe, K., *et al.* (2003). Negative regulation of Wnt signalling by HMG2L1, a novel NLK-binding protein. Genes Cells *8*, 677-684.

Yamada, M., Ohnishi, J., Ohkawara, B., Iemura, S., Satoh, K., Hyodo-Miura, J., *et al.* (2006). NARF, an nemo-like kinase (NLK)-associated ring finger protein regulates the ubiquitylation and degradation of T cell factor/lymphoid enhancer factor (TCF/LEF). J Biol Chem *281*, 20749-20760.

Yang, C.S., Wang, X., Lu, G., and Picinich, S.C. (2009). Cancer prevention by tea: animal studies, molecular mechanisms and human relevance. Nat Rev Cancer *9*, 429-439.

Yasuda, J., Tsuchiya, A., Yamada, T., Sakamoto, M., Sekiya, T., and Hirohashi, S. (2003). Nemo-like kinase induces apoptosis in DLD-1 human colon cancer cells. Biochem Biophys Res Commun *308*, 227-233.

Yasuda, J., Yokoo, H., Yamada, T., Kitabayashi, I., Sekiya, T., and Ichikawa, H. (2004). Nemo-like kinase suppresses a wide range of transcription factors, including nuclear factor-kappaB. Cancer Sci *95*, 52-57.

Yokoyama, N.N., Pate, K.T., Sprowl, S., and Waterman, M.L. (2010). A role for YY1 in repression of dominant negative LEF-1 expression in colon cancer. Nucleic Acids Res.

Yuan, J.S., Kousis, P.C., Suliman, S., Visan, I., and Guidos, C.J. (2010). Functions of notch signaling in the immune system: consensus and controversies. Annu Rev Immunol *28*, 343-365.

Zechner, D., Fujita, Y., Hulsken, J., Muller, T., Walther, I., Taketo, M.M., *et al.* (2003). beta-Catenin signals regulate cell growth and the balance between progenitor cell expansion and differentiation in the nervous system. Dev Biol *258*, 406-418.

Zeng, G., Apte, U., Micsenyi, A., Bell, A., and Monga, S.P. (2006). Tyrosine residues 654 and 670 in beta-catenin are crucial in regulation of Met-beta-catenin interactions. Exp Cell Res *312*, 3620-3630.

Zeng, X., Tamai, K., Doble, B., Li, S., Huang, H., Habas, R., *et al.* (2005). A dual-kinase mechanism for Wnt co-receptor phosphorylation and activation. Nature *438*, 873-877.

Zeng, Y.A., Rahnama, M., Wang, S., Sosu-Sedzorme, W., and Verheyen, E.M. (2007). Drosophila Nemo antagonizes BMP signaling by phosphorylation of Mad and inhibition of its nuclear accumulation. Development *134*, 2061-2071.

Zeng, Y.A., and Verheyen, E.M. (2004). Nemo is an inducible antagonist of Wingless signaling during Drosophila wing development. Development *131*, 2911-2920.

Zhang, J., Woodhead, G.J., Swaminathan, S.K., Noles, S.R., McQuinn, E.R., Pisarek, A.J., *et al.* (2010). Cortical neural precursors inhibit their own differentiation via N-cadherin maintenance of beta-catenin signaling. Dev Cell *18*, 472-479.

Zhang, J., Zhou, B., Zheng, C.F., and Zhang, Z.Y. (2003). A bipartite mechanism for ERK2 recognition by its cognate regulators and substrates. J Biol Chem *278*, 29901-29912.

Zhao, B., Schlesiger, C., Masucci, M.G., and Lindsten, K. (2009). The ubiquitin specific protease 4 (USP4) is a new player in the Wnt signalling pathway. J Cell Mol Med *13*, 1886-1895.

Zhou, T., Liang, B., Su, G.Y., Gong, W.L., Li, H.Y., Tian, L.F., *et al.* (2007). Identification of ubiquitin target proteins using cell-based arrays. J Proteome Res *6*, 4397-4406.

Zhu, J., Shibasaki, F., Price, R., Guillemot, J.C., Yano, T., Dotsch, V., *et al.* (1998). Intramolecular masking of nuclear import signal on NF-AT4 by casein kinase I and MEKK1. Cell *93*, 851-861.

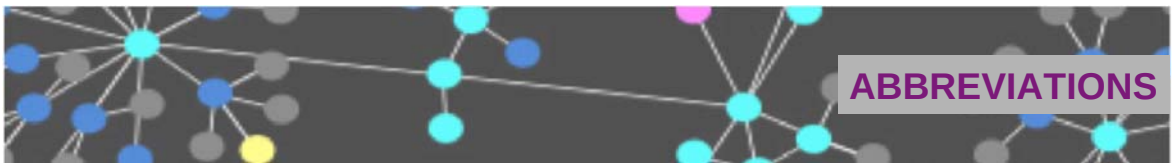

ABBREVIATIONS

Aa: amino acids

AD: Alzheimers' disease

AP4: activating enhancer binding protein 4

APC: adenomatous polyposis coli

APP: amyloid β precursor protein

ATP: adenosine triphosphate

BSA: bovine serum albumin

CAMKII: calcium/calmodulin-dependent protein kinase II

CBP: CREB-binding protein

CDK: cyclin-dependent kinase

CKI: casein kinase I

CLK: CDC-like kinase

CMV: cytomegalovirus

CNS: central nervous system

CRD: cysteine-rich domain

CREB: CRE-binding protein

CRY2: Cryptochrome-2

CtBP: C-terminal binding protein

C-terminal: carboxy-terminal

DAPI: 4,6-diamidino-2-phenylindole

DH-box: DYRK-homology box

Dll: Delta-like

DMEM: Dulbecco's Modified Eagle's Medium

DNA: desoxiribonucleic acid

DS: Down syndrome

DSCR: Down syndrome critical region

Dsh, Dvl: Dishevelled

DTT: dithiothreitol

DYRK: Dual-Specificity Tyrosine Phosphorylation-Regulated Kinase

EDTA: ethylendiamine tetracetic acid

EGCG: (-)-epigallocatechin-3-gallate

EGF: epidermal growth factor

EGFR: epidermal growth factor receptor

eIF2B: eukaryotic initiation factor 2B

ERK: extracellular signal-regulated kinase

FBS: foetal bovine serum

FGF: fibroblast growth factor

FITC: fluorescein isothiocyanate

FOXO: forkhead box, sub-group O transcription factor

Fzd: frizzled receptor

GFP: green fluorescent protein

GSK3: glycogen synthese kinase-3

GST: glutathione-S-transferase

HA: hemagglutinin

HDAC: histone deacetylase

HEPES: 4-(2-hydroxyethyl)-1-piperazineethanesulfonic acid

Hh: hedgehog

HIPK2: homeodomain-interacting protein kinase 2

HRP: horseradish peroxidase

HSA21: *Homo sapiens* autosome 21

IgG_H: immunoglobulin G heavy chain

IP: immunoprecipitation

IPTG: isopropyl-β-D-thiogalactopiranoside

IVK: *in vitro* kinase assay

JNK: c-Jun amino (N)-terminal kinase

kDa: kilodalton

LB: Luria Broth medium

LEF-1: lymphoid enhancer-binding factor-1

LRP5/6: low-density lipoprotein receptor-related protein 5/6

MAb: monoclonal antibody

MAP1B: microtubule-associated protein 1B

MAPK: mitogen-activated protein kinase

mnb: minibrain

mRNA: messenger RNA

NARF: NLK-associated ring finger protein

NES: nuclear export signal

NFAT: nuclear factor of activated T-cells

NGF: nerve growth factor

NICD: Notch intracellular domain

NLK: Nemo-like kinase

NLS: nuclear localization signal

NP-40: nonidet P-40

N-terminal: amino-terminal

ORF: open reading frame

PAGE: polyacrylamide gel electrophoresis

PBS: phosphate-buffered saline

PCR: polymerase chain reaction

PEST: region rich in Pro, Glu, Ser and Thr residues

PKA: c-AMP-dependent protein kinase

PKC: protein kinase C

RANKL: receptor activator for nuclear factor κ B ligand

RNA: ribonucleic acid

RNL: *Renilla* luciferase

RT: room temperature

RTK: receptor tyrosine kinase

SDS: sodium dodecil sulfate

SEM: standard error of the mean

shRNA: short hairpin RNA

SPRED: Sprouty-related Ena/vasodilator-stimulated phosphoprotein homology-1 (EVH1) domain-containing protein

Spry2: Sprouty 2

TAB2: TAK1-binding protein 2

TAK1: TGFβ-activated kinase 1

TCF-4: T-cell factor-4, official name TCF7L2, Transcription factor 7-like 2

TGFβ: Transforming growth factor beta

WB: western blot

wt: wild-type

Krisztina Arató was supported by an FPU predoctoral fellowship of the Spanish Ministry of Education and Science (AP20054558). This work was supported by the Spanish Ministry of Science and Innovation (BFU2007-61043/BMC), AGAUR (2009SGR1464) and the AnEUploidy EC grant. The group belongs to the Centro de Investigación Biomédica en Red de Enfermedades Raras (CIBERER).

Acknowledgements

Aquí tengo un poco de espacio para dirigirme a vosotros, los que habéis estado al lado mío durante estos 5 años de tesis o incluso antes y que habéis ayudado cada día para que yo llegué hasta escribir esta tesis con ganas, orgullo y disfrutándolo. Gracias a todos, por haber aguantado mis tonterías, sobre Hungría y la Unión Europea, y pido perdón por no entender nunca ningún chiste de doble sentido. Espero haber aportado algo a vuestras vidas, como mínimo, un poco de paz interior y alguna sonrisa.

Susana, primero de todo quisiera agradecerte de haberme dado la oportunidad de hacer la tesis contigo. Aprendí que todo el mundo puede tener una segunda oportunidad y si alguien quiere aprender hay que encontrar el profesor adecuado y el grupo adecuado, el entorno adecuado. Eres muy motivadora. Sabes, lo que más disfrutaba era enseñarte los resultados porque cada vez tenías completamente otra conclusión que yo, algo de que yo ni me di cuenta, aprendí mucho de esto. De ser siempre muy crítico con nuestros resultados, eso es muy difícil. Después, la cosa más importante que aprendí, y que me servirá para toda la vida, es aceptar si algo no funciona y dejarlo. Ai, es que soy una cabezona!!! Y gracias por ayudarnos en todo momento, económicamente y personalmente. En nombre de los guiris tengo que agradecerte que no tenemos que preocuparnos de si comemos el día siguiente o si estamos enfermos que medicamento tenemos que tomar, y mil otras cosas. Ojala te podría devolver una décima parte de esto!

Para los compis del lab: gracias a todos por crear un ambiente tan agradable, familiar. Tantas mujeres y sabíamos sacar provecho de ello! Gracias por todas las cotillas y charlas y lágrimas y cariño y chocolate. Y gracias a los chicos por aguantarnos…

Chiari, un día serás una superjefa y yo estaré orgullosa de que te enseñé donde estaban las cosas en el lab, porque mucho más no tenía que explicar. Me impresiona lo eficaz que eres. Era muy importante para mí que te guste tanto la biología como a mí y que forzaste siempre nuestras reuniones para discutir sobre resultados. Eres la mejor! Nunca lo dejes!

Esteban, eres el único que logró de verdad integrarse entre tantas mujeres, gracias por tratar nuestro género con tanto cariño. Estoy muy contenta por tenerte como amigo, es que compartimos tantas cosas. Por fin encontré a alguien que venga conmigo a los conciertos!

Ali, como Susana dijo, gracias por ser tan estupenda. Nadie aguantaría las mil preguntas que te hacemos cada cinco minutos por no encontrar nada y por pedir y pedir y pedir… este lab funciona tan bien porque nos llevas tan ordenados, jaja… gracias a ti y a Chiari también por ayudarme con los experimentos y por las cenas en tu casa adonde algunas veces logramos llegar.

Andrea, gracias por volverme a enseñar que hay que vigilar el cuerpo para tener una vida sana. Era el último empujón para comprarme la bici.

Mónica, sólo coincidimos el primer año, pero estás tan presente en este lab… casi todos los resultados tienen que ver algo contigo, cuanto trabajo! Gracias por traer tan buen rollo siempre.

Sergi, mil gracias por haberme enseñado los protocolos… Ai, como me machacabas con el Laemmli-buffer!!! Jajaja… y nosotras te machacábamos con nuestra feminidad… y ahora una niña, esto es tu destino… disfrútalo!

Salichs, espero que te hayas encontrado tu camino con lo de enseñar. Te veo muy bien allá, seguro que los niños te muestran mucho cariño que entre adultos no es tan fácil de enseñarlo. Y no dejes la música, si lo llevas tan a dentro.

Silvi, que risa me haces siempre. Me alegro de que estés contenta con la farmacia. Siempre me acordaré de nuestro viaje. O más bien la tuya, jaja…

Valentin, ai las risas que me vienen… gracias por ser el punto alegre. Y por compartir el DYRK4.

A Lali, a Ari y a Uli las felicito por enseñarnos de que es posible ser mamá y superinvestigadora a la vez. De dónde podéis sacar tanta energía? Mil besos a todas vuestras familias. Ari, gracias por enseñarnos “Compartir es estimar”, y Uli gracias por haberme sentido como si las dos viniéramos de la misma familia o de la misma escuela.

Mariona, gracias por ser mi segunda jefa en los labmeetings, en el comité… por compartir la habitación en Oviedo… por hacernos conocer a Alba.

Elisa, te queda un año para que acabes… y esto no lo digo para estresarte, más bien te veo bien, llegarás con buenos resultados, con la cabeza alta. Algunas veces tal vez lo dudabas, pero hay que dar tiempo a las cosas, y si trabajas con ratones aún más. Gracias por las cenas y fiestas en tu casa, eran las más divertidas.

María Jo, te admiro y te quiero. Gracias por todo el apoyo mental y emocional que nos das cada día.

Soni, a ver cuántas chicas conseguirás en cinco años para ir a rugby contigo, y en vez de volley jugaremos rugby en la playa. Gracias por las fiestas que hemos pasado juntas, por tus ataques de risa y por algunas charlas que tuvimos en la terraza entre las dos, que me gustaban mucho.

Erikín, cuanto chocolate hemos comido juntas!!! Aaaa, en este lab uno sólo se engorda… gracias por estar siempre allá conmigo, tanto por cotillar sobre tonterías como por ayudarme si necesitaba algo. Me encanta tu sentido de humor y tu risa. Pero mujer, aprende a descansar, no puedes trabajar tanto!!

Silvi Porta, juarrr!!! Un día tendré que mirar quién era este Krisztin Klanders… que pena que acabaste tantos años antes que yo…

Lauri, la gallega de todas, jeje, me quedé con la frase “Vaya nicki más chachi”… lo que tenía que aprender para entenderos… hace mucho que no sabemos nada de ti y tus mejillones, espero que estés contenta.

María José de radioactividad, muchísimas gracias por vigilarme durante el pulse-chase y de atenderme siempre con tanta paciencia frente cualquier problema.

Cristina y Henrik de proteómica, nuestra colaboración ha dado muy buenos frutos, gracias por hacer todo lo que os pedíamos.

Doy gracias al CRG por haber podido trabajar con tantas máquinas tan buenas, especialmente doy gracias a los inventores del FujiFilm de WBs, por poder revelar en incremento y no tener que poner films manualmente cada 30 segundos. Ésta máquina nos salva días de trabajo!

A magyaroknak:

Anyu, Apu, nektek köszönök mindent. Ez az egész doktori nem lenne nélkületek. Hiszen ha jól belegondolok, ez a biológia mánia otthonról jön, a sok állat, a sok növény, a telek… Köszönöm az örökös szeretetet, a biztos családi hangulatot, a játékkedvet; hogy sose hiányzott pénz tanulásra; hogy annyira nyitott szívűek vagytok felém, Pere felé, a barátaim felé és hogy ilyennek neveltetek. Köszönöm, hogy mindig bíztattatok, hogy bíztatok bennem, még ha ilyen fura szakmát is választottam, és hogy végül elengedtetek az utamra.

Gábor, neked azt köszönöm, hogy annyira szeretsz és kötődsz hozzám, még ha iszonyúan különbözőek vagyunk is. Jesszus, mikor gyerekek voltunk alig bírtuk elviselni egymást… hehe, Anyuék mesélhetnének… és most nézd meg, mennyi sok közös vonásunk van: tök fontosak számunkra a barátok, az otthon, imádunk bulizni, jó színvonalon élni, amiért persze meg is dolgozunk, és bármi rossz történik is velünk, újra talpra állunk. A tanulás számomra tök mindegy, nekem bejött, neked nem. Tudd, hogy számomra te egy remek ember vagy. Ez már csak abból is látszik, hogy egy ilyen szuper barátnőd van, mint a Móni. Móni, köszönöm, hogy vigyázol rá, hogy legyenek céljai a jövőre és hogy együtt sikerüljön betöltenetek ezeket.

Zitám, mi újat mondhatnék neked… tudod hogy szeretlek, hogy tisztellek, hogy a példaképem vagy, hogy az egész életemre hatással voltál/vagy/leszel; hogyha bajom van, téged hívlak; hogyha döntenem kell, rád gondolok, hogy mit tennél ezesetben. Sajnálom, hogy emiatt a hülye doktori miatt keveset mentem meglátogatni titeket; hogy annyi mindenről nem meséltem, de igazából ahhoz kettesben kéne lennünk néha, mint a régi időkben. És iszonyú nagy megtiszteltetés számomra, hogy Picúr életébe bevontok, mintha családtag lennék. Nézd meg, itt állok 29 évesen, és ez a legszeretettelibb dolog amit valaha értem tettek eddig. Köszönöm.

Adrinak és Máténak köszönöm a jelátviteles laborban eltöltött éveket, hogy annyira szuper kutatókká lettetek és példaképemül szolgáltok, és hogy a munkán kívül annyi sok hülyeségre is kaphatóak vagytok. A legjobb barátaim vagytok.

Para los de casa:

Perico, a ti que te puedo decir que no te haya dicho ya. Vine aquí con 23, con una maleta y sin ningún duro y fue tan difícil el primer año que si no fuera por ti me hubiera ido a casa. Pero decidí quedarme, entré en el grupo de Susana y desde entonces todo cambió. Estoy disfrutando cada día en Barcelona contigo, con nuestros amigos, con nuestro piso (vale de Ari y Sergi). Me he convertido en una persona tranquila, alegre y quien sabe lo que quiere hacer. Todo esto hubiera sido imposible sin tenerte al lado mío. Esta tesis te la dedico a ti, por los siete años de risas y por todos los días llorones que hayas aguantado.

A toda la familia de Pere, quisiera agradecer de haberme aceptado como una hija, desde el primer día que llegué; de haber cambiado el idioma de la familia al principio; de haber compartido los buenos y los malos momentos conmigo; de aconsejarme sobre cualquier problema que tenía; de avisarme sobre todas las noticias de Hungría; vamos, de hacerme sentir que tengo una familia aquí en Barcelona también. Gracias por todos los regalos y por estar tan orgullosos como mis padres ahora que me presentó a defender la tesis.

Hagen, Luisa, Jessica, Henrik, Adam, Martin, Renia, Helena, Tamara, Rasa, Philip, mi grupo de doctorado y sus familias, gracias por estos 5 años maravillosos, por las presentaciones que teníamos que hacer en el primer año, por las comidas, por las excursiones, por los embarazos, por las tesis... Luisa cariño, gracias por la portada y Hagen, no te preocupes, lo vas a conseguir, yo confío en ti, dos besos.

Carole, Xavi, Felix, mi familia preferida. Vuestro trío trasmite tanto amor que es imposible desengancharse. Otra vez, gracias por ser ejemplares en enseñar que se puede tener familia al lado de un trabajo duro.

Adam, you will laugh about it… I just said that it's funny I really started to talk to you because you are from Eastern Europe. In Hungary I would have never done that. But it really seems to work, at least you understand my jokes, even though I don't understand yours, hehe! You will always repeat me this… To you and to Kalli I can only say that the first year is hard, but you will overcome any problem, you are such nice people.

Vicky, gracias por ser la hermana que siempre quería tener. Ya sé que tú tienes muchas… Me encanta que eres tan franca como yo… ai, cuanto me haces reír!

Mónica, que bien me pasé en Budapest con vosotras, tu tranquilidad me hace relajar tanto.

Camilla, guapa, todo el mérito para ti por haber quedado en el CRG con nuevo grupo y nuevo proyecto, queriendo hacer el doctorado. Yo también aprendí que si alguien tiene una meta, la puede conseguir aunque al principio las cosas se hagan un poco difíciles. Eres estupenda! Que no pierdas nunca tu sonrisa y energía.

Dani, el primer argentino que conocí, y que hablaba catalán! No me pareciste ni argentino. Me impresiona que hayas ido a hacer un post-doc tan duro, y que nosotros casi nunca hablamos del trabajo! Eres una sorpresa cada día… nunca me cansaré de ti.

Elena, que divertido que nos hicimos amigas en el metro, y estas en el lab de al lado! De todas formas, antes o después, teníamos que encontrarnos una a la otra. Que mucho ánimo, que tu también estas muy cerca de presentarla, y que te quedará genial porque has trabajado mucho!! Un abrazo.

Iris, lo mismo, que llevamos 5 años en paralelo, siempre preguntando si has hecho ya el comité de tesis o no, trabajo o hobby, que tal el paper, cuando defendemos….? Me hizo mucha ilusión compartir todo esto contigo, uno se hace más seguro cuando ve que todo el mundo enfrenta los mismos problemas. Pero hay que aprender a relajarse!

Ignasi, tú todavía aquí… un día te harán una estatua de ti en el CRG o en el animalario o al lado de la pista de volley, jajaja… cuantos recuerdos… me acuerdo haber filmado el video para tu tesis en el otro edificio; los partidos de volley donde Salichs, Markus y tu nos habéis animado a ponernos delante de tíos altísimos y devolver la pelota; las buenas palabras de cada día en el pasillo… sé que siempre podré contar contigo.

Cedrik, eres único, nunca cambies!

Gracias a todos los miembros de Genes and Disease por las charlas en cultivos y en el pasillo. Xevi, a ti especialmente por haberme preguntado cada día "Qué tal la tesis?". Y a Laura por haberme enseñado el mundo de los lentivirus.

María, Celia, Yaiza, Roger, Rayane, Eli, Stephen, Paco, mis compis de 4 pisos, os agradezco a todos que hayáis compartido vuestra casa, comida, cultura conmigo. En todos